Modification of Bcl-x and Mcl-1 Pre-mRNA Splicing Using Splice-Switching Oligonucleotides

John A. Bauman

A dissertation submitted to the faculty of the University of North Carolina at Chapel Hill in partial fulfillment of the requirements for the degree of Doctor of Philosophy in the Department of Pharmacology

Chapel Hill
2010

Approved by:

Adviser: Dr. Ryszard Kole

Reader: Dr. Rudolph Juliano

Reader: Dr. Channing Der

Reader: Dr. Pilar Blancafort

Reader: Dr. Bert O'Neil

ABSTRACT

Modification of Bcl-x and Mcl-1 Pre-mRNA Splicing Using Splice-Switching Oligonucleotides

(Under the direction of Ryszard Kole)

Over 90% of multi-exon pre-mRNA transcripts undergo alternative splicing and up to one-half of disease-causing mutations affect splicing. Thus, alternative splicing has emerged as an important target for molecular therapies. Splice-switching oligonucleotides (SSOs) are chemically modified antisense oligonucleotides that hybridize to pre-mRNA sequences involved in splicing and block access to the transcript by splicing factors. As a result the splicing machinery is redirected to alternative splice sites thereby modifying the pattern of splicing and influencing protein expression. The efficacy of SSOs has been established in various animal disease models and clinical trials for Duchenne Muscular Dystrophy. However, the application of SSOs against cancer targets has been hindered by poor *in vivo* delivery of antisense therapeutics to tumor cells.

Bcl-x pre-mRNA is alternatively spliced to express anti-apoptotic Bcl-x_L and pro-apoptotic Bcl-x_S. Bcl-x_L expression is up-regulated in many cancers and confers chemoresistance, distinguishing it as an important target for cancer therapy. It was previously demonstrated that redirection of Bcl-x pre-mRNA splicing from Bcl-x_L to -x_S induced

apoptosis in breast and prostate cancer cells. In the research presented herein, the effect of SSO-induced Bcl-x splice-switching on metastatic melanoma was assessed in cell culture and B16F10 tumor xenografts. Delivery to tumor cells *in vivo* was achieved by encapsulating the SSO in targeted lipid nanoparticles. Administration of nanoparticle with Bcl-x SSO resulted in modification of Bcl-x pre-mRNA splicing in lung metastases and reduced tumor load, while nanoparticle alone or formulated with a control SSO had no effect. These findings demonstrate *in vivo* anti-tumor activity of SSOs that modulate Bcl-x pre-mRNA splicing.

Like Bcl-x, Mcl-1 pre-mRNA is alternatively spliced to produce proteins with opposing functions. Splicing of all three Mcl-1 exons produces anti-apoptotic Mcl-1_L, which is highly expressed in many malignancies and confers resistance to chemotherapeutic drugs. Skipping of exon 2 leads to expression of Mcl-1_S, a potent pro-apoptotic protein expressed at low levels in most cells. I designed and screened SSOs targeted to the 5′ and 3′ splice sites of exon 2 in Mcl-1 pre-mRNA, which resulted in redirection of Mcl-1 pre-mRNA from Mcl-1_L to -1_S. Mcl-1 splice-switching resulted in PARP cleavage and cell death in HeLa cells, indicative of apoptosis. Mcl-1 splice-switching also sensitized cells staurosporine. These findings validate Mcl-1 as a target for SSOs to induce apoptosis and sensitize cancer cells to chemotherapy.

ACKNOWLEDGEMENTS

I thank my adviser Ryszard Kole for providing me with many opportunities to improve as a scientific researcher, writer and speaker.

I thank my committee chair Rudy Juliano for his mentorship and for allowing me to work in his lab.

I thank the members of my committee, Channing Der, Pilar Blancafort and Bert O'Neil, for their time, patience and helpful suggestions.

I thank members of the Kole and Juliano Laboratories, past and present, especially Peter Sazani, Jennifer Roberts, Mike Fisher, Brian Buckley, Marysia Graziewicz, Jin Lee, Jing Wan, Natee Jearawiriyapaisarn, Thipperat Suwanmanee, Xin Ming, LeShara Fulton, Osamu Nakagawa.

I thank my collaborators Leaf Huang and Shyh-Dar Li for their time and efforts in our project.

I thank those who have mentored and taught me over the years, including Jerry Rich, Rebecca Sacra, Carla Green, Faye Cascio, Louis Cohen, Michael Bergman and Barbara Duman.

This work would not have been possible without the love, support and encouragement of my parents, John and Nancy, my sisters Leslie and Christina, and my brother-in-law David; I am grateful to each of them.

TABLE OF CONTENTS

LIST OF TABLES

LIST OF FIGURES

ABBREVIATIONS

2OMe – 2′-O-methyl

BPS – branch point sequence

CRCE1 – ceramide-responseive RNA *cis*-element

CXCL1 – chemokine (C-X-C motif) ligand 1

DMD – Duchenne muscular dystrophy

hnRNP – heterogeneous nuclear ribonucleoprotein

ESE – exonic splicing enhancer

ESS – exonic splicing silencer

FADD – Fas-associated death domain

IL-8 – interleukin-8

ISE – intronic splicing enhancer

ISS – intronic splicing silencer

LNA – locked nucleic acid

MOE – 2′-O-methoxyethyl

NMD – nonsense-mediated decay

OMM – outer mitochondrial membrane

PDE – phosphodiester

PMO – phosphoroamidate morpholino

PNA – peptide nucleic acid

PS – phosphorothioate

RT-PCR – reverse-transcriptase polymerase chain reaction

RSE – regulatory splicing element

RRM – RNA recognition motif

SR protein – serine-arginine-rich protein

snRNA – small nuclear RNA

snRNP – small nuclear ribonucleoprotein

TNF – tumor necrosis factor

U2AF – U2 auxiliary factor

Chapter 1 – Introduction

Pre-mRNA Splicing

Pre-mRNA splicing is the co-transcriptional process of intron removal and exon joining in eukaryotes (Goldstrohm et al., 2001). In humans, the average human gene is 28,000 nucleotides long and has 8.8 exons and 7.8 introns (Lander et al., 2001). The typical gene contains relatively short exons (e.g. 50–250 base pairs in length) separated by much larger introns (typically, hundreds of thousands of base pairs or more). Pre-mRNA splicing is mediated by the spliceosome, a dynamic complex of proteins and RNAs, which is assembled *de novo* on nascent transcripts. Sequence specificity and simultaneous plasticity of alternative splicing is achieved by tissue-dependent variability of spliceosome composition (Pollard et al., 2002; Pollard et al., 2000) and loose conservation of essential sequence elements in the pre-mRNA. These elements include splice sites, branch points, polypyrimidine tracts, and auxiliary exonic and intronic sequence elements known as splicing enhancers (ESEs and ISEs, respectively) and silencers (ESSs and ISSs, respectively) (Figure 1.1A). Splicing is thought to be controlled by competition among splice sites and splicing elements for splicing factors.

Importantly, up to 50% of human genetic diseases arise from mutations that affect splicing and aberrations in splicing have been associated with cancer parthogenesis. (Cartegni et al., 2002; Faustino and Cooper, 2003; Pagani and Baralle, 2004; Pagenstecher et al., 2006). Thus, pharmacological agents that modify pre-mRNA splicing would potentially have therapeutic value (Bauman et al., 2009).

Sequences Involved in Splicing

Sites in pre-mRNA that participate in every splicing reaction include the 5′ and 3′ ends of introns (referred to as 5′ and 3′ splice sites, respectively); the branch-point sequence

(BPS), an adenosine located upstream of the 3′ splice site; and the polypyrimidine tract, located between the branch point and the 3′ splice site (Figure 1.1 A). The first and last two nucleotides of an intron are conserved GU and AG, respectively. These absolutely conserved dinucleotides are flanked by loosely conserved splice site consensus sequences. The 5′ and 3′ splice sites, BPS and polypyrimidine tract are the sites of interaction with various components of the splicing machinery, and participate in the biochemical splicing reactions.

The core splicing elements are predicted to contain about half of the information required for splicing (Lim and Burge, 2001). The remaining information is derived largely from *cis*-regulatory sequence element (RSEs) that participate in splicing regulation. RSEs are classified as exonic and intronic splicing enhancers (ESEs and ISEs, respectively) and silencers (ESSs and ISSs, respectively) (Figure 1.1 A). SREs function by recruitment of sequence-specific RNA-binding factors that either activate or repress the use of adjacent splice sites. Interplay between these sequence elements is thought to control the outcome of each splicing event, providing the means for regulation of alternative splicing (Dominski and Kole, 1992). Many SREs have been identified through the study of disease-causing splicing mutations (Hua et al., 2007; Hua et al., 2008). Recently, high-throughput methods have accelerated the identification of SRE consensus sequences (Wang et al., 2004; Wang et al., 2006). The eventual goal is to decipher the "cellular code" of splicing regulation to improve our capacity to predict alternative splicing outcomes (Wang and Burge, 2008).

Chemical Reactions in Splicing

Splicing of pre-mRNA proceeds via two transesterification reactions (Figure 1.1 B). First, the 2′-hydroxel group of the branch point adenosine attacks the phosphate at the 5′ splice site. This leads to cleavage of the 5′ exon from the intron and the concerted ligation of

the intron 5′ end to the BPS 2′-hydroxyl. This step produces two reaction intermediates: a detached 5′ exon and an intron/3′-exon fragment in a lariat configuration containing a branched A nucleotide at the branch point. The second transesterification step is the attack on the phosphate at the 3′ end of the intron by the 3′-hydroxyl of the detached exon. This ligates the two exons and releases the intron in the form of a lariat (Black, 2003).

The Spliceosome: A Dynamic Ribonucleoprotein Machine

The spliceosome is a dynamic complex of small nuclear ribonucleoproteins (snRNPs) and accessory proteins, which is assembled *de novo* at every splicing event. The process of spliceosome assembly has been comprehensively reviewed and will be briefly summarized (Black, 2003; Staley and Guthrie, 1998; Wahl et al., 2009). The primary components of the spliceosome are the U1, U2, U4/U6 and U5 snRNPs. Each snRNP consists of an snRNA (two in the case of U4/U5), and a variable number of complex-specific proteins. Spliceosome assembly begins with ATP-independent binding of the U1 snRNP through base-pairing interactions of the 5′ end of the U1 snRNA to the 5′ splice site. In higher eukaryotes, this interaction is stabilized by members of the serine-arginine-rich (SR) protein family. At the same time, SF1/BBP protein binds the branch-point adenosine (Baughan et al., 2006), and U2 auxiliary factor (U2AF), a dimer composed of 65 kDa and 35 kDa subunits, binds the polypyrimidine tract (Gaur et al., 1995). These two proteins bind cooperatively; SF1/BBP interacts with the 65 kDa subunit of U2AF (U2AF65) through its C-terminal RNA recognition motif (RRM). In addition, the 35 kDa subunit of U2AF (U2AF35), binds the AG dinucleotide of the 3' splice site; this interaction is critical for introns with weak polypyrimidine tracts (Wu et al., 1999). Together, these molecular interactions yield the E

(early) complex and play crucial roles in the initial recognition of the 5′ splice site and 3′ splice site (Black, 2003; Wahl et al., 2009).

After the formation of the E complex, the U2 snRNA engages in an ATP-dependent base-pairing interaction with the branch-point, leading to the formation of the A complex (pre-spliceosome). This base-pairing interaction is stabilized by heteromeric protein complexes of the U2 snRNP and by the arginine-serine-rich (RS) domain of the U2AF65 protein (Valcarcel et al., 1996). Association of U2 leads to the displacement of SF1/BBP from the branch-point. The latter interaction is replaced by association of SF3b14a/p14 with the branch point adenosine. The SF3b155 protein now interacts with the C-terminal RNA recognition motif of U2AF65 (Wahl et al., 2009).

Following A complex formation, the U4/U6 and U5 snRNPs are recruited as a preassembled U4/U6.U5 tri-snRNP, forming the B complex. This process requires SR proteins (ASF, SC35 and SRp55) and ATP hydrolysis (Roscigno and Garcia-Blanco, 1995). At this point, the required snRNPs are all present in the B complex, but it is still catalytically inactive and requires conformational and positional rearrangements in order to facilitate the first transesterification step of splicing. During spliceosome activation, U1 and U4 are destabilized or released, giving rise to the activated spliceosome (the B* complex). The activated spliceosome then undergoes the first catalytic step of splicing, generating the C complex. Prior to the second catalytic step, additional rearrangements occur in the spliceosomal RNP network. After the second catalytic step, the spliceosome dissociates, releasing the U2, U5 and U6 snRNPs to be recycled for additional rounds of splicing (Wahl et al., 2009).

The dynamic process of spliceosome assembly illustrates three recurring principles of the splice process. First, the core splicing elements are recognized multiple times by RNA or protein to ensure the precision of the splicing reaction. Second, functionally important interactions among components of the spliceosome are often weak but are enhanced by a combination of multiple interactions. Third, RNP rearrangements during spliceosome assembly generally involve the handing over of one of more binding partners to new interaction partners (Wahl et al., 2009).

Splicing Factors

Most ESEs recruit members of the SR protein family. SR proteins are characterized by their ability to interact simultaneously with RNA and other protein components via an N-terminal RNA recognition motif (RRM) and through a C-terminal domain rich in arginine and serine residues, the RS domain (Caceres et al., 1997; Shepard and Hertel, 2009; Wang and Burge, 2008). For example, SR proteins facilitate binding of U1 snRNP to the 5′ splice site and U2AF65 to the polymyrimide tract (Staknis and Reed, 1994). SR proteins are also required from the pre-spliceosome (A complex) to spliceosome (B complex) transition, as their depletion inhibits spliceosome assembly (Roscigno and Garcia-Blanco, 1995).

ESSs are often bound by splicing repressors of the hnRNP class, a diverse group of proteins containing one or more RNA-binding domains and sometimes splicing inhibitory domains, such as glycine-rich motifs (Han et al., 2010). The hnRNP proteins vary in their mechanism of action: they can repress splicing by directly antagonizing the recognition of splice sites, or can interfere with the binding of proteins bound to enhancers (Martinez-Contreras et al., 2007). Polypyrimidine tract biding protein (PTB, also hnRNP I) blocks interactions between U1 and U2 snRNPs (Sharma et al., 2005), while hnRNP A1 inhibits

splicing by binding on either side and looping out exons, or by directly displacing snRNP binding (Nasim et al., 2002; Zhu et al., 2001).

There are fewer examples of well-characterized intronic rather than exonic RSEs. One example is G triplet or G run (G_n; $n \geq 3$), which are often present in clusters and can enhance recognition of adjacent splice sites (McCullough and Berget, 2000). Characterized ISSs include binding sites for the aforementioned PTB and hnRNP AI splicing repressors (Matlin et al., 2005), CA-rich sequences bound by hnRNP L (Hui et al., 2005), and specific octamers flanking exon IIIb of the FGFR2 gene (Wagner et al., 2005). Interestingly, intronic RSEs are thought to be of particular importance in regulating alternative splicing because the intronic regions surrounding alternatively spliced exons are far more conserved in mammals than those surrounding constitutive exons (Sorek and Ast, 2003). This increased conservation has been used to predict unannotated alternative exons (Sorek et al., 2004) and to predict intronic SREs (Yeo et al., 2007).

Alternative Splicing

Through alternative splicing, a single pre-mRNA transcript can give rise to multiple mature mRNA splice variants, which are then translated into variable protein isoforms. This is accomplished through various means, including exon exclusion, intron retention, exon shuffling, alternative 5′ and 3′ splice sites, alternative promoter usage and alternative polyadenylation site selection (Figure 1.2). According to deep sequencing analyses, over 90% of multi-exon genes undergo alternative splicing, approximately 86% with a minor isoform frequency of 15% or more (Wang et al., 2008). Most alternative splicing events affect the coding sequence, with half of these altering the reading frame and one-third apparently leading to nonsense-mediate decay of the RNA product (Thanaraj et al., 2003).

Regulation of alternative splicing is thought to involve the participation of core splicing elements and RSEs, with the precise combinations and relative ratios of factors dictating regulatory decisions. Tissue-specific splicing decisions might be determined by cellular codes comprised of particular combinations of splicing regulators specific to each cell type. As a result, many alternative splicing events involve a complex interplay between positive and negative regulators that function through cognate enhancers and silencers (Dominski and Kole, 1992; Matlin et al., 2005). The dynamic nature and the gene- and tissue-dependent variability of the splicing machinery and its interaction with pre-mRNA suggest a richness of potential targets for drugs that interfere with or redirect alternative splicing pathways for therapeutic purposes (Kole et al., 2004).

Splice-switching oligonucleotides

Antisense oligonucleotides (ASOs) can be broadly defined as oligonucleotides 8 to50 nucleotides in length that, entirely or in part, bind RNA through Watson-Crick base pairing and upon binding to RNA, modulate the function of the targeted RNA (Bennett and Swayze, 2010). These compounds act by various mechanisms either to promote the degradation of the RNA or to modify its function in some way without promoting degradation. Perhaps the best understood mechanism resulting in target RNA degradation is cleavage by ribonuclease H (RNase H), which cleaves DNA:RNA duplexes (Lima et al., 2008). Another widely studied mechanism of RNA degradation is RNA interference (RNAi), which involves loading of double-stranded mRNA substrates into a protein complex called RISC, followed by cleavage of the target mRNA by the enzymatic Argonaute protein (Sigova and Zamore, 2008). Antisense mechanisms of regulation that do not involve cleavage of the target RNA include

translation arrest (Deas et al., 2005), inhibition of translation initiation (Baker et al., 1997) and modification of splicing (Dominski and Kole, 1993).

Modification of pre-mRNA splicing was first demonstrated in cell-free extracts from cells expressing aberrantly-sliced β-globin. Dominski and Kole (1993) discovered that blocking an active splice site with an antisense oligonucleotide does not lead to the complete shut down of splicing in that transcript, but simply forces the spliceosome to select an alternative splicing pathway. In this study, human β-globin pre-mRNAs with splicing mutations were targeted with RNase H non-competent 2′-*O*-methyl antisense oligonucleotides in order to restore correct splicing. Antisense oligonucleotides targeted against aberrant 5′ and cryptic 3′ splice sites activated by IVS2-705 and IVS2-654 mutations in intron 2 significantly inhibited the aberrant splicing and restored the correct splicing pathway. This study demonstrated that oligonucleotides could compete with splicing factors for access to pre-mRNA sequence elements and modify the pattern of splicing. A subsequent study in mammalian cells expressing the IVS2-654 human β-globin gene confirmed that the oligonucleotide could enter the cell, reach the nucleus and modify the pattern of splicing in a sequence-specific manner in live cells (Sierakowska et al., 1996). Antisense oligonucleotides that modify splicing comprise a distinct class of antisense compounds and have been termed **splice-switching oligonucleotides** (SSOs).

Oligonucleotide Chemical Modifications

The SSO mechanism of action requires that it form very stable duplexes with its pre-mRNA target to enable successful competition with natural splicing factors for specific binding sequences. This must be achieved without activating RNase H. These requirements are met by incorporating various chemical modifications of the oligonucleotide backbone and

ribose ring that improve binding affinity and do not support RNase H cleavage (Sazani et al., 2001). Down-regulating ASOs are limited in the degree to which they can be modified because they require at least five contiguous deoxyribonucleotides to support RNase H cleavage (Monia et al., 1993). Chimeric ASOs, or "gapmers," consisting of a deoxyribonucleotide region flanked by modified nucleotides are RNase H-active and derive a partial benefit due to the modified flanks. Because some modified nucleotides interfere with loading into the RISC complex, siRNA is even more limited in the degree to which they can be modified.

In addition to RNase H non-competence, the SSO must be resistant to enzymatic degradation in the cellular environment and should demonstrate preferential tissue distribution and pharmacodynamics *in vivo*. The chemical modifications that best meet all the desired SSO criteria are discussed in the following sections.

Phosphorothioate Modification

In biological fluids, unmodified deoxyribonucleotides are highly susceptible to degradation by ubiquitous nucleases and *in vivo* they exhibit circulating half-lives of 1–2 minutes (Levin et al., 2008). Modifying the phosphodiester (PDE) backbone of DNA ASOs renders them resistant to cleavage by nucleases. The widely used phosphorothioate (PS) modification substitutes a sulfur for a non-bridging oxygen atom in the PDE linkages (Figure 1.3 A); this modification improves nuclease stability such that the plasma half-life of these ASOs is increased to 30–60 minutes. The PS modification does not impart RNase H non-competence, however, and must be used in conjunction with other modifications that do not support RNase H to be applied for splice-switching.

In addition to increased nuclease resistance, the PS modification confers enhanced protein binding (Brown et al., 1994). The reason PS ASOs bind more promiscuously to cellular proteins than PDE ASOs has not been fully elucidated, but may be due to increased lipophilicity and metal ion complexation (Levin et al., 2008). Interactions of the sulfurs in the PS ASOs with metal ions associated with specific proteins have been proposed for the affinity of PS ASOs for proteins (Eckstein, 2000). Binding of PS ASOs to several abundant serum proteins including albumin, fibrinogen, and γ-globulin, has been reported (Yu et al., 2000). The increased binding of PS ASOs to serum proteins may contribute to increased cellular toxicity of these drugs. In primates, a PS DNA ASO activated the complement cascade following rapid infusion and in some cases, led to cardiovascular collapse and death; however, lower doses used in human clinical trials have been well-tolerated (Nemunaitis et al., 1999). In addition, increased serum protein binding protects PS ASOs from renal filtration and contributes to the increased serum half-life (Levin, 1999). The PS modification imparts slightly reduced binding affinity towards complementary RNA compared to unmodified ASOs. Thus, the enhanced nuclease stability of PS ASOs comes at the expense of target binding affinity and increased toxicity. These drawbacks can be compensated for by incorporation of other modifications. Unless specifically stated otherwise, all 2OMe, MOE and LNA SSOs described in this manuscript contained PS internucleotide linkages.

2′-Modifications of Ribose

Substitutions at the 2′ position of ribose impart RNase H non-competence to fully-modified SSOs. The two most widely studied in this group are the 2′-O-methyl (2OMe) and 2′-O-methoxyethyl (MOE) modifications (Figure 1.3 B, C). Oligonucleotides that employ these ribose modifications, coupled with PS internucleotide linkages, exhibit diminished

toxicity and enhanced target sequence binding compared to PS DNAs. The first report showing *in vivo* activity of SSOs utilized both of these chemistries (Sazani et al., 2002). Since then, numerous groups have used 2OMe (Lu et al., 2003; Lu et al., 2005; Mann et al., 2001) and MOE (Hua et al., 2008; Vickers et al., 2006) SSOs to modulate splicing *in vivo*. Among the chemistries employed for oligonucleotide therapeutics, the MOE modification has been studied in the most detail, with 15 MOE ASOs currently in clinical trials (www.isispharm.com/pipeline).

Locked nucleic acids (LNA) consist of a ribonucleotide containing a methylene bridge that connects the 2′-oxygen of the ribose with the 4′-carbon (Figure 1.3 D). Introduction of LNAs into a DNA ASO induces a conformational change of the DNA-RNA duplex towards the A-type helix, and therefore prevents the RNase H cleavage of the target RNA. Chimeric DNA-LNA ASOs exhibit enhanced stability against nucleolytic degradation and remarkably high target affinity (Wahlestedt et al., 2000). The enhanced binding affinity enables the use of lower SSO concentrations *in vitro* and *in vivo* (Roberts et al., 2006). A study of SSOs consisting of various proportions of DNA, 2OMe and LNA monomers demonstrated that the introduction of LNA monomers enhanced antisense activity (Guterstam et al., 2008). However, this study also found that, due to their high target affinity, LNA monomers also confer low mismatch discrimination to the SSO, which could result in increased off-target effects and related toxicity. This potential drawback could be addressed by using shorter oligonucleotides or by tuning of the proportion of LNA monomers in an SSO to optimize the trade-off between splice-switching efficiency and risk for off-target effects.

Backbone Modifications

Phosphoroamidate morpholinos (PMOs) are nonionic DNA analogs in which the ribose is replaced by a morpholino moiety and phosphoroamidate intersubunit linkages are used instead of PDE bonds (Figure 1.3 E). They have high nuclease resistance, high duplex stability and do not activate RNase H (Morcos, 2007). Because they are uncharged, PMOs are unlikely to form unwanted interactions with nucleic acid-binding proteins; however, their cellular uptake is limited (Sazani et al., 2002). In cynomolgus monkeys, no toxicity was detected at the maximum feasible dose (320 mg/kg) (Sazani et al., 2010) and no adverse effects were reported following intramusculuar injection in human clinical trials (Kinali et al., 2009).

Peptide nucleic acids (PNA) consist of a DNA analog wherein the deoxyribose phosphate backbone is replaced by polyamide linkages (Figure 1.3 F). PNAs exhibit high target affinity, are nuclease and peptidase-resistant and do not activate RNase H. However, they are electrostatically neutral and their ability to cross cell membranes is limited. This limitation can be overcome by the addition of positively charged amino acids at the 5′ or 3′ end (Abes et al., 2006; Sazani et al., 2002; Sazani et al., 2001).

Delivery of SSOs

In order for the SSO to affect splicing, it must reach its pharmacological site of action in the nucleus. In cell culture, antisense activity of free SSOs is generally modest and as a result commercially available transfection reagents, such as Lipofectamine2000 (Wan et al., 2008) and DMRIE-C (Mercatante et al., 2001), are commonly used to improve delivery. Without the aid of delivery agents, uncharged or positively charged SSOs (e.g. morpholino, PNA) reached the nucleus more efficiently than negatively-charged compounds (e.g. 2OMe,

MOE) (Sazani et al., 2001). The poor efficacy of the 2OMe and MOE SSOs appeared to be due not to poor cellular uptake but to sequestration of these compounds in the cytoplasm or cytoplasmic vesicles (e.g. endosomes) following uptake. Incorporation of G-clamp and phenoxazine analogs of cytidine into MOE SSOs resulted in a modest increase in antisense activity compared to unmodified MOE SSOs (Sazani et al., 2003). The addition of four positively-charged lysines increased the antisense activity of a PNA SSO (Sazani et al., 2001). Treatment with endosome-disrupting agents resulted in a dramatic increase in the antisense activity of a PNA SSO conjugated with eight lysines without improving the activity of the free PNA SSO, suggesting that the former efficiently entered the cell but was sequestered in endosomal vesicles (Abes et al., 2006).

In vivo delivery of SSOs presents additional challenges that are not encountered in cell culture. The biological barriers to effective SSO delivery and how they may be overcome are discussed in the following sections.

Biological Barriers Encountered by SSOs In Vivo

Several major biological barriers must be overcome in order for SSOs to be useful as therapeutic agents. The first barrier encountered by the SSO *in vivo* is comprised of ubiquitous nucleases in plasma and tissues. The major activity in plasma is a 3′ exonuclease, however cleavage of the internucleotide bonds also takes place (Juliano et al., 2009a). In general, oligonucleotides accumulate in most tissues, particularly the liver and kidney, but not the central nervous system. The precise pharmacokinetics and functional distribution of an SSO depend on its chemical composition (Sazani et al., 2002). However, the biodistribution of an oligonucleotide does not predict the tissues in which it will be functionally active (Roberts et al., 2006).

Another consideration is clearance by macrophages of the reticuloendothelial system (RES). The RES is composed of phagocytic cells, including circulating monocytes and macrophages, whose physiological function is to clear the body of foreign pathogens, remove cellular debris that is generated during tissue remodeling, and clear cells that have undergone apoptosis (Mosser and Edwards, 2008). Tissue macrophages are most abundant in the liver (Kupffer cells) and spleen, tissues that also receive high blood flow and exhibit fenestrated vasculature (Underhill and Ozinsky, 2002). Thus is it not surprising that these organs accumulate high concentrations of oligonucleotide (Geary et al., 2008; Roberts et al., 2006).

In order to reach a particular tissue, the oligonucleotide must cross the endothelial cells that line the vasculature. These cells adhere tightly to the underlying extracellular matrix via integrins and form junctions with one another via cell-cell adhesion molecules. A model has been proposed that describes normal endothelium as having abundant 45 Å diameter pores as well as relatively scarce large pores of 250 Å (Rippe et al., 2002). Based on the molecular weights of oligonucleotides, they should be able to extravasate from circulation via these small pores. There is controversy regarding the role of the large pore system and it is not known whether its contributes to extravasation of oligonucleotides (Juliano et al., 2009a).

In contrast to normal endothelium, tumor vasculature presents abnormalities that provide opportunities and obstacles to oligonucleotide delivery. The transvascular permeability of tumors is generally higher than that of normal tissue, likely due to an increased number and size of the “large pore” component (Jain, 1999). Tumor vasculature tends to be more highly fenestrated than normal tissue and exhibit poor lymphatic drainage. These characteristics might enable macromolceules to more easily cross into and persist in

tumor tissue, the so-called enhanced permeability and retention (EPR) effect (Brannon-Peppas and Blanchette, 2004). However, tumors also frequently exhibit high interstitial fluid pressure, which works against the uptake of macromolecules (Juliano et al., 2009a).

Oligonucleotides enter cells by some form of endocytosis, which requires coordination of cellular uptake, vesicular trafficking and endosomal release. Injection of mice with increasing doses of a nonsense ASO in combination with a constant concentration of a therapeutic MOE SSO resulted in an increase in antisense activity of the latter, suggesting the presence of a nonproductive bulk uptake pathway (Geary et al., 2009). The SSO site of action is the nucleus (Sazani et al., 2003), thus their pharmacological effect depends not only on total cell update but also on intracellular trafficking of the SSO, which to date is poorly understood (Alam et al., 2008).

Systemic Administration of Free SSOs

The simplest approach to *in vivo* delivery of SSO is systemic administration of free oligonucleotide. This was first documented by Sazani and colleagues, who engineered an animal model for the study of SSO activity *in vivo*. The assay is based on a transgenic mouse that ubiquitously expresses the coding sequence for enhanced green fluorescence protein (EGFP) with an aberrantly spliced intron of human β-globin intron 2 (IVS-654; see earlier section on origins of SSOs for more detail), such that basal expression of EGFP protein is essentially zero (Sazani et al., 2002). Delivery of SSO to the nuclei of cells corrects the aberrant splicing and leads to generation of mRNA containing the correct EGFP reading frame and renders the cells fluorescent, providing a positive readout of nuclear oligonucleotide activity.

With the advent of the so-called EGFP-654 mouse, the *in vivo* efficacies of systemically delivered SSOs containing various chemical modifications could be compared in a controlled system. In contrast to earlier observations in cell culture (Sazani et al., 2001), MOE SSOs demonstrated strong antisense activity in a number of tissues, including liver, small intestine, lung and heart (Sazani et al., 2002). Neutral morpholino and PNA SSOs exhibited only modest activity; however addition of four lysines significantly enhanced their activity (PNA-4K). LNA SSOs were found to be active almost exclusively in the liver and, to a lesser extent, the small intestine and colon (Roberts et al., 2006). The LNA SSO was considerably more potent than the 2OMe SSO in these tissues. In the liver, the LNA SSO exhibited an EC_{50} that was approximately 17-fold higher than that of the 2OMe SSO. This was likely due to higher binding affinity conferred by the LNA bases. Little activity was seen in the kidney, the tissue with by far the greatest LNA SSO accumulation, indicating that the sites of SSO biodistribution do not necessarily predict the sites of its pharmacological activity (Roberts et al., 2006). Taken together, these results indicated that systemically delivered free SSOs exhibited distinct functional activity profiles depending on their chemical composition in the EGFP-654 model system.

Administration of free SSOs did not result in detectable antisense activity in tumor cells in various tumor xenograft models. Over the course of several related studies, over 254 mice were implanted with subcutaneous tumor xenografts (508 total tumors) using different cell lines. Despite using more aggressive dosing regimens than were used in the studies described above (25 mg/kg daily injections over two weeks vs. 25–50 mg/kg daily injections over four days), the investigators failed to detect antisense activity of MOE SSOs (Adams and Kole, unpublished data). The investigators also failed to detect SSO activity in orthotopic

liver xenografts (42 mice implanted). In summary, antisense activity could not be confirmed in tumor xenografts following systemic administration of free SSO.

Peptide Conjugates to Improve Delivery

Two main strategies have emerged for improving delivery of oligonucleotide therapeutics: cell targeting or cell penetrating peptide (CPP) conjugates and nanoparticles (see next section). Because the SSO mechanism of action enables up-regulation of reporter gene expression, SSOs constitute ideal tools for investigating novel delivery agents for oligonucleotides in general (Kang et al., 1998). As a result, to date many peptide conjugates have been investigated in cell culture (Alam et al., 2008; Kang et al., 2008; Marlin et al., 2010). However, fewer peptide conjugates have been validated *in vivo*. Jearawiriyapaisarn et al. screened in the EGFP-654 mouse a panel of putative cell penetrating peptides containing different combinations of arginine, 6-aminohexanoic acid, and β-alanine conjugated to PMO SSOs (Jearawiriyapaisarn et al., 2008). Many of the peptide-conjugated PMOs (PPMOs) exhibited potent antisense activity in numerous tissues. In particular, one PMO-peptide conjugate, PPMO-B, induced significant antisense activity in body-wide skeletal muscle, diaphragm and cardiac muscle, distinguishing the PPMO-B peptide as potentially useful for muscle-related targets. Others have reported similar results with arginine-rich CPPs (McClorey et al., 2006; Moulton et al., 2007; Wu et al., 2008; Yin et al., 2008a; Yin et al., 2008b), several of which are currently being investigated in the clinic for the modification of splicing in the Duchenne Muscular Dystrophy (see later section on DMD).

Lipid Nanoparticles for Oligonucleotide Delivery

Because they cannot tolerate many chemical modifications, efforts to improve siRNA delivery have involved nanoparticle encapsulation to protect them from premature degradation by nucleases. As a result, there is a large body of research on nanoparticle delivery of siRNAs *in vivo* (Akhtar and Benter, 2007*)*. In contrast, to date only one study has utilized a non-peptide conjugate delivery aid for SSOs *in vivo*: a commercially available triblock copolymer, Pluronic F127, delivered 2OMe SSOs to body-wide skeletal muscle following i.v. injection, resulting in a low but detectable level of antisense activity (Lu et al., 2005). It seems likely that nanoparticle formulations that prove successful in delivery siRNA may be applied for the delivery of SSOs.

Among the formulations that have proven effective in the delivery of siRNA *in vivo* are lipid-based nanoparticles. Cationic lipids can condense nucleic acids into a cationic particle known as a lipoplex. Lipoplex formations protect the nucleic acid cargo from enzymatic degradation and can deliver it into cells by interacting with the negatively charged cell membrane. However, lipoplexes suffer high toxicity—likely related to charge—and have performed poorly in clinical trials (Edelstein et al., 2004; Lv et al., 2006). To overcome toxicity issues and to extend circulation time, the nucleic acid cargo can be encapsulated into a polyethylene glycol (PEG)-shielded cationic liposomal bilayer using scalable formulation methods (Choi et al., 2003; Harvie et al., 2000; Jeffs et al., 2005; Li et al., 2005; Wheeler et al., 1999; Zhang et al., 1999). These PEG-shielded cationic particle differ from lipoplexes by having a bilayer shell around the nucleic acid cargo, a smaller particle diameter (<100 nm) and better stability *in vivo*.

Li and Huang recently developed a multi-component lipid nanoparticle that effectively delivered siRNA and RNase H-active ASOs to tumor cells in culture, and siRNA to tumor xenografts *in vivo* (Li and Huang, 2006a). The formulation was prepared by encapsulating the siRNA using calf thymus DNA as a carrier DNA, providing protection against nucleases (See Figure 2.4 for schematic representation). The complex was condensed using protamine and then coated with cationic liposomes consisting of cholesterol and a cationic lipid. PEG lipids were inserted into the liposomal bilayer to shield the positive charge, reduce aggregation and increase circulation time in the blood. PEGylated nanoparticles have been reported to accumulate in highly vascularized tissues (the aforementioned EPR effect) (Brannon-Peppas and Blanchette, 2004). To increase cellular uptake, ligands may be tethered to the distal end of PEG to trigger receptor-mediated endocytosis. Li and Huang used anisamide, a ligand that binds the sigma receptor, which is aberrantly expressed at the tumor cell surface in various cancers (Banerjee et al., 2004; Bem et al., 1991). Based on its composition, Li and Huang referred to this lipid-based nanoparticle as a liposome-polycation-DNA complex, or LPD.

In its first application, the LPD NP delivered either siRNA or ASO targeted to survivin into sigma receptor-expressing H1299 lung cancer cells, resulting in reduced survivin mRNA and protein expression, and increased apoptosis and chemosensitization (Li and Huang, 2006b). These effects were significantly diminished in the presence of haloperidol, a high affinity sigma receptor ligand, suggesting that the conjugation of anisamide improved cell uptake. Li and Huang used this study to optimize the LPD formulation by fine-tuning the ratio of siRNA/ASO:protamine:liposome.

Next, Li and Huang used the LPD NP to deliver siRNA to tumor cells *in vivo*. LPD NP carrying siRNA targeted to EGFR was administered by three consecutive daily injections of 1.2 mg siRNA/kg to mice bearing H460 lung cancer subcutaneous xenografts (Li et al., 2008a). This treatment resulted in significant knockdown of EGFR expression, a modest induction of apoptosis (~15% vs. ~3 in PBS-treated animals), and reduced tumor growth. These effects were not seen in animals treated with LPD NP carrying a scrambled control siRNA. Non-targeted LPD NP carrying EGFP siRNA showed an intermediate level of tumor cell uptake that was greater than free siRNA but less than targeted LPD NP; however, it failed to silence EGFR or inhibit tumor growth. This suggested that improved uptake facilitated by the anisamide ligand was necessary for anti-cancer effects.

Li and colleagues next employed a common tumor model wherein sigma receptor-expressing B16F10 murine melanoma cells are injected into the tail vein and rapidly colonize the lungs. Using cells stably expressing luciferease, they demonstrated that LPD NP carrying luicferase siRNA could achieve 70–80% knock-down expression of reporter gene expression following a single 0.15 mg siRNA/kg i.v. injection (Li et al., 2008b). No cytokine induction was detected and uptake was relatively specific for tumor cells. LPD NP carrying three siRNAs targeted to MDM2, c-myc, and VEGF dramatically reduced tumor burden (by 70–80%) following two consecutive daily injections of 0.45 mg total siRNA/kg (0.15 mg each siRNA/kg) (Li et al., 2008c). This regimen improved survival time by 30%. Once again, target gene silencing and anti-tumor effects were absent in non-targeted LPD NP and LPD NP carrying scrambled siRNA. Higher doses of LPD NP (≥1.2 mg siRNA/kg) resulted in induction of IL-12 and IL-6 cytokines.

The impressive results using the LPD NP carrying siRNA prompted us to ask whether it could also be used to deliver SSO to the nucleus in tumor xenografts. This hypothesis was tested in Specific Aim 1.

Examples of SSO targets

SSOs may be applied in several ways: (i) to restore correct splicing of an aberrantly spliced transcript, (ii) to shift existing alternative splicing patterns from one splice variant to another, and (iii) to induce a novel splice variant that is not normally expressed (Figure 1.4) (Sazani P, 2007). The following section provides examples of how these splice-switching strategies have been applied against therapeutically relevant targets. This list is not comprehensive, but includes targets that have been thoroughly characterized *in vitro* and *in vivo*: β-globin, SMN2, TNFR2, MyD88, HER2 and ATM (Bcl-x is discussed in a later section). Special attention is devoted to SSOs applied to restore dystrophin expression in Duchenne Muscular Dystrophy because this is the first application to progress to clinical trials.

β-thalassemia

The blood disease β-thalassemia is caused by mutations in the β-globin a gene, many of which disrupt pre-mRNA splicing of introns one and two. Among the common β-globin mutations that disrupt splicing are IVS-654 and IVS-705, which create aberrant 5′ splice sites at positions 654 and 705, respectively, and activate the same cryptic 3′ splice site in intron 2. These mutations cause a portion of the intron to be retained in the spliced transcript, which introduces a shift in the reading frame that produces a premature stop codon. Dominksi and Kole showed that oligonucleotides targeted to these mutations restored normal splicing of β-

globin mRNA (Dominski and Kole, 1993). This study demonstrated that oligonucleotides could compete with splicing factors for access to pre-mRNA sequence elements and modify the pattern of splicing. A subsequent study in mammalian cells expressing the IVS2-654 human beta-globin gene confirmed that the oligonucleotide could enter the cell, reach the nucleus and modify the pattern of splicing in a sequence-specific manner in live cells (Sierakowska et al., 1996).

In erythroid progenitor cells isolated from peripheral blood of patients carrying IVS2-654 or -745 mutations, a single treatment with PMOs targeted to aberrant 5′ splice sites by syringe loading resulted in correction of β-globin pre-mRNA splicing and production of hemoglobin A (HbA) (Lacerra et al., 2000). Moreover, the PMOs were freely taken up by erythroid progenitor cells isolated from bone marrow of β-thalassemic mice carrying the human βIVS2-654 mutation (Lewis et al., 1998) and from peripheral blood of patients carrying IVS2-654 mutation, leading to effective splicing correction (Suwanmanee et al., 2002b). Free uptake of PMOs was also shown to be effective in splicing correction and HbA restoration in progenitor cells isolated from patients carrying a hemoglobin E mutation that activates a cryptic 5′ splice site in exon 1 (Suwanmanee et al., 2002a). These results suggested that PMO would be applicable *in vivo*, in mouse models of β-thalassemia.

Using an arginine-rich peptide, PMO SSO was delivered to a mouse model of IVS2-654 thalassemia. The SSO restored normal splicing resulting in significant expression of hemoglobin in peripheral blood, improving the number and quality of erythroid cells (Svasti et al., 2009).

SMN2

Spinal muscular atrophy (SMA) is characterized by the progressive degeneration of the motor neurons leading to a muscle wasting caused by homozygous mutations or deletions in the survival of motor neuron 1 gene (*SMN1*). *SMN1* is ubiquitously expressed and encodes SMN protein, which is necessary for assembly of snRNPs involved in splicing, an essential process for cell survival (Wan et al., 2005). In humans there is a second, *SMN* gene copy, *SMN2*, which differs from *SMN1* in the C-to-T transition at position 6 of SMN2 exon 7. It has been proposed that this transition disrupts an ESE sequence (Cartegni and Krainer, 2002), creates an ESS sequence (Kashima and Manley, 2003), or strengthens an inhibitory RNA stem loop at the 5′ end of exon 7 (Singh et al., 2004), leading to exon 7 exclusion in most of SMN2 transcripts that yields an unstable truncated SMN protein. *SMN2* is a modifying gene in SMA patients, as the number of copies of *SMN2* is inversely correlated to the severity of SMA (Mailman et al., 2002). Therefore, a strategy to include exon 7 and up-regulate expression of full-length, fully functional SMN protein from the intact copies of *SMN2* present in SMA patients can offer a therapeutic approach for SMA. Indeed, masking the 3′ splice site of SMN2 intron 7 using a 2OMe SSO impaired splice site recognition and forced the splicing machinery to re-couple the 5′ and 3′ splice sites in intron 6, leading to increased inclusion of exon 7 in cell culture (Lim and Hertel, 2001).

Targeting exon 7 by SSOs either linked to serine/arginine-rich splicing factors or including a “tail” that serves as a splicing factor binding site, called exon-specific splicing enhancement by small chimeric effectors (ESSENCE) (Cartegni and Krainer, 2003) and targeted oligonucleotide enhancer of splicing (TOES) (Skordis et al., 2003), respectively, have also been shown to promote exon 7 inclusion. A synthetic ESSENCE molecule

containing a PNA SSO targeted to exon 7 coupled to ten arginine-serine (RS) repeats significantly induced exon 7 inclusion in a cell-free splicing system. Although the PNA SSO lacking the RS repeats was active, efficacy was much lower than the ESSENCE molecule. The TOES was designed to have two components; the first was complementary to exon 7 and second was a non-complementary sequence which was designed to mimic an ESE to recruit trans-splicing factors. This bifunctional SSO increased SMN2 exon 7 inclusion *in vitro* and in SMA patient fibroblasts, which led to partial restoration of gem number, an indicator of SMN protein increase, suggesting that SSO bound to exon 7 in the transcript did not interfere with translation.

In a subsequent study, SMN2 exon 7 was saturated with overlapping MOE SSOs (Hua et al., 2007). The cell culture experiments revealed that the most effective SSOs, which promoted exon 7 inclusion and increased full-length SMN protein in SMA patient fibroblasts, were targeted to two putative exon splicing silencers (ESS) close to the 3′ and 5′ splice sites, respectively. These results imply that blocking of the ESS is sufficient to induce exon inclusion and that ESSENCE or TOES modifications, although most likely helpful, are not essential.

SSO targeted to a putative ISS in intron 6 identified also prompted an increase in exon 7 inclusion in the context of a SMN2 minigene (Miyajima et al., 2002). The ISS, called ISS-N1, was subsequently identified immediately downstream of the 5′ splice site of intron 7 (Singh et al., 2006). An extensive SSO screen of sequences downstream of the 5′ splice site in intron 7 identified the same ISS (Hua et al., 2008). Recently, MOE-PS SSO targeted to ISS-N1 was administered to human SMN2 (hSMN2) transgenic mice by biweekly i.v. injections at 25 mg/kg. Significant exon 7 inclusion was observed in the liver and kidney, but

not in the spinal cord of treated mice (Hua et al., 2008). In order to achieve the therapeutic effect of this strategy in SMA, the SSO would need to cross the blood-brain barrier or be delivered directly to the central nervous system.

TNFR

The cytokine tumor-necrosis factor-α (TNF-α) plays an important role in inflammatory diseases such as rheumatoid arthritis and hepatitis. TNF-α signaling is mediated by two membrane-bound receptors, TNFR1 and TNFR2, which trimerize upon ligand binding, leading to downstream activation of the transcription factor NF-κB. Approved anti-TNF-α macromolecular drugs etanercept (a dimerized TNFR2 receptor:Fc fusion protein), and infliximab and adalimumab (anti-TNF-α monoclonal antibodies), bind TNF-α in circulation and inhibit its inflammatory effects.

Graziewicz and colleagues hypothesized that exclusion of the transmembrane domain-encoding exon 7 would create a novel soluble protein, Δ7TNFR2, capable of antagonizing TNF-α signaling. They screened 16-mer SSOs consisting of alternating LNA-DNA nucleotides with PS linkages in L929 mouse cells and identified SSO3274, which efficiently blocked the 5′ splice site of exon 7 in TNFR2 pre-mRNA, inducing exon skipping in a sequence-specific and dose-dependent manner. SSO3274-induced exon skipping resulted in the expression of soluble Δ7TNFR2 protein, which was detected in the culture medium and which exhibited anti-TNF activity (Graziewicz et al., 2008).

LNA-containing SSOs are remarkably potent in the liver, where TNFR2 is highly expressed (Roberts et al., 2006). This led to an approach to utilize the liver as a "protein factory," producing soluble Δ7TNFR2 for release into circulation to antagonize TNF-α. As expected, SSO3274 induced sequence-specific, dose-dependent, persistent splice-switching

in the mouse liver after five daily i.p. injectons at 25 mg/kg/day. Δ7TNFR2 protein was detected in the serum of SSO3274-treated animals at 8,000–10,000 pg/ml, exhibited potent anti-TNF activity and was detectable in circulation up to 35 days after the last injection. Serum containing Δ7TNFR2 from SSO3274-treated mice (25 mg/kg/day i.p. once daily for 10 days) was 10-fold more potent at than that from mice treated with etanercept (50 μg i.p. once daily for 5 days). Evidently etanercept was subject to *in vivo* degradation that reduced its activity, while SSO3274 continually induced additional Δ7TNFR2 protein, replenishing degraded or inactivated protein in circulation. Importantly, no SSO-induced toxicity was reported. Because SSOs induce the expression of endogenous protein the likelihood of immune toxicity is very low. The ability of SSOs to produce therapeutic splice variants, such as Δ7TNFR2, for extended time periods and with a low likelihood of immune toxicity is a distinct advantage over biological drugs such as etanercept.

In a mouse model of inflammatory liver disease, SSO3274 injected i.p. for 10 days at 25 mg/kg/day protected the liver from TNF-α insult and prevented liver damage. The observed anti-inflammatory effects were likely enhanced by the ability of SSO3274 to simultaneously down-regulate TNFR2 while inducing Δ7TNFR2 in the liver. Importantly, etanercept administered at a dose comparable to the amount of Δ7TNFR2 induced by SSO3274 elicited no such protection. The 10-day dosing regimen also delayed the course of disease in a mouse model of collagen-induced rheumatoid arthritis. These results are notable given that 30% of rheumatoid arthritis patients do not respond to currently available treatments (Olsen and Stein, 2004; Pincus et al., 1999).

MyD88

MyD88 is an adapter protein that mediates pro-inflammatory cytokine signaling through IL-1 and Toll receptors. Upon receptor activation, MyD88 interacts with the receptor intracellular domain and recruits IL-1R-associated kinase-1 (IRAK-1) and IRAK-4, leading to the phosphorylation of IRAK-1 and the subsequent activation of the transcription factor NF-κB. Skipping of the second exon of MyD88 produces naturally occurring splice variant, $MyD88_S$. $MyD88_S$ retains its receptor binding function but is defective in its ability to recruit IRAK-4 and induce IRAK-1 activation; thus, $MyD88_S$ functions as a dominant-negative regulator of IL-1R and Toll receptor signaling (Janssens et al., 2002). Vickers et al. screened 20-mer MOE-PS SSOs targeted to the 5′ and 3′ splice sites of exon 2 and selected ISIS 337846, an SSO that switched splicing from MyD88 to $MyD88_S$ in mouse and human cells. ISIS 337846 induced redirection of MyD88 mRNA splicing in the liver, adipose tissue, and intestine of mice i.p. injected three times per week for three weeks with 50 mg/kg SSO. $MyD88_S$ protein was not detected, although this could be due to insufficient recognition of the splice variant by available antibodies. The SSO regimen abrogated pro-inflammatory IL-1β signaling in the liver (Vickers et al., 2006).

HER2

HER2 is a member of the epidermal growth factor receptor (EGFR) family of receptor tyrosine kinases. EGFR family members are comprised of three functional domains: an extracellular ligand-binding domain, a transmembrane domain, and an intracellular tyrosine kinase domain. Ligand-binding to a monomeric receptor promotes homo- or hetero-dimerization, which leads to auto- or trans-phosphorylation in the cytoplasmic domain and downstream signaling, primarily through mitogen-activated protein kinase (MAPK) and

phosphatidylinositol 3-kinase (PI3K)/protein kinase B (Akt) pathways(Yarden and Sliwkowski, 2001). Therefore, EGFR receptors play critical roles in cell proliferation, differentiation and survival (Olayioye et al., 2000). Deregulation of EGFR receptors has been implicated in numerous types of tumors (Hsieh and Moasser, 2007). HER2 is amplified and/or overexpressed in many human malignancies, including 25–30% breast cancers. HER2 overexpression correlates with enhanced tumor aggressiveness and decreased patient survival.

The transmembrane domain of HER2 is encoded by a single exon, exon 15. Wan et al. screened a series of MOE SSOs and identified one, SSO111, that induced exon 15 skipping in a sequence-specific, dose-dependent manner, thereby down-regulating full-length HER2 while producing a novel splice variant lacking the transmembrane domain, Δ15HER2 (Wan et al., 2008). In SK-BR-3 human breast cancer cells, which highly express HER2, SSO111-induced splice-switching potently inhibited cell growth and induced apoptosis. This effect was less pronounced in MCF7 cells, in which HER2 expression is 100-fold lower, despite the fact that splice switching was still observed, confirming that SSO111-induced growth inhibition was HER2-dependent. This was consistent with the previously reported correlation of SSO potency with increased target gene expression (Mercatante et al., 2002). It also indicates that tumors highly expressing HER2 would be more sensitive to SSO treatment than surrounding healthy tissue. It was further demonstrated that His-tagged Δ15HER2 protein potently down-regulated HER2 protein expression and inhibited HER3 activation in dose-dependent manner in SK-BR-3 cells (Wan et al., 2008).

ATM

Ataxia-telangiectasia (A-T) is an autosomal recessive disorder characterized by neurodegeneration, immune defects and predisposition to malignancy. A-T is caused by mutations in the ataxia-telangiectasia mutated (*ATM*) gene, half of which disrupt splicing (Teraoka et al., 1999). Recently, 25-mer PMO SSOs were used to block the activation of cryptic splice sites in cell lines representing three types of A-T splicing defect: a 5′ exonic cryptic splice site in TAT[C] cells, a 3′ exonic cryptic splice site in IRAT9 cells, and a pseudoexon inclusion in AT203LA cells (Du et al., 2007). In each case dose-dependent, sequence-specific splice correction was achieved, leading to upregulation of functional ATM protein. These findings are especially promising in light of evidence that only a small amount of functional protein (5-20% wild-type levels) is necessary to significantly ameliorate the disease phenotype (Gilad et al., 1998).

DMD

Duchenne Muscular Dystrophy is a fatal genetic disease characterized by severe and progressive muscle wasting. It is caused by deletions and other mutations in the *DMD* gene, which cause premature termination of translation and result in lack of dystrophin protein. Deletions that maintain the reading frame in *DMD* gene produce internally deleted but partially functional dystrophin, causing the milder Becker muscular dystrophy (BMD) (Monaco et al., 1988). It has been reported that rare, naturally occurring revertant (i.e. dystrophin-positive) fibers are expressed sporadically in muscles tissues of the *mdx* mouse, a mouse model of DMD (Hoffman et al., 1990) and in DMD patients (Nicholson et al., 1989). The dystrophin in these revertant fibers consists of internally deleted dystrophin generated by omission of the mutated exon through alternative splicing of dystrophin pre-mRNA, resulting

in restoration of the translational reading frame of *DMD* transcripts (Klein et al., 1992; Lu et al., 2000). A goal of DMD research has been to mimic this natural phenomenon to convert the DMD phenotype to the BMD phenotype by removing one or more exons to create shortened but in-frame dystrophin transcripts generating partially functional dystrophin. This approach was validated using SSOs that blocked pre-mRNA splicing elements, thereby excluding the mutation-containing exon and restoring the reading frame in *DMD* transcripts in cell-free extracts, (Takeshima et al., 1995), human lymphoblastoid cells (Pramono et al., 1996), and primary *mdx* myoblast cultures (Dunckley et al., 1998; Wilton et al., 1999).

The use of SSOs to induce exon-skipping in DMD has been further validated in animal models and clinical trials. The SSO chemistry first used in DMD studies was 2OMe, which was tested in primary myoblasts derived from DMD patients carrying different deletions and a nonsense mutation (Aartsma-Rus et al., 2003; van Deutekom et al., 2001). In *mdx* mice, which carry a nonsense mutation in exon 23 of the *DMD* gene, dystrophin expression was restored by intramuscular (i.m.) injections of 2OMe SSO targeted to the 5′ splice site of intron 23 complexed with cationic liposomes (Mann et al., 2001), or the nonionic block copolymer F127 (Lu et al., 2003). In the latter case, SSO treatment led to functional improvement of the treated muscle. Because all muscles are affected by DMD, it is important to induce dystrophin expression in skeletal, smooth, and cardiac muscles. Intravenous injections of 2OMe complexed with F127 induced dystrophin expression in body-wide skeletal but not cardiac muscle in *mdx* mice without detectable toxicity (Lu et al., 2005).

Significant progress in DMD research was achieved in *mdx* mice i.v. injected with 2 mg uncomplexed PMO SSO at weekly intervals, which led to functional improvement of

tibialis anterior muscles after three injections (Alter et al., 2006). After seven weekly injections, levels of dystrophin expression in gastrocnemius and quadriceps of treated *mdx* mice reached 50% normal expression. Additionally, serum creatinine kinase (CK) levels were dramatically reduced, suggesting improvement of the underlying disease. The potential of PMO SSOs for DMD treatment was further demonstrated in canine X-linked muscular dystrophy (CXMD), a clinically severe canine model of DMD. Systemic infusions of PMO cocktails inducing skipping of exons 6 and 8 restored dystrophin expression in skeletal muscles and ameliorated exercise ability in CXMD canines (Yokota et al., 2008). Other chemistries such as LNA, ethylene brdiged nucleic acid (ENA), PNA have been tested in cell culture and *in vivo* but they do not seem to be particularly useful in treatment of DMD (Aartsma-Rus et al., 2004; Surono et al., 2004; Yin et al., 2008a).

Another major advance in exon skipping in DMD has been application of cell penetrating peptide-conjugated PMOs (PPMOs). These compounds have shown enhanced efficacy in exon 23 removal in *mdx* mice compared to unconjugated PMO. A PPMO carrying $(RXR)_4XB$ peptide, (where R is arginine, X is 6-aminohexanoic acid, and B is β-alanine), induced normal levels of dystrophin expression in diaphragm and low levels in colon, gut and skeletal muscles of *mdx* mice treated as neonates with four weekly i.p injections at 5 mg/kg, a significantly lower dose than that used for unconjugated PMO (Fletcher et al., 2007; Moulton et al., 2007). However, none of the above studies in animal models showed restoration of dystrophin expression in cardiac muscle. Intra-cardiac injections of PMO in *mdx* mice induced only very low level of dystrophin expression (Vitiello et al., 2008). Because cardiomyopathy is one of the major causes of death in DMD patients, induction of dystrophin expression in cardiac muscle is critical for DMD treatment. Jearawiriyapaisarn

and colleagues demonstrated that systemic treatment of *mdx* mice with PPMO-B carrying $(RXRRBR)_2XB$ peptide induced in cardiac muscles high levels of exon 23-skipped mRNA and produced 20–30% of normal dystrophin protein (Jearawiriyapaisarn et al., 2008). This treatment resulted in reduced inflammatory cell infiltration in the heart. Exon 23-skipped mRNA and restored dystrophin protein expression remained detectable for at least 2–3 months after treatment, especially in diaphragm and quadriceps, where 100% exon-skipping was maintained. These data suggested that the PPMO-B/PMO is very stable in muscle tissues because the half-life of dystrophin mRNA is only about 16 hours (Tennyson et al., 1996). The sustained dystrophin expression led to a decrease of serum CK to near wild-type levels, confirming that the rescued dystrophin protein was functional. Further study revealed that treatment with PPMO-B preserved cardiac sarcolemma integrity and prevented cardiac hypertrophy and diastolic dysfunction (Jearawiriyapaisarn et al., 2010). Sustained dystrophin expression induced by PPMO-B SSO would be desirable for clinical application due to the potential for infrequent re-administration.

The pre-clinical results described above have led to three clinical trials for oligonucleotide-induced exon-skipping in DMD patients. PRO051, a 2OMe SSO targeted to an internal sequence of exon 51, was investigated for its ability to induce exon 51 skipping in DMD patients (van Deutekom et al., 2007). In this study, a single local i.m. injection of 0.8 mg PRO051 specifically excluded exon 51 in four DMD patients, thereby restoring the translational reading frame. Dystrophin expression equivalent to approximately 3–12% normal levels was detected in muscle biopsies taken four weeks after injection. However, biopsies from control-treated tissues were not examined making it impossible to determine

the background level of dystrophin expression (i.e. from spontaneous revertant fibers) in each patient.

Clinical trials exploring the efficacy of PMO SSOs for DMD are also underway. AVI-4658, a PMO SSO that induces exon 51 skipping, was tested in a single-blind, placebo-controlled, dose-escalation study in patients with deletions in the open reading frame of DMD that are responsive to exon 51 skipping. Unlike the PRO051 trial, this study compared dystrophin expression in treated muscles with that of saline-injected contralateral muscles, an important negative control that accounts for background dystrophin expression. AVI-4658 administered i.m. resulted in a 26–32% increase in dystrophin expression locally within treated muscles. The level of dystrophin expression is predicted to be sufficient to avoid skeletal muscle symptoms (Neri et al., 2007). AVI-4658 was well-tolerated and there were no significant drug-related serious adverse events.

A trial to evaluate systemic administration of AVI-4658 was recently completed. Patients received one of six doses ranging from 0.5 to 20 mg/kg once weekly for 12 weeks by intravenous infusion. Treatment resulted in substantial dystrophin expression that was related to dose, with patients exhibiting up to 55% dystrophin-positive muscle fibers (www.avibio.com/ and (Kole, 2010)). CD3, CD4 and CD8 counts, markers of inflammation, were reduced, suggesting amelioration of the underlying disease. The drug was well-tolerated and there were no drug-related serious adverse events or severe adverse events. Data from clinical trials indicating safety of PMOs are consistent with the results from a study in cynomolgus monkeys in which AVI-4658 was well-tolerated at the maximum feasible dose (320 mg/kg) (Sazani et al., 2010). Still unanswered questions, regarding SSO

bioavailability, therapeutic index and long term effects, are being addressed in ongoing pre-clinical and clinical studies for DMD.

Summary of the Unique Properties of SSOs

Modification of pre-mRNA splicing as a therapeutic strategy has several important advantages over alternative molecular therapies. Unlike RNase H-sensitive ASOs and siRNA, which are limited to down-regulation of target expression, SSOs down-regulate one transcript and simultaneously up-regulate the expression of a therapeutic splice variant. Importantly, up-regulation of protein expression by SSOs does not alter the DNA in any way; this precludes the potential for off-target gene disruptions caused by virus-mediated therapies. Furthermore, SSOs induce expression of endogenous proteins, reducing the likelihood of stimulating an immune response.

In the TNFR2 application described earlier, LNA SSO was active primarily in hepatocytes, where it induced expression of a soluble secreted decoy receptor that was released into systemic circulation (Graziewicz et al., 2008). Cells that take up the SSO are thus converted into factories that manufacture the therapeutic splice variant. Because synthetic oligonucleotide chemistries such as LNA are resistant to nucleases, SSOs bearing these modifications are functionally active *in vivo* for long periods of time (e.g., 35+ days following five 25 mg/kg i.p. injections). SSOs applied in this way would thus require relatively infrequent dosing.

The magnitude of the effect of splice-switching is largely dependent on the level of expression of the pre-mRNA transcript. For example, Mercatante et al. found that cells expressing higher levels of endogenous Bcl-x were more sensitive to Bcl-x splice-switching than cells expressing lower levels. She concluded that cells expressing higher levels of Bcl-x

generated more Bcl-x pre-mRNA that could be converted into pro-apoptotic Bcl-x_S, rendering them more sensitive to Bcl-x SSO-induced apoptosis (Mercatante et al., 2002). This phenomenon provides a layer of target cell specificity because splice-switching will have the greatest effect in cells expressing the highest levels of target gene expression. Moreover, RNase H-sensitive ASOs and siRNA become less effective as their target gene expression increases. This is due to the fact that, as more target mRNA is expressed, incomplete repression of target gene expression becomes more consequential. In contrast, increased target gene expression enhances the effects of splice-switching strategies.

Apoptosis

Apoptosis is the process of programmed cell death marked by distinct morphological characteristics and biochemical mechanisms, including DNA fragmentation, chromatin condensation, membrane blebbing, cell shrinkage, and disassembly into membrane-enclosed vesicles, called apoptotic bodies, which are subsequently engulfed by macrophages and other cells (Jacobson et al., 1997; Kerr et al., 1972). This program is essential for normal development, maintenance of tissue homeostasis, and immune-system function in multicellular organisms. Dysregulation of apoptotic signaling contributes to numerous pathological conditions, from degenerative disorders to cancer (Cory and Adams, 2002). Indeed, the ability of tumor cells to evade apoptosis is one of the hallmarks of cancer and has been the focus of intense research (Adams and Cory, 2007; Hanahan and Weinberg, 2000).

Caspases

There are two major apoptotic pathways, the extrinsic or death receptor-mediated pathway, and the intrinsic pathway (Figure 1.5). Both pathways converge on the activation of

cystein aspartate proteases called caspases, which function in cell disassembly (effectors) and in initiating this disassembly in response to pro-apoptotic signals (initiators). Caspases are expressed as proenzymes that contain three domains: an NH2-terminal domain, a large subunit (~20 kDa) and a small subunit (~10 kDa) (Zimmermann et al., 2001). Activation involves proteolytic processing between domains, followed by association of the large and small subunits to form a heterodimer. When initiator caspases, such as caspase-8 and -9, are activated by oligomerization, they cleave the precursor forms of effector caspases, such as caspase-3, -6 and -7. Activated effector caspases in turn cleave a specific set of cellular substrates, resulting in the biochemical and morphological changes that characterize the apoptosis phenotype (Thornberry and Lazebnik, 1998). One of the targets of caspase cleavage is Poly (ADP-ribose) polymerase (PARP), an enzyme involved in single strange DNA nick repair (Boulares et al., 1999). The detection of PARP cleavage in cells is indicative of an activated caspase cascade. Caspases cleave their cellular targets following an aspartic acid; recognition of at least four amino acids downstream of the cleavage is also required. The preferred tetrapeptide recognition motif varies among the caspases and explains the diversity of their biological function (Thornberry et al., 1997).

Precisely how the cleavage of cellular substrates causes apoptosis has not been fully elucidated. One role caspases play is the destruction of proteins that protect living cells against apoptosis. In addition, caspases contribute to cell disassembly by cleaving lamina polymers that constitute the rigid structure underlying the nuclear lamina (Takahashi et al., 1996). In addition, they cleave proteins involved in cytoskeleton regulation (Thornberry and Lazebnik, 1998). In many cases, caspases cleave their target such that the substrate protein's regulatory and effector domains are dissociated and thus the function is dysregulated.

Examples include proteins involved in DNA repair, mRNA splicing and DNA replication (Thornberry and Lazebnik, 1998). In some cases, caspase cleavage creates truncated proteins with altered function compared. For example, the anti-apoptotic protein Bcl-2 can be cleaved into a truncated form with pro-apoptotic activity (Cheng et al., 1997).

Extrinsic and Intrinsic Pathways

The extrinsic pathway is mediated by the so-called death receptors, which include members of the TNF receptor family, such as Fas or TNF receptor-1 (TNFR1) (Figure 1.4). Binding of ligands such as FASL and TNF to to FAS and TNFR, respectively, recruits the adapter protein Fas-associated death domain (FADD) to the intracellular domain of the receptors. FADD mediates activation of caspase-8, which leads to the activation of downstream effector caspases (Okada and Mak, 2004).

The intrinsic pathway is triggered by intracellular and extracellular stresses, such as growth factor withdrawal, hypoxia and DNA damage. Signals that are transduced in response to these stresses converge on the mitochondria. A series of biochemical events is induced (see next section) that results in the permeabilization of the outer mitochondrial membrane (OMM) and the release of pro-apoptotic molecules, including Cytochrome C. Cytochrome C binds APAF1 and leads to assembly of a heptameric protein ring called the apoptosome, which can bind pro-caspase-9 and induce its activation through a conformational change. (Figure 1.5) (Wang, 2001). Permeabilization of the OMM is regulated by the Bcl-2 family of proteins, however once cytochrome C is released, the downstream cascade of caspase activation is irreversible.

Bcl-2 Family of Apoptotic Regulators

The Bcl-2 family of apoptotic regulators is divided into three classes, based on sequence homology: the pro-apoptotic Bax-like proteins, the anti-apoptotic Bcl-2 homologs, and the pro-apoptotic BH3-only proteins (Figure 1.6 A).

Bax-like Proteins

The first class in the Bcl-2 family consists of the pro-apoptotic Bax-like proteins, Bax, Bak and Bok (Adams and Cory, 2007). These proteins directly initiate apoptosis by oliomerizing at the mitochondrial membrane, leading to a change in the outer mitochondrial membrane potential. This results in membrane permeabilization and consequent efflux of pro-apoptotic factors, such as cytochrome C.

Bax and Bak contain four Bcl-2 homology (BH) domains BH1, BH2, BH3 and BH4, whereas Bok has BH domains 1-3, but lacks BH4 (Figure 1.6 A). All three Bax-like proteins encode C-terminal hydrophobic regions that enable them to associate with the OMM. Structural analysis indicates that the BH1, -2 and -3 domains form a hydrophobic groove that form a binding pocket for the BH3-domain of other Bcl-2 family proteins. In addition, in its inactive conformation, the C-terminal membrane anchor domain of Bax fits into its own BH1–3 hydrophobic pockets and Bax resides in the cytosol. (Nechushtan et al., 1999).

Bax and Bak may have some redundancy of function, as loss of either gene has little effect in most cells and tissues. However, absence of both genes completely blocks apoptosis in many cell types (Wei et al., 2001b), and results in drastic developmental defects and typically perinatal death (Lindsten et al., 2000). While Bax and Bak are widely expressed, Bok expression is restricted to ovary, testis and uterus; it does not appear to play as crucial a role in apoptotic signaling (Hsu et al., 1997).

In non-apoptotic cells, Bak is associated with the mitochondrial membrane and Bax is present in the cytosol with its C-terminal membrane-anchoring domain sequestered in its own BH1–3 hydrophobic pocket. Apoptotic stimuli prompt a conformational change in Bax causes its translocation to the mitochondria and exposes its C-terminal hydrophoic tail, which enables it to associate with the OMM (Nechushtan et al., 1999). Because Bak is already present at the OMM, it may be keep inactive by interaction with anti-apoptotic Bcl-2 family members (Cuconati et al., 2003).

Anti-apoptotic Proteins

The anti-apoptotic Bcl-2 family members include Bcl-2, Bcl-x_L, Mcl-1_L, Bcl-w and Bfl-1/A1. Bcl-2, Bcl-x_L and Bcl-w each have all four BH domains, Mcl-1_L has BH domains 1, 2 and 3 and Bfl-1/A1 has only BH domains 1 and 2 (Figure 1.5 A). As in the Bax-like proteins, BH domains 1–3 form a hydrophobic binding pocket that serves as a binding site for the BH3 domains of other Bcl-2 family proteins. In addition, Bcl-2, Bcl-x_L, Bcl-w and Mcl-1_L each have a C-terminal hydrophobic domain, which is responsible for membrane localization.

The anti-apoptotic Bcl-2 proteins prevent cells from committing to apoptosis by interacting with and antagonizing Bax and Bak proteins (Adams and Cory, 2007). Bax can form heterodimers via its BH3 domain with all five major anti-apoptotic Bcl-2 homologs, suggesting that all the anti-apoptotic family members participate in Bax regulation. Bak forms heterodimer with Mcl-1_L and Bcl-x_L, however it appears to bind Mcl-1_L with several fold higher affinity than Bcl-x_L (Willis et al., 2005). Bcl-2 does not appear to play a role in regulating Bak (Willis et al., 2005).

Three additional putative anti-apoptotic Bcl-2 family proteins, Bcl-RAMBO, Bcl-B, and Bcl-G, contain multiple BH domains and share high sequence homology with other Bcl-2 family members. However, they are less well studied and as a result their roles in apoptosis have not been elucidated (Youle and Strasser, 2008).

BH3-only Proteins

The third class of the Bcl-2 family is comprised of the BH3-only proteins and includes Bad, Bid, Bim, Bmf, Bik, Hrk, Noxa and Puma. As their name suggests, these proteins each contain a BH3 domain, but they are otherwise largley unrelated in sequence to either Bcl-2 or each other (Willis and Adams, 2005) (Figure 1.5 A). The BH3 domain is required for their pro-apoptotic activity and is involved in binding pro-survival Bcl-2 family members at the OMM (Chang et al., 1999; Petros et al., 2004).

The BH3-only proteins promote apoptosis upon activation by pro-apoptotic signals. Puma and Noxa are transcriptionally up-regulated in a p53-dependent manner in response to DNA damage (Nakano and Vousden, 2001; Oda et al., 2000). Noxa is also transcriptionally activated by c-MYC in response to proteasome inhibition (Nikiforov et al., 2007). Bim expression is activated by the transcription factors FOXO3A and CEBPα in response to growth factor deprivation (Dijkers et al., 2000) and endoplasmic reticulum stress (Puthalakath et al., 2007), respectively. Bad is dephosphorylated in response to growth factor deprivation, causing its release from 14-3-3 proteins and translocation to the mitochondria (Zha et al., 1996). Two splice variants of Bim, BimEL and BimL, are sequestered in inactive conformations at the microtubules-associated dynein complex in healthy cells. Likewise, Bmf is sequestered to myosin V motors by association with dynein light chain 2. Apoptotic stimuli such as serum withdrawal or anoikis prompt the translocation of BimEL, BimL and

Bmf to the mitochondria. Bid normally exists in the cytosol in its full-length inactive form. Death receptor activation activates caspase-8, which then cleaves Bid into its truncated, active form, tBid, which translocates to the mitochondria (Li et al., 1998). Bid thus provides a means for crosstalk between the death receptor-mediated and mitochondrial death pathways.

The BH3-only proteins exhibit widely varying binding affinities for the anti-apoptotic Bcl-2 proteins (Chen et al., 2005). For example, PUMA binds Bcl-2, Bcl-x_L, Mcl-1_L and Bcl-w with high affinity, whereas NOXA binds only Mcl-1_L with high affinity (Adams and Cory, 2007). Likewise, the anti-apoptotic Bcl-2 homologs bind Bax and Bak with different affinities. Both Bim and tBid appear to have affinity for Bcl-2 (Opferman et al., 2005).

Indirect Activation of Apoptosis by BH3-only Proteins

Activation of BH3-only proteins does not trigger apoptosis in cells lacking Bak and Bax, indicating that they act upstream of Bax and Bak (Cheng et al., 2001). Apoptotic stimuli trigger conformational changes in Bax and Bak and prompt their localization to and oligomerization at the OMM. At the OMM, however, Bax and Bak are bound by the anti-apoptotic Bcl-2 homologs, sequestering them and preventing oligomerization. A preponderance of evidence indicates that activated BH3-only proteins induce apoptosis by competing with Bax/Bak for binding with the anti-apoptotic Bcl-2 homologs, thereby displacing Bax/Bak and freeing them to oligomerize at the OMM (Figure 1.5 B)(Chen et al., 2005; Lacerra et al., 2000; Willis et al., 2005; Willis et al., 2007). In this model, BH3-only proteins act as damage sensors that indirectly trigger apoptosis by directly antagonizing the anti-apoptotic Bcl-2 proteins (Adams and Cory, 2007).There is some evidence that certain BH3-only proteins can directly activate apoptosis, as Bim and tBid have been shown to

synergize with Bax in cell-free membrane permeabilization assays (Lacerra et al., 2000). However, this concept has been called into question by the inability to definitively show direct interactions between Bid, tBid or Bim with Bax or Bak, and by the observation that apoptosis is not abrogated in *Bim/Bid* double knock mice (Willis et al., 2007).

Bcl-2 Family in Cancer

The balance of BH3-only and anti-apoptotic Bcl-2 proteins determines whether the cell will commit to apoptosis. Up-regulation of the anti-apoptotic Bcl-2 homologs, enables them to overcome antagonism by BH3-only proteins, inhibiting apoptosis. Consequently, overexpression of an anti-apoptotic family member, or loss of a pro-apoptotic relative can be oncogenic. Because many chemotherapeutic drugs induce apoptosis through activation of BH3-only proteins, the overexpression of Bcl-2 anti-apoptotic proteins promotes chemoresistance (Huang and Strasser, 2000). A screen of somatic copy-number profiles from 3,131 cancers across more than two dozen cancer types found that the *bcl-x* and *mcl-1* genes were amplified with significant frequency suggesting that up-regulation expression of these genes may be a common mechanism for cancers to increase survival (Beroukhim et al., 2010).

Due to their roles in cancer progression and chemoresistance, the anti-apoptotic Bcl-2 homologs are the targets of numerous inhibitors in clinical development (Storey, 2008). For example, the small molecule ABT-737 binds Bcl-2, Bcl-x_L and Bcl-w proteins with nanomolar affinity. It induced apoptosis in lymphoma and small-cell lung carcinoma cells in culture, and caused tumor regression and improved survival in preclinical studies (Oltersdorf et al., 2005). An orally bioavailability analog of ABT-737, ABT-263, is currently in Phase I/II clinical trials to evaluate its single agent efficacy for refractory chronic lymphocytic

leukemia, refractory lymphoid malignancies, and advanced small cell lung cancer (www.clinicaltrials.gov). Another small molecule, GX015-070, binds Mcl-1 with high affinity. This agent induced apoptosis in multiple myeloma cells (Trudel et al., 2007) and showed antitumor activity in mouse tumor xenografts derived from colon, prostate and cervical cancer cells (Nguyen et al., 2007). GX015-070 is currently being evaluated combination therapy in Phase II clinical trials for refractory multiple myeloma and refractory and advanced-stage small cell lung cancer (www.clinicaltrials.gov). Clearly, pharmacological agents that promote apoptosis by affecting the Bcl-2 family hold promise as potential anti-cancer therapeutics.

Bcl-x

The *Bcl-x* gene contains three exons, the first of which is untranslated. Its pre-mRNA transcript undergoes alternative splicing at the 5′ splice site of exon 2 to produce protein isoforms with opposing functions, Bcl-x_L (long) and Bcl-x_S (short). A third isoform, Bcl-xβ, results from an unspliced transcript (Ban et al., 1998; Gonzalez-Garcia et al., 1994). *Bcl-x* is widely expressed in human and mouse (Gonzalez-Garcia et al., 1995; Gonzalez-Garcia et al., 1994; Krajewski et al., 1994). Bcl-x_L is widely expressed, particularly in tissues containing long-lived post-mitotic cells such as adult brain. Bcl-xβ has not been well-studied, however one study in mouse suggested that its patter of expression is similar to that of Bcl-x_L, albeit at lower levels (Gonzalez-Garcia et al., 1995). In neurons, Bcl-xβ protected cells against apoptosis (Gonzalez-Garcia et al., 1995), while rat Bcl-xβ promoted apoptosis in promyeloid cells (Shiraiwa et al., 1996). Bcl-x_S is expressed in cells that undergo high rate of turnover, such as developing lymphocytes (Boise et al., 1993).

Splicing at the downstream (Bcl-x_L) alternative splice produces the major isoform, Bcl-x_L (Boise et al., 1993). Bcl-x_L is a anti-apoptotic Bcl-2 homolog that contains all four BH domains (BH1-BH4) and a C-terminal hydrophobic region responsible for localization to the OMM. It promotes cell survival by binding and sequestering Bak and Bax with high affinity. Bcl-x_L expression also induces the proangiogenic interleukin-8 (IL-8) and chemokine (C-X-C motif) ligand 1 (CXCL1) *in vitro* and *in vivo* (Giorgini et al., 2007; Karl et al., 2007). Increased expression of Bcl-x_L enables tumor cells to evade apoptosis and promotes resistance to a broad range of chemotherapeutic agents (Amundson et al., 2000). Not surprisingly, Bcl-x_L overexpression has been detected in multiple myeloma (Tu et al., 1998), small cell lung carcinoma (Reeve et al., 1996), breast cancer (Olopade et al., 1997), prostate cancer (Castilla et al., 2006; Mercatante et al., 2002), metastatic melanoma (Tang et al., 1998), hepatocellular carcinoma (HCC) (Takehara et al., 2001; Watanabe et al., 2002), and colorectal cancer (Backus et al., 2002). Downregulation of Bcl-x_L using 2OMe gapmer ASOs sensitized colon cancer cells to ionizing radiation (Wacheck et al., 2003). Likewise, Bcl-x ASOs triggered apoptosis in HCC cells (Takehara et al., 2001).

Use of the upstream (Bcl-x_S) 5′ alternative splice site of Bcl-x exon 2 produces Bcl-x_S (Boise et al., 1993). Bcl-x_S lacks 189 bases from the C-terminal end of exon 2, though the reading frame is maintained; as a result Bcl-x_S encodes only the BH3 domain. Exogenous expression of Bcl-x_S was found to inhibit the ability of Bcl-2 and Bcl-x_L to protect cells from apoptotic stimuli (Boise et al., 1993; Minn et al., 1996) in a BH3 domain-dependent manner (Chang et al., 1999). Bcl-x_S was also found to directly bind Bcl-x_L and Bcl-2 (Minn et al., 1996; Sato et al., 1994). Thus, Bcl-x_S is thought to act as a pro-apoptotic BH3-only protein, indirectly inducing apoptosis through antagonism of Bcl-x_L and Bcl-2 (Willis et al., 2007).

Conditional expression of Bcl-x_S under the control of a Tetracycline-inducible promoter reduced the growth of human melanoma tumor xenografts (Hossini et al., 2003).

Regulation of Bcl-x Alternative Splicing

Several studies have been published describing regulation of Bcl-x alternative splicing (summarized in Figure 1.7). F and H hnRNP proteins were found to bind 10–30 nucleotides downstream of the Bcl-x_S alternative splice site. Addition of these proteins to HeLa cell extract stimulated Bcl-x_S expression and their abolition by siRNA reduced Bcl-x_S expression in cells in culture (Garneau et al., 2005).

The lipid molecule ceramide, a regulator of various stress responses and growth mechanisms, was found to direct Bcl-x splicing from Bcl-x_L to -x_S in a protein phosphatase 1 (PPN1)-dependent manner (Chalfant et al., 2002). The chemotherapeutic nucleoside analog gemcitabine shifted splicing from Bcl-x_L to -x_S splicing via induction of ceramide lipid synthesis in A549 lung cancer cells. This activity involves the splicing factor SAP155, which binds a ceramide-responsive *cis*-element, CRCE1, upstream of the Bcl-x_S splice site (Massiello et al., 2006).

The RNA-binding protein Sam68 has also been implicated in the regulation of Bcl-x alternative splicing. Depletion of Sam68 led to the accumulation of Bcl-x_L whereas Sam68 upregulation led to increased expression of Bcl-x_S (Paronetto et al., 2007). Tyrosine phosphorylation of Sam68 by the Fyn kinase, a Src-like tyrosine kinase, inverted this effect and favored usage of the Bcl-x_L splice site. Overexpression of the splicing factor SF2/ASF blocked Bcl-x_S expression by Sam68. In addition to Bcl-x, Sam68 was found to bind endogenous mRNAs of Bak, Bax, and Bim.

The transcription factor E2F1 plays a key role during S phase progression and apoptosis. Among the transcriptional targets of E2F1 is *sc35*, a component of the spliceosome. Expression of E2F1 under the control of an inducible promoter activated the Bcl-x_S splice site in an SC35-dependent manner (Merdzhanova et al., 2008). This effect was recapitulated in cells treated with DNA damaging agents, which induced E2F1 transactivation of *sc35* and a shift in Bcl-x alternative splicing from Bcl-x_L to -x_S.

The splicing factor RBM25 was found to activate the Bcl-x_S splice site binding an ESE (CGGGCA) situated 64–69 nucleotides upstream of the Bcl-x_S splice site and associating with hLuc7A, a U1 snRNP-associated factor (Zhou et al., 2008). RBM25 thereby facilitates recruitment of U1 snRNP to and subsequent spliceosome assembly at the weaker Bcl-x_S splice site.

In addition to the regulators of Bcl-x alternative splicing enumerated above, there are likely many more that remain to be identified. Control of Bcl-x alternative splicing is thus complex, with multiple exonic and intronic control elements that allow Bcl-x splicing to respond differently to a variety of signals in distinct cellular contexts.

Direction of Bcl-x Alternative Splicing with SSOs

Previously, our lab applied SSOs to switch the pattern of Bcl-x pre-mRNA splicing from anti-apoptotic Bcl-x_L to pro-apoptotic Bcl-x_S. Mercatante et al. used 2OMe SSOs targeted to the Bcl-x_L splice site and demonstrated that this resulted in a dose-dependent and sequence-specific manner that induced apoptosis in PC-3 and Mcf-7 cells (Mercatante et al., 2001). Importantly, modulation of splicing was more effective at inducing apoptosis than antisense-mediated down-regulation of Bcl-x_L. Bcl-x splice-switching also sensitized cells to treatment with γ-irradiation and chemotherapeutic drugs, including etoposide, 5-fluorouracil,

cisplatin, 5-fluorodeoxyuridine and doxorubicin. Subsequent study revealed that sensitivity to SSO-induced apoptosis correlated with the level of endogenous Bcl-x_L expression (Mercatante et al., 2002), presumably due to the cell's dependence on the anti-apoptotic activity of Bcl-x_L for survival. Moreover, higher Bcl-x_L expression also provides more pre-mRNA that can be converted into pro-apoptotic Bcl-x_S, which antagonizes both Bcl-x_L and Bcl-2. Thus, cancers with high Bcl-x_L expression, and those that depend on Bcl-x_L expression for survival, represent good candidates for treatment with SSOs targeting Bcl-x (Mercatante et al., 2002).

Another group used MOE SSOs to modify Bcl-x splicing in A549 lung cancer cells, sensitizing them ultraviolet B radiation and cisplatin (Taylor et al., 1999). Wilusz et al. targeted Bcl-x for splice-switching using a chimeric PNA oligonucleotide conjugated to a polypeptide containing eight Ser-Arg repeats (Wilusz et al., 2005). This compound shifted Bcl-x splicing and induced apoptosis in HeLa cells, recapitulating the findings of Mercatante and colleagues.

Based on the *in vitro* studies described above, modification of Bcl-x splicing holds promise as an anti-cancer strategy; however, the effects of Bcl-x splice-switching has yet to be evaluated in a more realistic *in vivo* setting. The *in vivo* effect of Bcl-x splice-switching was addressed in Specific Aim 1 of this dissertation.

Mcl-1

Mcl-1 is an immediate-response gene that is widely expressed in human tissues and is required for survival of hematopoietic stem cells (Opferman et al., 2005) and myeloid cells (Edwards et al., 2004). *Mcl-1* expression is rapidly induced in response to signals for cell differentiation, including granulocyte-macrophage colony-stimulating factor, stem cell factor

and interleukin (IL)-3, IL-5, IL-6, IL-7 and IL-15 in various cell types (Warr and Shore, 2008; Wei et al., 2001a). Expression is also induced in response to certain cytotoxic agents, including colchicine and vinblastine (Yang et al., 1996). Mcl-1 mRNA is rapidly turned over, with a half-life between 30 min and a few hours depending on the cell type and culture conditions (Nijhawan et al., 2003; Yang et al., 1996).

Mcl-1 pre-mRNA consists of three exons which are alternatively spliced to produce a longer isoform, Mcl-1_L, encoding all three exons, and a short form, Mcl-1_S, encoding only exons 1 and 2 (Bae et al., 2000; Bingle et al., 2000). Mcl-1_L is the predominant isoform while Mcl-1_S expression is absent or very low in healthy adult cells (Bae et al., 2000; Bingle et al., 2000; Legartova et al., 2009). The first 229 amino acids are identical in Mcl-1_L and -1_S; however, due to skipping of exon 2, Mcl-1_S contains a novel 42-amino acid C-terminus. Both proteins encode PEST domains (sequences rich in proline, glutamic acid, serine and threonine) near the N-terminus, which are associated with high-turnover proteins (Bae et al., 2000; Bingle et al., 2000). As described earlier, Mcl-1_L encodes BH domain 1−3, which form a hydrophobic pocket that serves as a binding site for the BH3 domain of other Bcl-2 family members. Pro-apoptotic Bak binds at this site via its BH3 domain, inhibiting Bak-mediated apoptosis (Willis et al., 2005; Zhai et al., 2008). The rapid up-regulation of *Mcl-1* gene and Mcl-1_L protein expression in response to cytokines, coupled with its rapid turnover suggest that Mcl-1_L provides short-term protection against cell death during critical transitions in cell fate (Craig, 2002).

Certain apoptotic stimuli, such as DNA damage by etoposide or UV irradiation, prompt Mcl-1_L ubquitination by Mule/Arf-BP1 E3 ligase and subsequent proteasomal degradation (Zhong et al., 2005). Elimination of Mcl-1_L, by decreased transcription or

proteasomal degradation, is an early and required step for apoptosis induced by DNA damaging agents, including UV irradiation, cisplatin and etoposide (Nijhawan et al., 2003). The deubiquitinase USP9X stabilizes Mcl-1_L and promotes tumor survival (Schwickart et al., 2010).

In a manner similar to Bcl-x_L, overexpression of Mcl-1_L enables tumor cells to resist apoptosis and has been reported in a number of malignancies, including multiple myeloma (Zhang et al., 2002), acute myeloid leukemia (Konopleva et al., 2006), melanoma (Boisvert-Adamo et al., 2009), cervical cancer (Wei et al., 2001a) and poor-prognosis breast cancer (Ding et al., 2007). Amplification of the *Mcl-1* gene was found to be significantly enriched in a broad range of cancers, suggesting a general role for its predominant splice variant, Mcl-1_L, in cancer pathogenesis. Cancer cell lines insensitive to ABT-737, a small molecule inhibitor of Bcl-2, Bcl-x_L and Bcl-w, were found to express high levels of Mcl-1_L (Tahir et al., 2007). Down-regulation of Mcl-1_L was required to sensitize resistant cells to ABT-737 (Chen et al., 2007; Tahir et al., 2007; van Delft et al., 2006). Chronic treatment of SCLC cells with ABT-737 led to a progressive decrease in Bcl-2 and Noxa levels, and a concomitant increase in Mcl-1_L levels (Tahir et al., 2007). Knock-down of Mcl-1 deubiquitinase USP9X increases Mcl-1 polyubiquitination, which enhances Mcl-1 turnover and sensitivity to ABT-737. Taken together, these findings indicate an important role for Mcl-1_L in the development and chemoresistance of a broad range of cancers. Importantly, Mcl-1_L appears to at least partially compensate for loss of other anti-apoptotic Bcl-2 proteins.

Because skipping of exon 2 causes a shift in the reading frame, Mcl-1_S encodes only the BH3 domain and thus resembles a BH3-only protein. Mcl-1_S was found to bind Mcl-1_L in a yeast two-hybrid assay and its overexpression induced apoptosis in CHO cells (Bae et al.,

2000; Bingle et al., 2000). Mcl-1_L was found to completely counteract Mcl-1_S-induced apoptosis in CHO cells, while Bcl-x_L and Bcl-w could only partially counteract this effect (Bae et al., 2000). Little is known about the regulation of Mcl-1_S, but it may play a role during developmental stages or in high turnover cell types. For example, it was up-regulated under hypoxic conditions in placental cells (Soleymanlou et al., 2007).

In summary, Mcl-1 pre-mRNA undergoes alternative splicing to produce splice variants with opposing functions in the regulation of apoptosis. A shift in Mcl-1 pre-mRNA splicing from Mcl-1_L to -1_S would be expected to induce apoptosis and/or render tumor cells more sensitive to chemotherapeutics. Mcl-1 thus constitutes an ideal target for SSOs.

Dissertation Specific Aims

Specific Aim 1: Experiments in Aim 1 were designed to test the hypothesis that redirection of Bcl-x pre-mRNA splicing from Bcl-x_L to -x_S could elicit pro-apoptotic effects in melanoma cells and tumor xenografts. Experimental results support this hypothesis and are discussed in chapter 2.

Specific Aim 2: Experiments in specific aim 2 were designed to test the hypothesis that the alternative splicing pattern of Mcl-1 pre-mRNA can be shifted using SSOs targeted to the 5′ or 3′ splice site of alternatively spliced exon 2. Additional experiments in aim 2 were designed to test the hypothesis that redirection of Mcl-1 pre-mRNA splicing induces apoptosis and/or sensitizes cells to chemotherapeutic agents. Experimental results that support these aims are discussed in chapter 3.

Results of both aims are briefly summarized in chapter 4 and future studies are proposed. Progress in the development oligonucleotide therapeutics is also discussed.

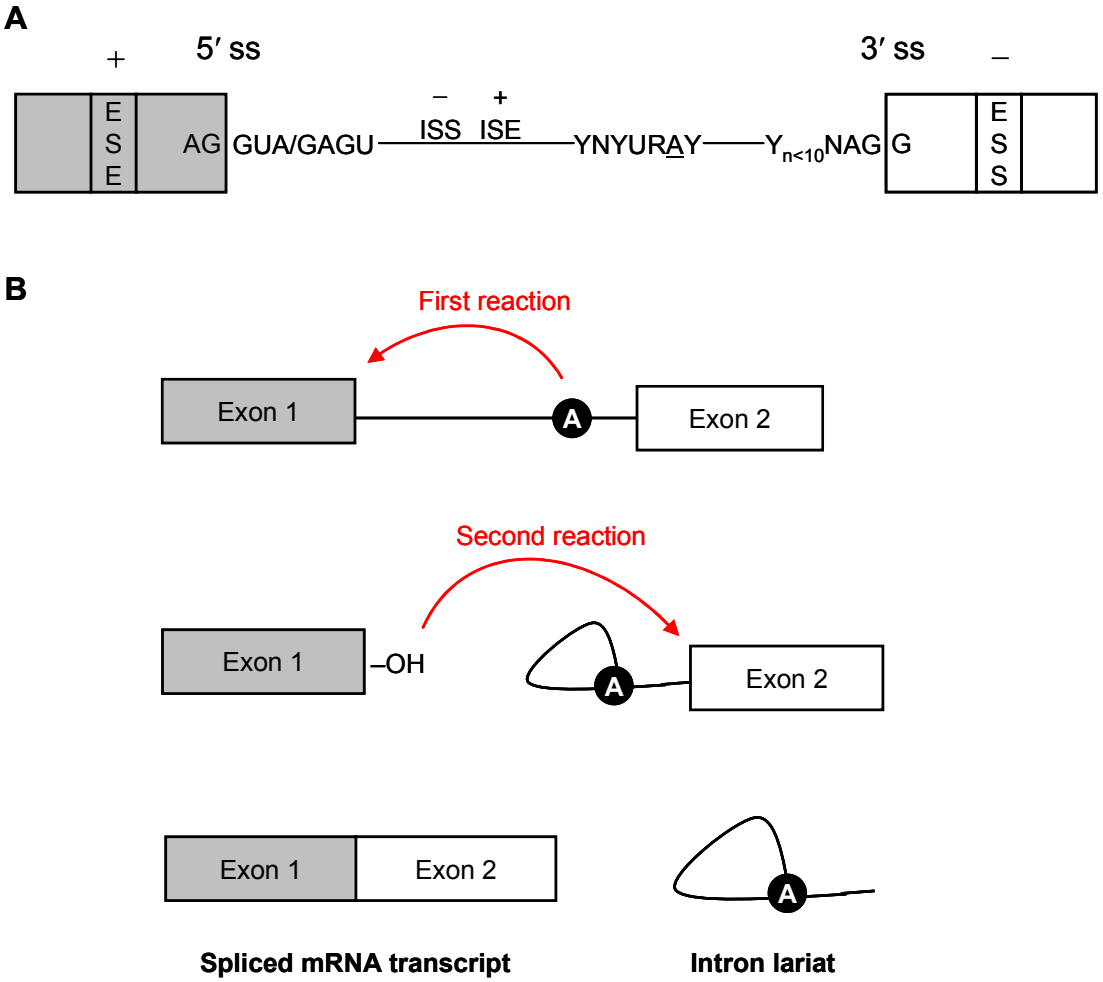

Figure 0.1 Schematic representation of pre-mRNA splicing.
(A) Schematic exon-intron-exon structure. The conserved pre-mRNA sequences involved in splicing are shown, including the 5′ splice site (ss), branch point, polypyrimidine tract ($Y_{n<10}$), and 3′ splice site and splicing regulatory elements (ESE, ISS, ISE and ESS). Y denotes either pyrimidine base, R denotes either purine base, N denotes any base. (B) Pre-mRNA splicing proceeds via two consecutive transesterification reactions. The first transesterification reaction is triggered by the 2′-OH of the branch point A. This group acts as a nucleophile to attack the phosphoryl group of the conserved G in the 5′ splice site. As a consequence, the phosphodiester bond between the sugar and the phosphate at the junction between the intron and the exon is cleaved and the freed 5′ end of the intron is joined to the A within the branch site. Thus, in addition to the 5′ and 3′ backbone linkages, a third phosphodiester extends from the 2′-OH of the A to create a three-way junction. The 5′ exon is a leaving group in the first reaction. In the second reaction, the newly liberated 3′-OH of the 5′ exon reverses its role and becomes a nucleophile that attacks the phosphoryl group at the 3′ splice site. This reaction joins the two exons and releases the intron as a lariat.

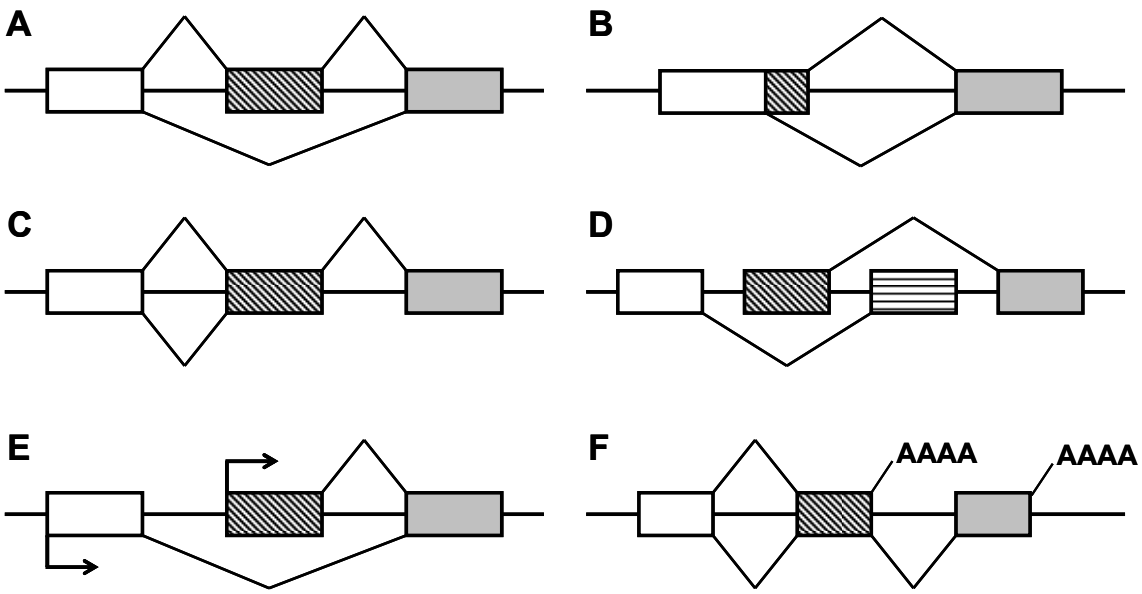

Figure 0.2 Examples of patterns of alternative splicing.
(A) Exon skipping. (B) Alternative 5' splice site. (C) Intron retention. (D) Mutually exclusive exons. (E) Alternative start sites. (F) Alternative polyadenylation sites.

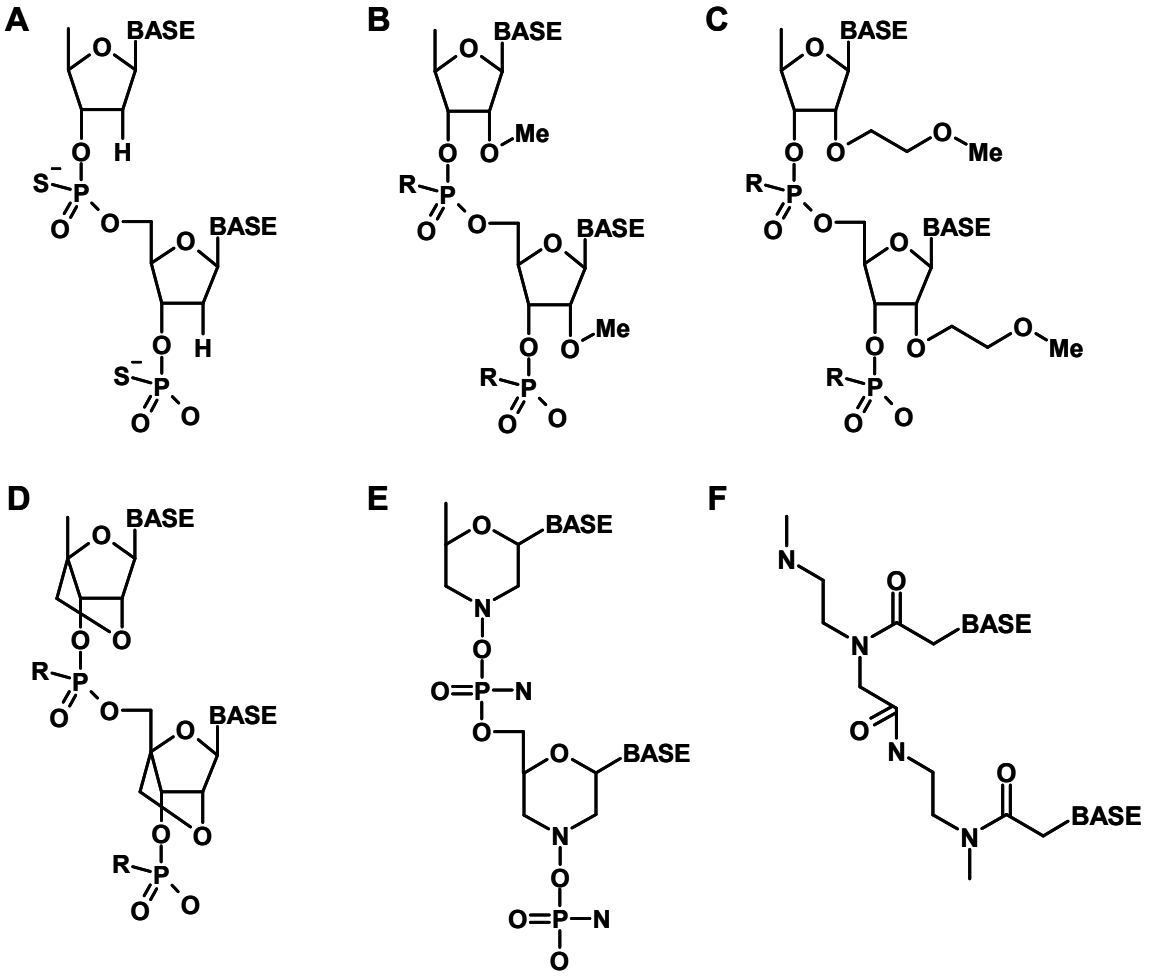

Figure 0.3 Synthetic oligonucleotide chemistries useful for splice-switching applications. R denotes H or S (for phosphorothioate). (A) DNA phosphorothioate. Phosphorothioate (PS) internucleotide linkages greatly increase resistance to nuclease degradation, rendering PS oligonucleotides stable in plasma, tissues and cells. The PS modification can be used in combination with 2′-modifcations; however PS alone does not confer RNAse H resistance. (B) 2′-O-methyl (OMe) oligoribonucleotide. (C) 2′-O-methoxyethyl (MOE) oligoribonucleotide. The 2OMe and MOE 2'-modifications confer increased binding affinity and enhance nuclease resistance, including RNAse H non-competence. (D) Locked nucleic acid (LNA). The LNA modification confers dramatically increased binding affinity and improved nuclease resistance, including RNAse H non-competence. (E) Phosphorodiamidate morpholino (PMO). The PMO backbone modification confers nuclease resistance, including RNAse H non-competence; however, PMO oligonucleotides are neutral and thus have difficulty crossing cell membranes unaided. (F) Peptide nucleic acid (PNA). The PNA modification confers increased binding affinity and nuclease resistance, including RNAse H non-competence. Like PMO, PNA oligonucleotides are neutral and thus have difficulty crossing cell membranes.

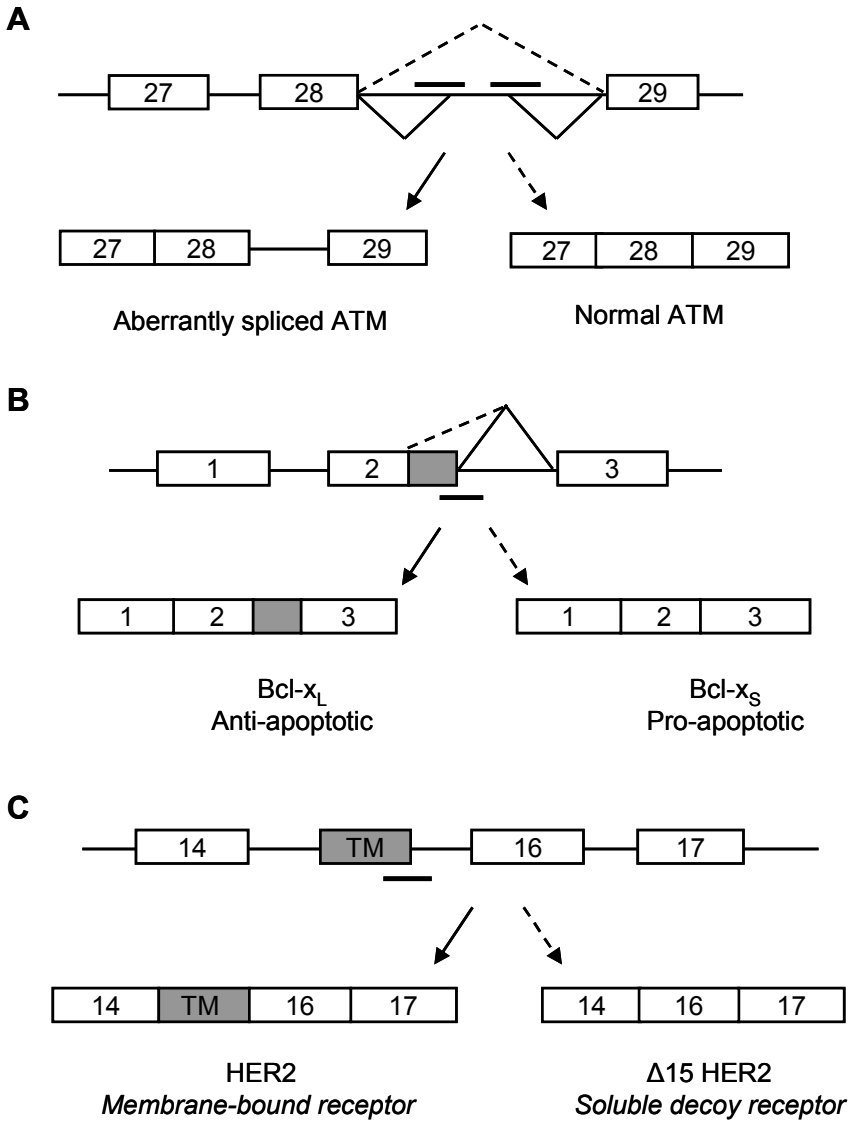

Figure 0.4 Applications of splice-switching oligonucleotides (SSOs)
SSOs can be applied to correct aberrant splicing, to modify alternative splicing to up-regulate an existing splice variant, or two modify pre-mRNA splicing to induce expression of a novel splice variant. (A) Correction of aberrant splicing of ATM gene transcripts leads to production of functional ATM protein (Du et al., 2007). (B) Manipulation of Bcl-x alternative splicing switches production from anti-apoptotic Bcl-x_L to pro-apoptotic Bcl-x_S. See text for details (Mercatante et al., 2001). (C) Production of a novel splice variant, Δ15HER2, which is a soluble decoy receptor (Wan et al., 2008).

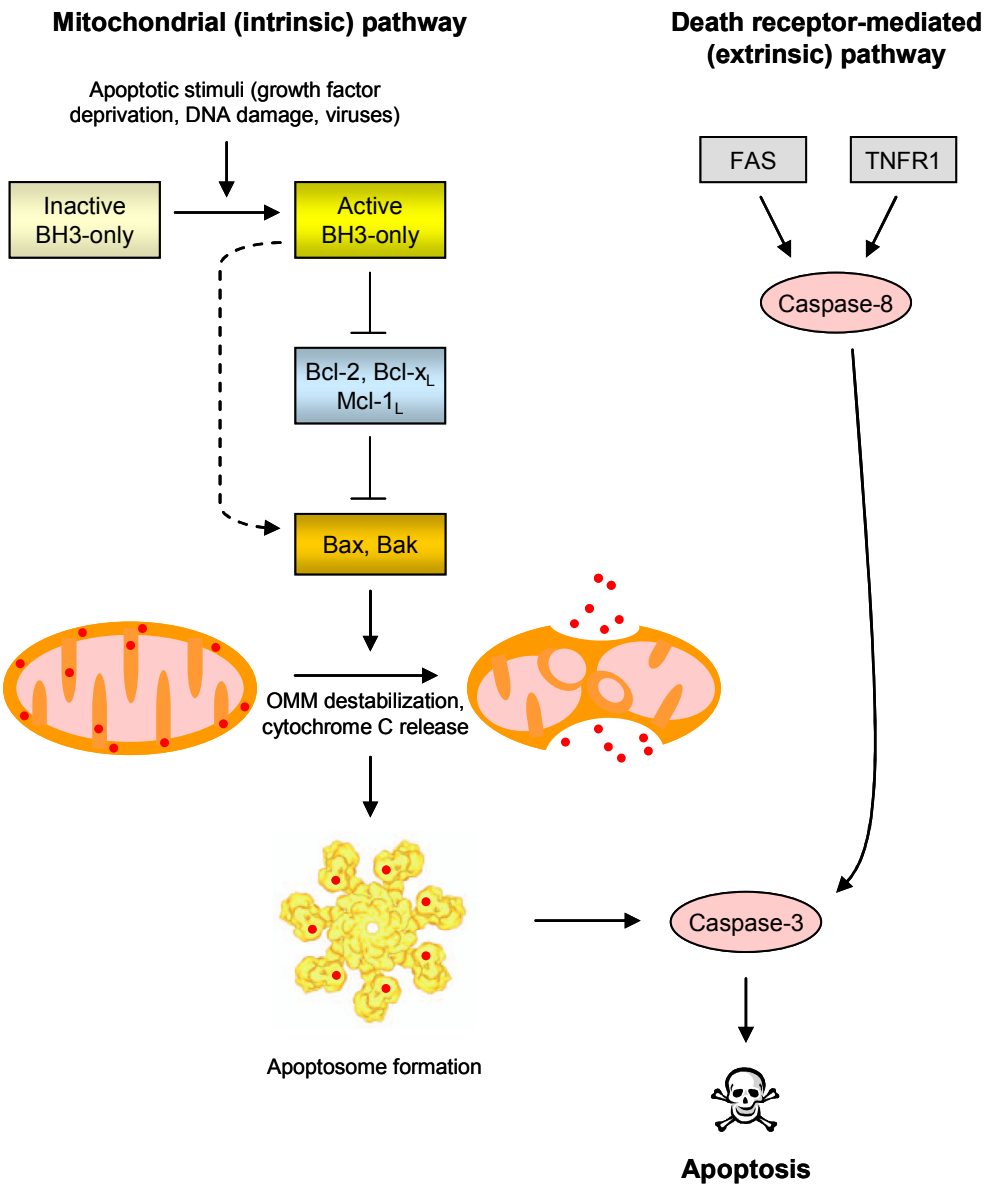

Figure 0.5 Scheme depicting mitochondrial (intrinsic) and death receptor-mediated (extrinsic) pathways of apoptosis.
Apoptosis can be induced by various genotoxic agents, metabolic insults or transcriptional cues (mitochondrial pathway) or by cell surface receptors, such as Fas and TNFR2 (death receptor-mediated pathway). The mitochondrial pathways is initiated when apoptotic stimuli activate BH3-only members of the Bcl-2 family, which indirectly induce apoptosis through antagonism of anti-apoptotic Bcl-2 proteins. See text for details.

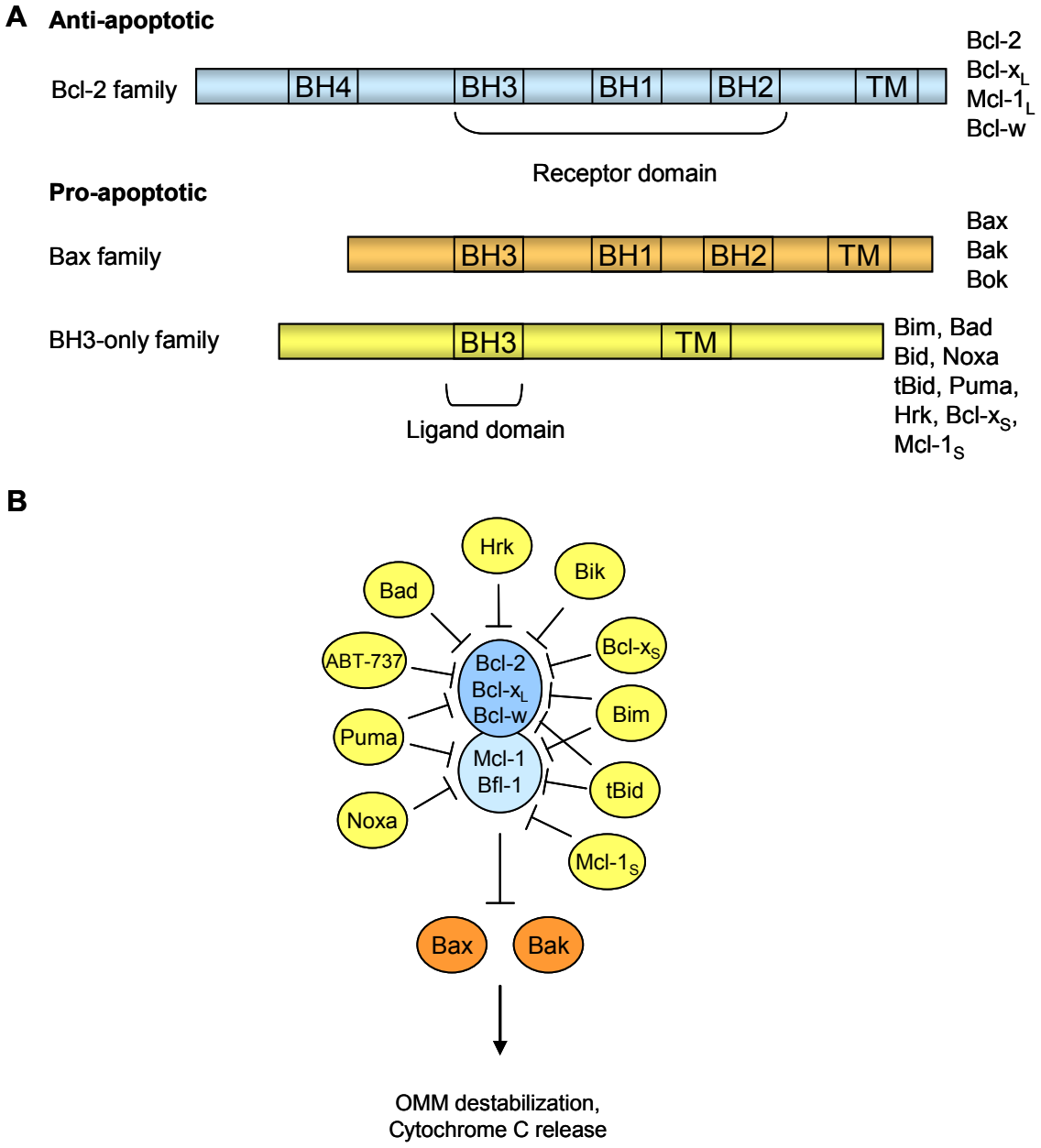

Figure 0.6 Regulation of apoptosis by Bcl-2 family proteins.
The Bcl-2 family regulates apoptosis via the mitochondrial pathway. (A) The Bcl-2 family is comprised of three subfamilies. The anti-apoptotic Bcl-2 homologs encode multiple basic helix (BH) domains. The pro-apoptotic Bax-like proteins contain BH domains 1-3. Finally, the pro-apoptotic BH-3 only proteins encode only the BH3 domain. (B) Upon activation by apoptotic stimuli, Bax and Bak proteins oligomerize at the outer mitochondrial membrane (OMM), causing membrane destabilization and efflux of pro-apoptotic factors such as cytochrome C. The anti-apoptotic Bcl-2 homologs block apoptosis by binding and antagonizing Bax and Bak. Apoptotic stimuli activate BH3-only protein, which indirectly induce apoptosis by binding and antagonizing the anti-apoptotic Bcl-2 homologs.

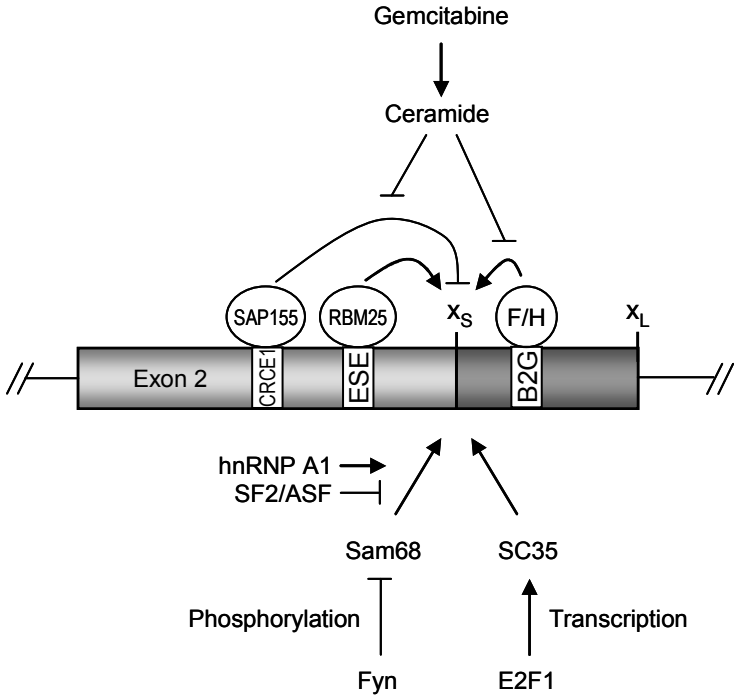

Figure 0.7 Regulation of Bcl-x alternative splicing.
Splicing at the downstream or upstream 5′ alternative splice site of exon 2 produces Bcl-x_L or Bcl-x_S, respectively. The RNA-binding protein SAP155 binds the CRCE1 element and inhibits splicing at the Bcl-x_S splice site. Gemcitabine-induced ceramide indirectly activates Bcl-x_S splicing by repressing SAP155. RBM25 and hnRNP F/H proteins bind exonic splicing enhancer elements and activate the Bcl-x_S splicing. The RNA-binding protein Sam65 activates Bcl-x_S splicing. This activity is inhibited by SF2/ASF and phosphorylation by Fyn kinase; it is induced by hnRNP A1. Bcl-x_S splicing is also activated by SC35, under transcriptional regulation of E2F1.

Chapter 2 – Modification of splicing and anti-tumor effects of Bcl-x splice-switching oligonucleotides *in vivo*

Abstract

Alternative splicing has emerged as an important target for molecular therapies. Splice-switching oligonucleotides (SSOs) modulate alternative splicing by hybridizing to pre-mRNA sequences involved in splicing and blocking access to the transcript by splicing factors. Recently, the efficacy of SSOs has been established in various animal disease models; however, the application of SSOs against cancer targets has been hindered by poor *in vivo* delivery of antisense therapeutics to tumor cells. The apoptotic regulator Bcl-x is alternatively spliced to express anti-apoptotic Bcl-x_L and pro-apoptotic Bcl-x_S. Bcl-x_L is up-regulated in many cancers and is associated with chemoresistance, distinguishing it as an important target for cancer therapy. Out lab previously showed that redirection of Bcl-x pre-mRNA splicing from Bcl-x_L to -x_S induced apoptosis in breast and prostate cancer cells. In this study, the effect of SSO-induced Bcl-x splice-switching on metastatic melanoma was assessed in cell culture and B16F10 tumor xenografts. SSOs were delivered *in vivo* using lipid nanoparticles. Administration of nanoparticle with Bcl-x SSO resulted in modification of Bcl-x pre-mRNA splicing in lung metastases and reduced tumor load, while nanoparticle alone or formulated with a control SSO had no effect. Our findings demonstrate *in vivo* anti-tumor activity of SSOs that modulate Bcl-x pre-mRNA splicing.

Introduction

Over 90% of multi-exon pre-mRNA transcripts undergo alternative splicing (Wang et al., 2008) and up to one-half of disease-causing mutations affect splicing (Lopez-Bigas et al., 2005). Thus, in addition to its significant contribution to proteome diversity, alternative splicing constitutes an important therapeutic target (Cooper et al., 2009). Slice-switching oligonucleotides (SSOs) modulate alternative splicing by hybridizing to pre-mRNA sequences involved in splicing and blocking access by various splicing factors (Dominski and Kole, 1993; Sierakowska et al., 1996). Unlike siRNA and traditional antisense approaches, which lead to RNA degradation by RISC and RNase H-mediated cleavage, respectively, direction of pre-mRNA splicing requires that the SSO-targeted RNA is not degraded. This is achieved by altering the oligonucleotide sugar-phosphate backbone as in, for example, the 2′-O-methoxyethyl (MOE) ribose modification (Sazani et al., 2003; Sazani et al., 2001). In order to realize their full therapeutic utility, SSOs must be efficiently delivered to the pharmacological site of action *in vivo* (Juliano et al., 2009b). This can be achieved by exploiting the inherent pharmacodynamic properties of the SSO chemistry (Graziewicz et al., 2008; Sazani et al., 2002), conjugation of cell penetrating peptides (Jearawiriyapaisarn et al., 2008; Svasti et al., 2009; Wu et al., 2008), and the use of nanoparticle carriers (Rimessi et al., 2009). As a result, *in vivo* efficacy has been established for SSOs in animal models of inflammatory disease, β-thalassemia, and Duchenne muscular dystrophy (DMD) [For a recent review, see (Bauman et al., 2009)], and early phase clinical trials using SSOs to treat DMD have yielded promising results (Kinali et al., 2009; van Deutekom et al., 2007).

Previously, this laboratory and others applied SSOs to manipulate the splicing pattern of the apoptotic regulator Bcl-x. Through alternative splicing, the Bcl-x gene yields two major protein isoforms with opposing functions, anti-apoptotic Bcl-x_L and pro-apoptotic Bcl-x_S (Boise et al., 1993) (Figure 1A). Bcl-x_L is up-regulated in a number of cancers and confers resistance to a broad range of chemotherapeutic drugs (Amundson et al., 2000). Bcl-x_S antagonizes the anti-apoptotic activity of Bcl-x_L and another anti-apoptotic protein, Bcl-2 (Lindenboim et al., 2001; Minn et al., 1996). Redirection of Bcl-x splicing from Bcl-x_L to -x_S induced apoptosis and increased chemosensitivity in cancer cells in culture (Mercatante et al., 2001; Mercatante et al., 2002; Taylor et al., 1999); however, the anti-tumor effect of this strategy remains to be demonstrated *in vivo*.

Because the SSO effectively converts Bcl-x_L to Bcl-x_S, cancers expressing high levels of Bcl-x_L represent good candidates for treatment with Bcl-x SSO (Mercatante et al., 2002). Metastatic melanoma is an aggressive malignancy with poor prognosis and disease progression is associated with increased Bcl-x_L expression (Leiter et al., 2000; Zhuang et al., 2007). Xenografts of murine B16F10 melanoma cells provide a good model of this aggressive cancer because they express Bcl-x_L and are syngeneic to C57BL/6 mice, obviating the need for immunocompromised animals and providing a more realistic environment for drug testing. In this model, B16F10 murine melanoma cells localize to the lungs shortly after injection into the tail vein, providing a concise and predictable experimental time-course. In addition, the cell line used here expressed luciferase, providing an easily quantified measure of the tumor load. We previously failed to detect activity of systemically-delivered free SSOs in tumor xenografts. Thus, for this work we employed a liposome-DNA-polycation (LPD) nanoparticle (NP) formulation designed by the Huang laboratory (Li et al., 2008a; Li and

Huang, 2006a; Li and Huang, 2006b), which delivered siRNA to tumor cells in the B16F10 xenograft model (Li et al., 2008b; Li et al., 2008c). In previous work, Huang and colleagues demonstrated enhanced tumor cell-specific uptake of this NP formulation by surface-modification with anisamide, a ligand of the sigma receptor, which is up-regulated in many cancers (John et al., 1995; Vilner et al., 1995) and is expressed in B16F10 cells (Banerjee et al., 2004; Li et al., 2008b; Li et al., 2008c; Li and Huang, 2006a).

Our findings show that delivery of Bcl-x SSO by the LPD NP resulted in modification of Bcl-x mRNA splicing in lung metastases and reduction of tumor load. This marks the first demonstration of SSO-induced splicing modification in tumor cells *in vivo* and provides support for Bcl-x splice-switching as a potential anti-tumor strategy.

Materials and Methods

Materials

2′-O-methoxyethyl (MOE)-phosphorothioate SSOs (Figure 2.1) were synthesized by ISIS Pharmaceuticals (Carlsbad, CA). The Bcl-x SSO was targeted to the 5′ splice site of exon II in Bcl-x pre-mRNA (5′-TGGTTCTTACCCAGCCGCCG-3′, ISIS 105751) (Zhang et al., 2007). An oligonucleotide targeted to aberrantly spliced human β-globin intron (5′-GCTATTACCTTAACCCAG-3′, ISIS 18204) (Sazani et al., 2002) was used as negative control. For nanoparticle preparation cholesterol, protamine sulfate, calf thymus DNA and cloning water were purchased from Sigma-Aldrich (St. Louis, MO). DOTAP stock solution (20 mg/ml) was purchased from Avanti Polar Lipids (Alabaster, AL).

Cell culture and transfection

B16F10 mouse melanoma cells expressing sigma receptors were used as model cells in this study (Pham et al., 2007). B16F10 cells stably expressing the firefly luciferase gene were provided by Dr. Pilar Blancafort (University of North Carolina, Department of Pharmacology, NC) (Li et al., 2008b). The cells were maintained in high-glucose Dulbecco's modified Eagle's medium supplemented with 10% fetal bovine serum and a 5% penicillin/streptomycin solution (GIBCO, Grand Island, NY) at 37ºC and 5% CO_2. Cells were seeded in 96, 24 or 6-well plates at 7.5×10^3, 7.0×10^5 and 5.0×10^5 cells/well, respectively, approximately 24 hours prior to transfection. Cells were transfected with LipofectAmine 2000 (Invitrogen) in Opti-MEM (Invitrogen) per the manufacturer's recommendation.

RNA Isolation and analysis

Total RNA from cells or tissue was isolated using TRI Reagent (Molecular Research Center, Cincinnati, OH, USA) according to the manufacturer's protocol using 800 µl for ~5 mg tissue samples. Next, 200 ng of total RNA was subjected to RT-PCR (5′-CATGGCAGCAGTGAAGCAAG-3′, Bcl-x forward primer; 5′-GCATTGTTCCCGTAGAGATCC-3′, Bcl-x reverse primer; 5′-GTGCAGCGCAACCACGAGAC-3′, Mcl-1 forward primer; 5′-GCAGCACATTTCTGATGCCG-3′, Mcl-1 reverse primer) with rTth polymerase (Applied Biosystems, Foster City, CA). Cycles of PCR proceeded at 95ºC for 3 min, followed by 22 cycles of 95ºC for 30 s, 56ºC for 30 s, and 72ºC for 1 min. The PCR contained Cy5-conjugated dCTP (GE Healthcare) for visualization. The PCR products were separated on a 10% nondenaturing polyacrylamide gel (Invitrogen) and bands were visualized on a Typhoon

9400 Imager (GE Healthcare). Images were quantified using ImageQuant analysis software (Version 5.2, Molecular Dynamics). The percentage of Bcl-x_S in each lane was determined by dividing the intensity of the 162 bp band (Bcl-x_S) by the total intensities of the 351 (Bcl-x_L) and 162 bp (Bcl-x_S) bands. The identity of the 162 bp band was confirmed by sequencing by the UNC-CH Genome Analysis Facility.

Cell viability assay

Cell viability in response to SSO treatment was assessed, with slight modifications, by a previously described clonogenic assay (Mercatante et al., 2002). Briefly, 24 h after oligonucleotide transfection in 6-well plates, 250 cells were re-plated in 10-cm plates. After 10 days under normal culture conditions surviving colonies were stained with 2% methylene blue (Sigma) in 50% ethanol for 10 min. Colonies larger than 50 cells were counted.

Western Blot Analysis

Cells (5.0×10^5 cells/well in a 6-well plate) were washed twice with ice-cold PBS and lysed in RIPA buffer (radioimmune precipitation assay buffer; 50 mM Tris-HCl, 150 mM NaCl, 5 mM EDTA, 1% Triton X-100, 0.1% SDS, and 1% sodium deoxycholate) and a cocktail of protease inhibitors (Sigma). Total protein was quantified with the Quick Start Bradford Protein Assay Kit (Bio-Rad Laboratories, Inc., Hercules, CA). Total protein (20 µg) was separated by electrophoresis on a 4-12% pre-cast Bis-Tris gel (Invitrogen) and electrotransferred to a polyvinylidene difluoride (PVDF) membrane. Membranes were stained with Ponceau's stain to confirm equal loading and transfer. Membranes were blocked for 1 hour in BLOTTO (5% w/v nonfat dry milk in TBS, 0.1% Tween) or StartingBlock Buffer (Pierce) and incubated overnight at 4ºC with primary antibodies: polyclonal Bcl-x

antibody (1:2000; BD Transduction Labs), polyclonal PARP antibody (1:2000; Cell Signaling 9452) and mouse anti-β-actin monoclonal antibody (1:10,000; Sigma). Membranes were then incubated for 1 hour with horseradish peroxidase-conjugated anti-mouse (1:100,000; Sigma) or goat anti-rabbit (1:10,000; Abcam) secondary antibodies. Blots were developed with ECL Plus reagents (GE Healthcare) and exposed to film (GE Healthcare). Bcl-x_L, Bcl-x_S, β-actin, cleaved PARP and full-length PARP migrated at 30, 22, 42, 89 and 116 kDa respectively. β-actin was used to confirm equal protein loading.

For the detection of Bcl-x_S levels, B16F10 cells were plated at 2.0×10^5 cells/plate in 60 mm^2 plates. Cells were transfected with 4 ug Bcl-x_S plasmid DNA (pcDNA3.1-Bcl-x_S graciously provided by Dr. Reuven Stein, Tel Aviv University, Tel Aviv, Israel) using LipoFectamine 2000 according to the manufacturer's protocol. Approximately 24 hours later, the transfected cells were rinsed twice with PBS and suspended using Trypsin-EDTA. B16F10 cells tranfected with pcDNA3.1-Bcl-x_S were then diluted in un-transfected B16F10 cells at various ratios: 1:2, 1:5, 1:10, 1:25, 1:50 and 1:100. Cells were then subjected to RNA and protein isolation and analysis as described above.

Preparation of SSO-containing nanoparticles

Liposome-protamine-DNA (LPD) nanoparticles (NP) were prepared as previously described (Li et al., 2008b; Li et al., 2008c). Briefly, naked NP were obtained by quickly mixing 150 μl suspension A (16.6 mM liposomes (DOTAP/cholesterol molar ratio = 1: 1, and 400 μg/ml protamine in 5% dextrose) with 150 μl solution B (320 μg/ml oligonucleotide and 320 μg/ml calf thymus DNA in 5% dextrose) followed by incubation at room temperature for 10 min. The naked NP suspension (300 μl) was further incubated with 75.6 μl micellar solution of DSPE-PEG_{2000}-anisamide (10 mg/ml) (synthesized in the Huang

lab as reported earlier (Banerjee et al., 2004)) at 50°C for 10 min and then allowed to stand at room temperature for 10 min. The resulting formulation was used within 20 min for the following experiments. These methods resulted in encapsulation of >90% oligoncuelotide or siRNA in previous studies (Chono et al., 2008; Li and Huang, 2006b; Li and Huang, 2009).

Animal Studies

Female C57BL/6 mice of ages 6–8 weeks (16–18 g) were purchased from Charles River Laboratories (Wilmington, MA). All experiments performed on the animals were in accordance with and approved by the Institutional Animal Care and Use Committee at the University of North Carolina. The mouse model was established by i.v. injection of 2×10^5 luciferase-expressing B16F10 cells on day 0. In the preliminary study, tumor-bearing animals were seven days after tumor inoculation injected i.v. with NP formulated with Bcl-x SSO at 2.4 mg/kg either (a) everyday for a total of nine injections, or (b) every other day for a total of five injections. The negative control group received no treatment. Animals were euthanized one day following the final injection (day 16 after tumor inoculation). RNA was isolated from tumor nodules and analyzed by RT-PCR. Following this preliminary experiment, a larger-scale study was designed and implemented in which animals were i.v. injected with vehicle only (PBS), NP only (2.4 mg/kg), control or Bcl-x SSO NP (2.4 mg/kg), or free control or Bcl-x SSO (2.4 or 10 mg/kg) on days 3–6 after tumor inoculation. On day 7, some animals were euthanized for analysis of RNA splicing. For animals treated with free SSO, only RNA was analyzed. For animals treated with NP, blood was collected for analysis of toxicity marker. On day 17 the remaining animals were euthanized for the analysis of tumor load. Tumor load was determined by measuring luciferase activity within tumor-bearing lungs, as described previously (Li et al., 2008b; Li et al., 2008c).

Toxicity Assays

Twenty-four hours after the final injection, blood samples were collected and serum was isolated. Analyses of serum aspartate aminotransferase and alanine aminotransferase were performed at the Animal Clinical Laboratory Core Facility (University of North Carolina) using a Vitro 250 Chemical Analyzer (Ortho-Clinical Diagnostics, Rochester, NY). Serum interleuikin-12 was measured with the enzyme-linked immunosorbant assay (ELISA) according to the manufacturer's protocol (BD Biosciences, San Diego, CA).

Statistical Analysis. Luciferase data were analyzed by one-way analysis of variance (ANOVA) and Tukey's post-test using Prism statistical software (GraphPad, version 4.03).

Results

Modification of Bcl-x pre-mRNA in melanoma cells

Transfection of B16F10 cells with MOE-PS Bcl-x SSO targeted to the downstream 5′ splice site of Bcl-x exon 2 (Figure 2.1) induced a dose-dependant shift in splicing of Bcl-x pre-mRNA from anti-apoptotic Bcl-x_L to pro-apoptotic Bcl-x_S, while a control SSO had no effect on splicing (Figure 2.2 A, B). Consistent with these results, probing of total protein from treated cells with anti-Bcl-x antibody showed SSO-dependent reduction in the level Bcl-x_L protein (Figure 2.2 C). We were unable to detect the expected Bcl-x_S protein because the endogenous level of murine Bcl-x_S expression was below the threshold required by available antibodies (Figure 2.3). Importantly, SSO treatment resulted also in a dose-dependant decrease in cell viability, as evidenced by a clonogenic cell death assay. (Figure 2.4 A). This was accompanied by cleavage of poly (ADP-ribose) polymerase (PARP), indicating that the observed cell death was due to apoptosis (Figure 2.4 B). These effects

were absent in untreated and mock-transfected cells, and cells transfected with a control SSO. In addition, the Bcl-x SSO had no effect on the pre-mRNA splicing of Mcl-1, a closely related gene that shares sequence homology at the 5′ splice site, supporting sequence specificity of the Bcl-x SSO (Figure 2.5).

Activity of Bcl-x SSO in vivo

To facilitate SSO delivery to cancer cells in tumor-bearing mice, an LPD NP developed by the Huang laboratory was used (Li et al., 2008b; Li et al., 2008c). The SSO and a carrier DNA (calf thymus DNA) were complexed by protamine into a compact core which was then coated with cationic lipids to form the NP (Figure 2.6). The surface of the NP was further modified with an anisamide ligand-conjugated polyethylene glycol (PEG)-lipid for targeting the sigma receptor-expressing B16F10 cells. This NP formulation could efficiently, specifically and with low toxicity deliver siRNA to tumor cells in the B16F10 tumor model, as shown previously (Li et al., 2008b; Li et al., 2008c).

B16F10 murine melanoma cells localize in the lungs shortly after injection into the tail vein of C57BL/6 mice. In the absence of treatment, the mice die approximately 22 days following inoculation (Li et al., 2008c). This rapid course of disease dictated the treatment protocol (see Materials and Methods). RT-PCR analysis of total RNA from the tumor-bearing lungs of animals euthanized on day 7 showed induction of Bcl-x_S mRNA expression in animals treated with the Bcl-x SSO NP formulation. This effect was dose-dependant, as increasing the number of injections resulted in a greater degree of Bcl-x splice-switching from Bcl-x_L to Bcl-x_S mRNA in the tumor nodules (Figure 2.7). In contrast, Bcl-x_S mRNA levels in animals treated with control SSO NP formulation or free SSO were no different than in animals treated with PBS only (Figure 2.7, 2.8 A). Modification of Bcl-x splicing in the

liver was barely detectable in Bcl-x SSO-treated animals and undetectable in animals treated with control SSO NP or PBS only (Figure 2.8A). As a measure of tumor load, luciferase activity was assayed in lysates from tumor-bearing lungs of animals euthanized on day 17. A dramatic reduction in luciferase activity was seen in animals treated with Bcl-x SSO NP compared to animals treated with NP only, control SSO NP, or PBS only (Figure 2.8 B, C). Statistical analysis (ANOVA, Tukey's post-test) revealed that the reduction in luciferase activity in animals treated with Bcl-x SSO NP was significant compared to animals treated with PBS only ($P < 0.001$), NP only ($P < 0.05$) and control SSO NP ($P < 0.05$) (Figure 2.8 B).

Toxicity studies

To determine the potential toxicities of NP and SSO treatment, serum levels of toxicity markers were analyzed in mice euthanized on day 7 following tumor inoculation. Tissues with a leaky endothelial wall, such as the liver, allow significant uptake of nanoparticles (Li and Huang, 2008). Accordingly, we analyzed serum aspartate aminotransferase (AST) and alanine aminotransferase (ALT) levels as markers of liver toxicity. No significant elevation in serum AST or ALT among treatment groups was observed (Figure 2.9 A, B). To test the possibility that components of the NP formulation might trigger an inflammatory response, serum levels of the pro-inflammatory cytokine IL-12 were also analyzed. Elevated IL-12 levels relative to the PBS control were observed in NP treatment groups (Empty NP, $P<0.01$; Control SSO $P<0.001$) (Figure 2.9 C).

Discussion

Alternative splicing has emerged as an important target for molecular therapies (Bauman et al., 2009). Clinical trials using SSOs to treat DMD have yielded promising preliminary results (Kinali et al., 2009; van Deutekom et al., 2007), while numerous recent reports have confirmed the *in vivo* efficacy of SSOs in treating animal models of disease (Bauman et al., 2009). SSOs have been applied against cancer targets *in vitro* (Mercatante et al., 2001; Mercatante et al., 2002; Wan et al., 2009), however *in vivo* validation of their efficacy has been hindered by the poor delivery of antisense therapeutics to tumor cells *in vivo* (Bennett, 2008; Juliano et al., 2009b). Here we show that an SSO in LPD NP formulation was effective in delivery to tumor cells in the B16F10 model system (Li et al., 2008b; Li et al., 2008c; Li and Huang, 2006a).

Our data indicate that SSO-induced redirection of Bcl-x pre-mRNA splicing from Bcl-x_L to -x_S induced apoptosis and subsequent cell death in a dose-dependant manner in B16F10 melanoma cells in culture (Figure 2.2, 2.3). *In vivo*, redirection of Bcl-x pre-mRNA splicing was associated with a significant reduction of tumor burden in rapidly growing and highly tumorigenic B16F10 lung metastases (Figure 5A-C). This finding is consistent with our *in vitro* data, as well as previous work in prostate and breast cancer cells (Mercatante et al., 2001; Mercatante et al., 2002). Interestingly, in this model both in cell culture and *in vivo* xenografts, modification of Bcl-x pre-mRNA splicing alone induced cell death, whereas in non-small cell lung carcinoma (A549) cells adjuvant chemotherapy was needed (Taylor et al., 1999). Bcl-x_L expression may therefore be critical for survival of B16F10 cells, consistent with reports that increased Bcl-x_L expression is associated with melanoma progression and metastasis (Leiter et al., 2000; Zhuang et al., 2007). Thus, other

pharmacological agents that target Bcl-x_L may warrant further investigation in metastatic melanoma.

Our cell culture data are consistent with the predicted SSO mechanism of action. Namely, that Bcl-x SSO-induced modulation of Bcl-x pre-mRNA splicing, reduced the level of Bcl-$x_{L,}$ and increased the level of Bcl-x_S splice variants, causing apoptosis of cancer cells. This is evident at the RNA level, and is further supported by the dramatic reduction of Bcl-x_L protein and by induction of PARP cleavage (Figure 2C, 3C). Although SSO induced Bcl-x_S mRNA we were unable to confirm concomitant production of Bcl-x_S protein by immunoblotting procedures. This was in spite of screening several commercially available antibodies and including attempts to concentrate the protein by immunoprecipitation prior to Western analysis. This is likely because the maximum level of endogenous Bcl-x_S protein that could be induced by the SSO was below that which could be detected by available antibodies (Supplementary Figure 1).

In vivo, RT-PCR analysis of total RNA from tumor-bearing lungs demonstrated that Bcl-x splicing was shifted approximately 10% from Bcl-x_L to the -x_S splice variant. Yet this treatment led to marked reduction of tumor load in treated animals. Two interpretations of these results are possible. One, that *in vivo* even a minor reduction of Bcl-x_L levels and concomitant increase in Bcl-x_S, leads to death of cancer cells or at least inhibits their proliferation. However, it is also possible that the cells which took up the SSO more efficiently were more effectively killed by apoptosis and thus eliminated from the tissue subjected to subsequent analysis. If this is the case, RT-PCR underestimates the actual level of SSO-induced splice-switching.

BH3 mimetics comprise a novel class of cancer drugs that competitively antagonize the Bcl-2 anti-apoptotic proteins (Chonghaile and Letai, 2008). For example, the small molecule ABT-737 binds Bcl-2, Bcl-x_L and Bcl-w proteins with nanomolar affinity. It induced apoptosis in lymphoma and small-cell lung carcinoma cells in culture, and caused tumor regression and improved survival in preclinical studies (Oltersdorf et al., 2005). By modifying the splicing pattern of Bcl-x, the SSO can be thought of as prompting the tumor cell to produce an endogenous BH3 mimetic, Bcl-x_S, capable of antagonizing Bcl-2 and Bcl-x_L and promoting apoptosis.

Nanoparticles are known to accumulate non-specifically in the liver due to the fenestrated vasculature (Li and Huang, 2008). We did not observe significant Bcl-x splice-switching in the liver (Figure 5A), and ALT and AST serum levels were not significantly elevated in treatment groups relative to the PBS control (Figure 6). This suggests that liver uptake of the NP was limited and did not translate into significant biological activity or toxicity. We did detect a modest elevation of serum IL-12 levels in NP treatment groups relative to the PBS control (Figure 6). A previous report with the LPD NP showed more pronounced induction of inflammatory toxicity at doses ≥1.2 mg/kg (Li et al., 2008a; Li et al., 2008c). However, that study analyzed local toxicity from lung lysate, whereas we analyzed serum from systemic circulation. It is unclear whether this small but statistically significant increase is biologically relevant. Elevated IL-12 could be due to unmethylated CpG motifs present in the calf thymus DNA component of the NP. While we cannot exclude the possibility that the observed IL-12 increase contributed to the anti-tumor effect of the Bcl-x SSO, this seems unlikely because IL-12 induction was observed in all NP treatment

groups, whereas reduction of tumor load was only evident in animals treated with the Bcl-x SSO.

The inclusion of calf thymus DNA in the NP complicates the use of this formulation from a pharmaceutics and regulatory perspective. Recently, Chono et al. replaced calf thymus DNA with a high molecular weight anionic polysaccharide, hyaluronic acid, resulting in a NP containing cationic liposome, protamine and hyaluronic acid (LPH) (Chono et al., 2008). The LPH formulation delivered siRNA *in vivo* with potency similar to that of the LPD formulation; however, induction of both IL-6 and IL-12 cytokines by LPH was significantly lower than that of the corresponding LPD containing the calf thymus DNA. The LPH NP formulation could be employed for delivery of SSOs to tumors in future studies.

Despite the caveats described above, it is encouraging that this NP formulation, developed primarily for *in vivo* delivery of siRNA, was found to deliver functionally active SSO to tumor cells. As mentioned in the Introduction, siRNAs do not support extensive chemical modifications because of specifications imposed by the RISC-loading process. As a result, efforts to improve siRNA delivery *in vivo* have been a major source of progress in the development of NP formulations. Our results suggest that advances in the NP-aided delivery of siRNA may be leveraged for the delivery of non-siRNA oligonucleotide therapeutics, including SSOs and RNase H-active ASOs. However, it should be noted that the LPD NP and similar iterations could not be sued to deliver uncharged oligonucleotides, such as PNA and PMO, because charge is necessary for association with and condensing by polyanionic protamine.

Tumor xenograft models, such as the one used in this study, are widely used for the preclinical evaluation of putative anti-cancer drugs. These models have drawn criticism

because they do not always predict which drugs will succeed in the clinic (Sharpless and Depinho, 2006). To address this criticism, SSOs targeting Bcl-x and other cancer targets could be tested in alternative cancer models such as orthotopic tumor or genetically engineered mouse models (Kerbel, 2003).

Our results extend previous findings on the LPD NP formulation, which delivered siRNA to the cytoplasm, the site of dicer activity, to oligonucleotides that function in the nucleus, the site of splicing modulation. Thus, through delivery of SSOs, liposome-based NP formulations may be used not only to down-regulate, but also to up-regulate endogenous gene expression, as is evidenced by the induction of Bcl-x_S mRNA we observed. In addition, our findings are consistent with Bcl-x pre-mRNA splice-switching as a possible anti-tumor strategy in melanoma as well as other malignancies expressing Bcl-x_L.

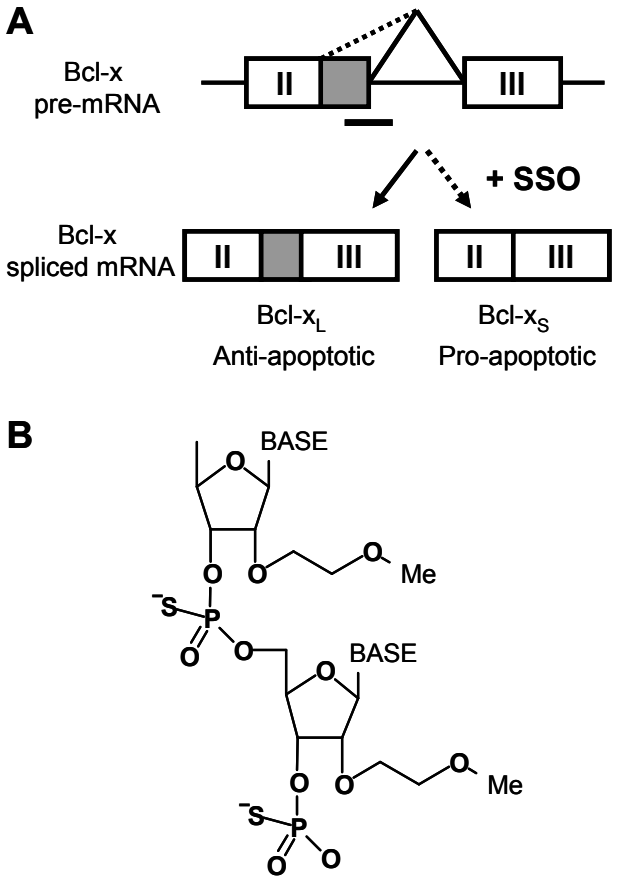

Figure 2.1 Direction of Bcl-x alternative splicing by SSO.
(A) Use of the downstream or upstream alternative 5′ splice site within exon II of Bcl-x pre-mRNA yields anti-apoptotic Bcl-x_L or pro-apoptotic Bcl-x_S, respectively. SSO targeted to the downstream splice site redirects the splicing machinery to the upstream alternative splice site, resulting in a simultaneous decrease in production of Bcl-x_L and increase in production of Bcl-x_S. (B) Chemical structure of 2′-O-methoxyethyl (MOE) phosphorothioate (PS) oligonucleotide. The MOE ribose modification confers RNAse-H non-competence and increased affinity for target mRNA, while the phosphorothioate inter-nucleotide linkage improves serum stability and bioavailability.

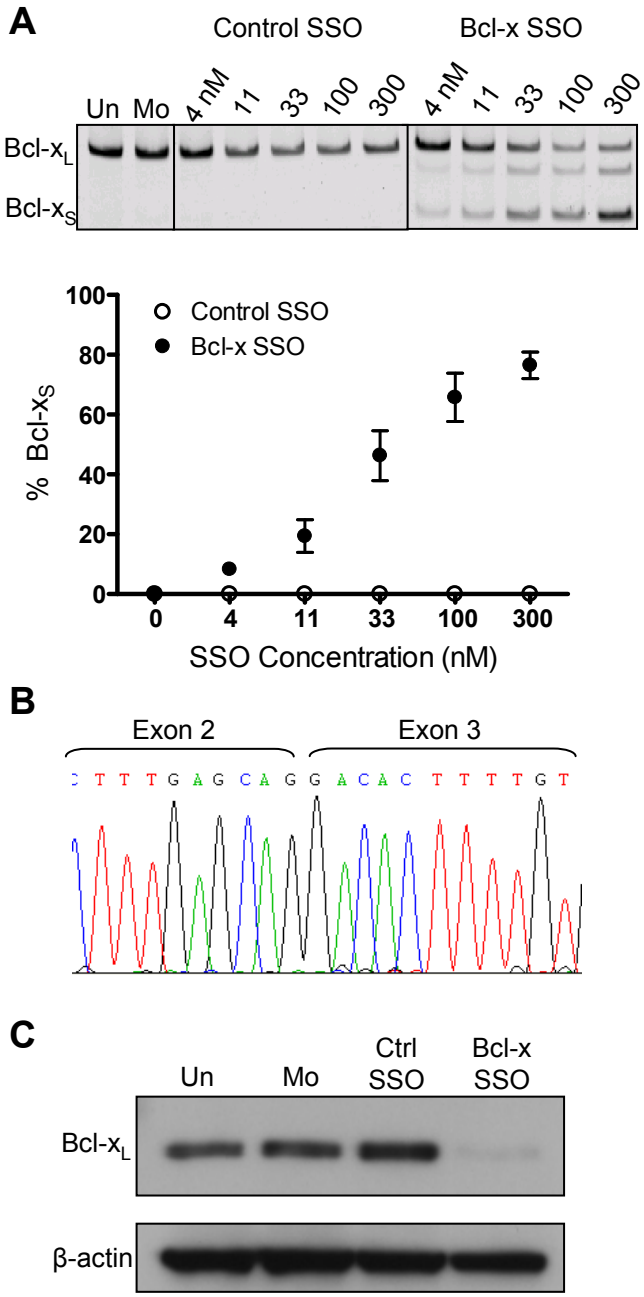

Figure 2.2 SSO induced Bcl-x splice-switching in B16F10 murine melanoma cells. (A) RT-PCR analysis of Bcl-x mRNA from cells transfected with control and Bcl-x SSO 24 hours post-transfection. The Bcl-x SSO induces dose-dependant switching of Bcl-x mRNA splicing from anti-apoptotic Bcl-x_L to pro-apoptotic Bcl-x_S. Error bars indicate mean ± SD (n=3). (B) Sequence analysis of the RT-PCR product corresponding to Bcl-x_S showing exons 2 and 3 joined at the upstream alternative splice site. (C) Immunoblot analysis of cells treated with 100 nM Bcl-x SSO 48 hours post-transfection. The SSO induces a reduction in the Bcl-x_L protein isoform. Detection of β-actin confirms equal loading.

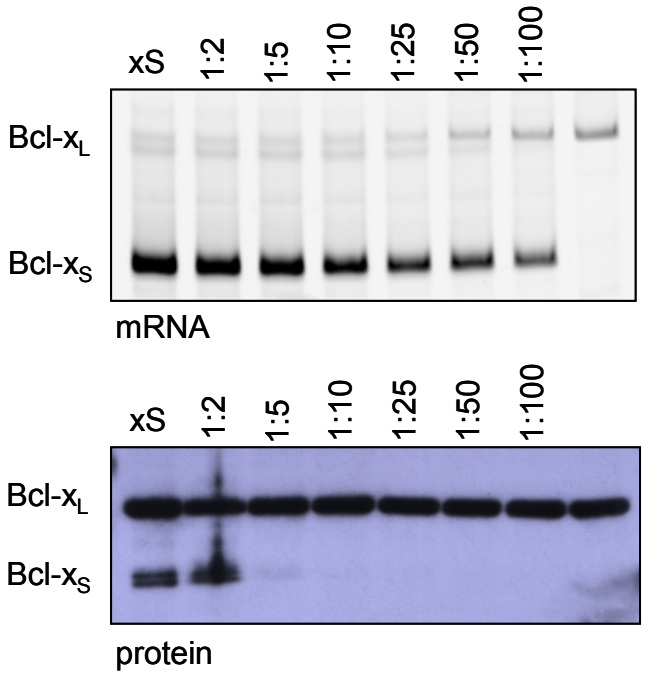

Figure 2.3 Bcl-x_S detection by RT-PCR and Western Blot.
B16F10 cells transfected with pcDNA3.1-Bcl-x_S were diluted with untransfected cells at various ratios (undiluted, 1:2, 1:5, 1:10, 1:25, 1:50, 1:100). RNA and protein were isolated and analyzed by RT-PCR and Western Blot, respectively. Bcl-x_S mRNA was readily detected even at the 1:100 dilution, though it was not detected in untransfected cells. Bcl-x_S protein could be detected up to the 1:5 dilution, but was not seen in more dilute samples. The level of Bcl-x_S mRNA corresponding to the 1:5 dilution is greater than can achieved endogenously through alternative splicing.

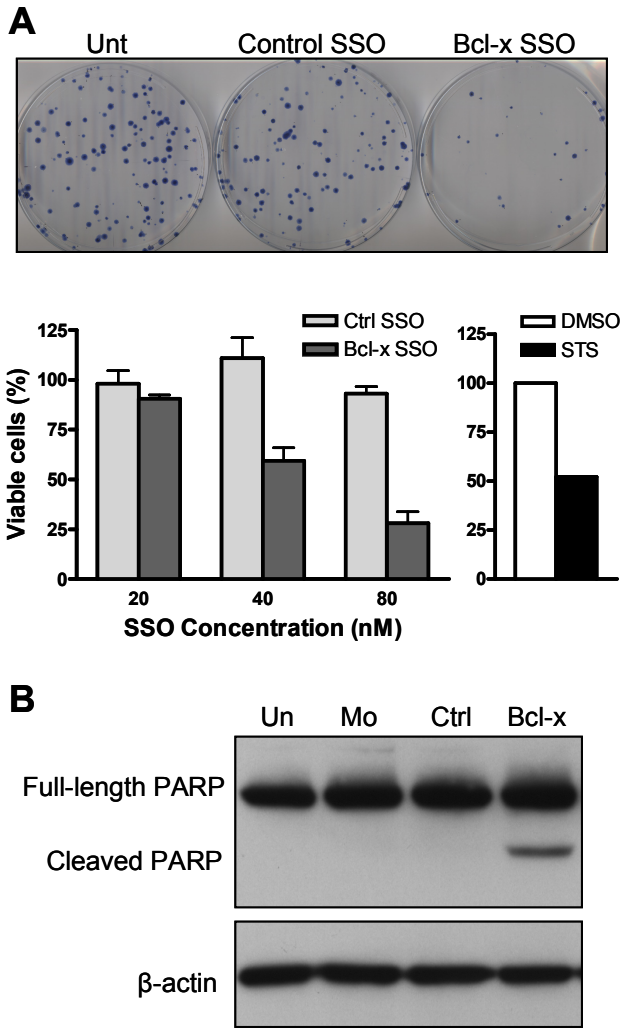

Figure 2.4 Bcl-x SSO induces cell death in B16F10 murine melanoma cells.
(A) Effect of Bcl-x and control SSO on cell viability as determined by a clonogenic assay. Top panel shows images of representative plates at 80 nM concentration. Bottom left panel expresses viability of SSO-treated cells relative to untreated cells. Error bars indicate mean ± SD (n=3-4). Bottom right panel shows viability of cells treated with 1 μM staurosporine (STS) relative to DMSO-treated cells. (B) Western blot of protein from cells treated with control and Bcl-x SSOs for 24 hours. The presence of PARP cleavage in Bcl-x SSO-treated cells confirms that the observed decrease in cell viability is due to apoptosis. Detection of β-actin confirms equal loading.

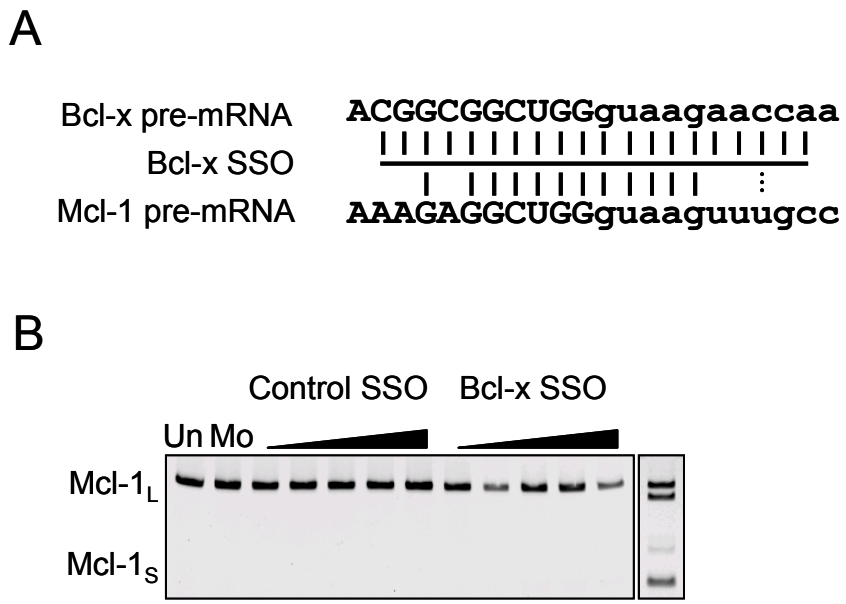

Figure 2.5 Bcl-x SSO does not affect Mcl-1 alternative pre-mRNA splicing.
(A) The Bcl-x and Mcl-1 share a high degree of sequence conservation at the 5′ splice site of exon 2. As a result the Bcl-x SSO matches 13 out of 20 bases in Mcl-1 pre-mRNA (including one G-U pair). (B) RNA from Bcl-x SSO-transfected B16F10 cells was subjected to RT-PCR using primers flanking exon 2 of mouse Mcl-1. Mcl-1 pre-mRNA can be alternatively spliced to produce a transcript that lacks exon 2. However, the Bcl-x SSO fails to redirect Mcl-1 splicing, despite matching 13 out of 20 bases in Mcl-1. SSO concentrations used were 4, 11, 33, 100 and 300nM.

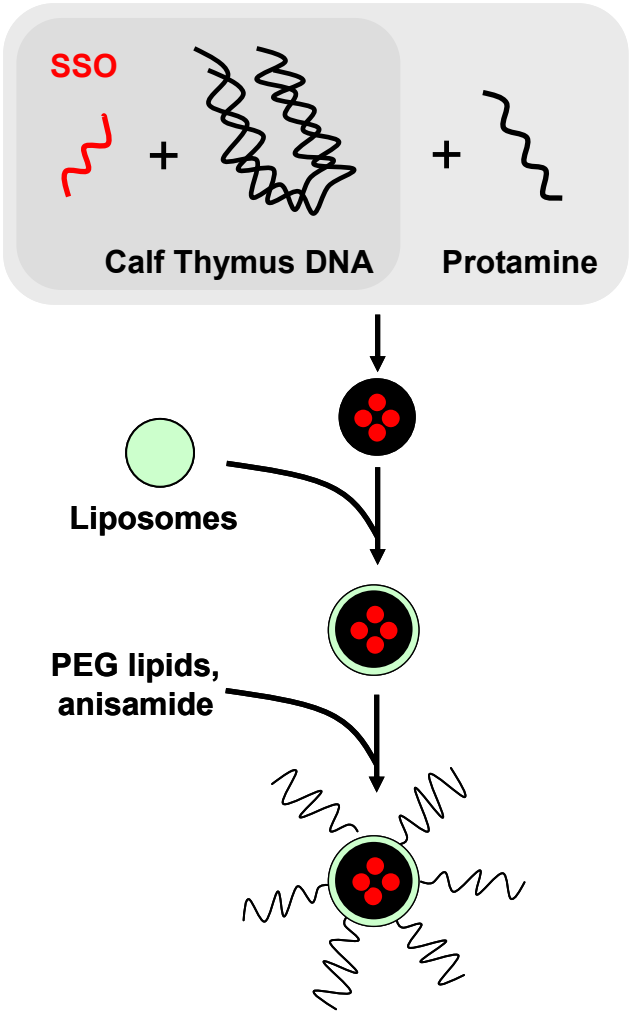

Figure 2.6 Schematic depiction of the preparation of SSO encapsulated LPD NP. The SSO was encapsulated into a condensed core with a high molecular weight polyanion (calf thymus DNA) and protamine, which was then coated with cationic liposomes. PEG lipids were inserted into the resultant bilayer to shield the positive charge and prevent aggregation in circulation. Anisamide, a commonly used targeting ligand that binds the sigma receptor, was conjugated to the distal end of the PEG lipids.

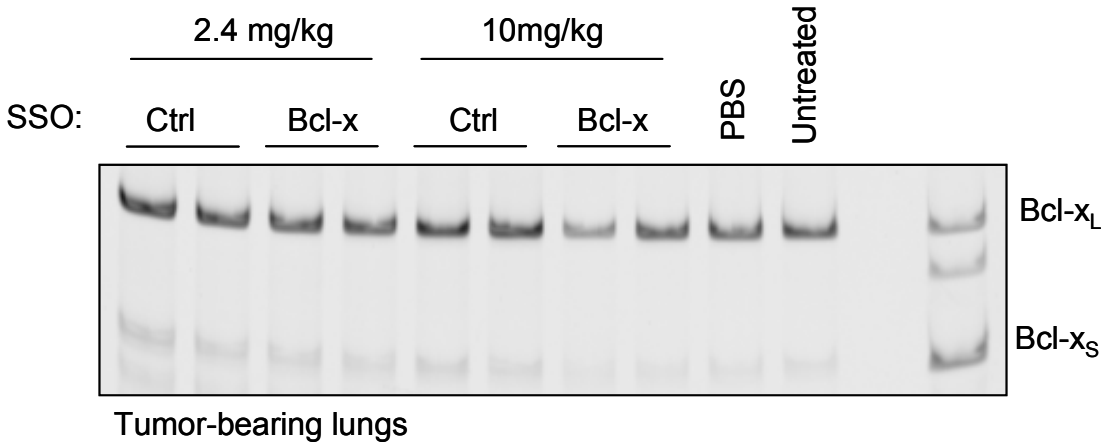

Figure 2.7 Systemically-delivered free Bcl-x SSO has no effect on Bcl-x pre-mRNA splicing in tumor xenografts.
Tumor-bearing animals were injected with vehicle only (PBS) or with free SSO (control SSO or Bcl-x SSO) in PBS at 2.4 or 10 mg/kg on days 3-6 following tumor inoculation. On day 7 animals were euthanized and RNA from tumor-bearing lungs was isolated and analyzed by RT-PCR.

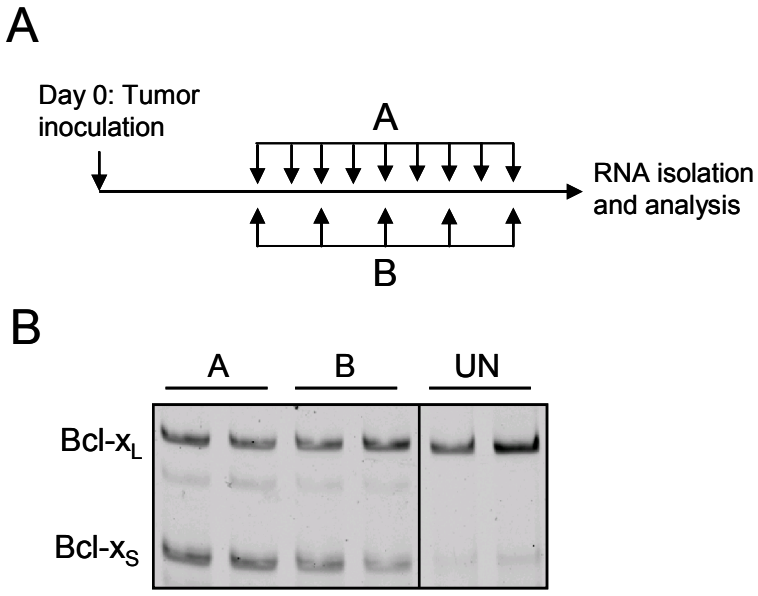

Figure 2.8 Bcl-x splice-switching depends on the dose of Bcl-x SSO NP formulation. (A) Bcl-x SSO NP was systemically delivered (tail-vein injection) every day (9 injections, group A) or every over day (5 injections, group B) to mice bearing B16F10 tumors. (B) RT-PCR analysis of Bcl-x pre-mRNA isolated from lung tumor nodules from mice injected with 2.4 mg/kg NP formulated with Bcl-x SSO every day (9 injections, group A) or every over day (5 injections, group B) revealed robust Bcl-x splice-switching.

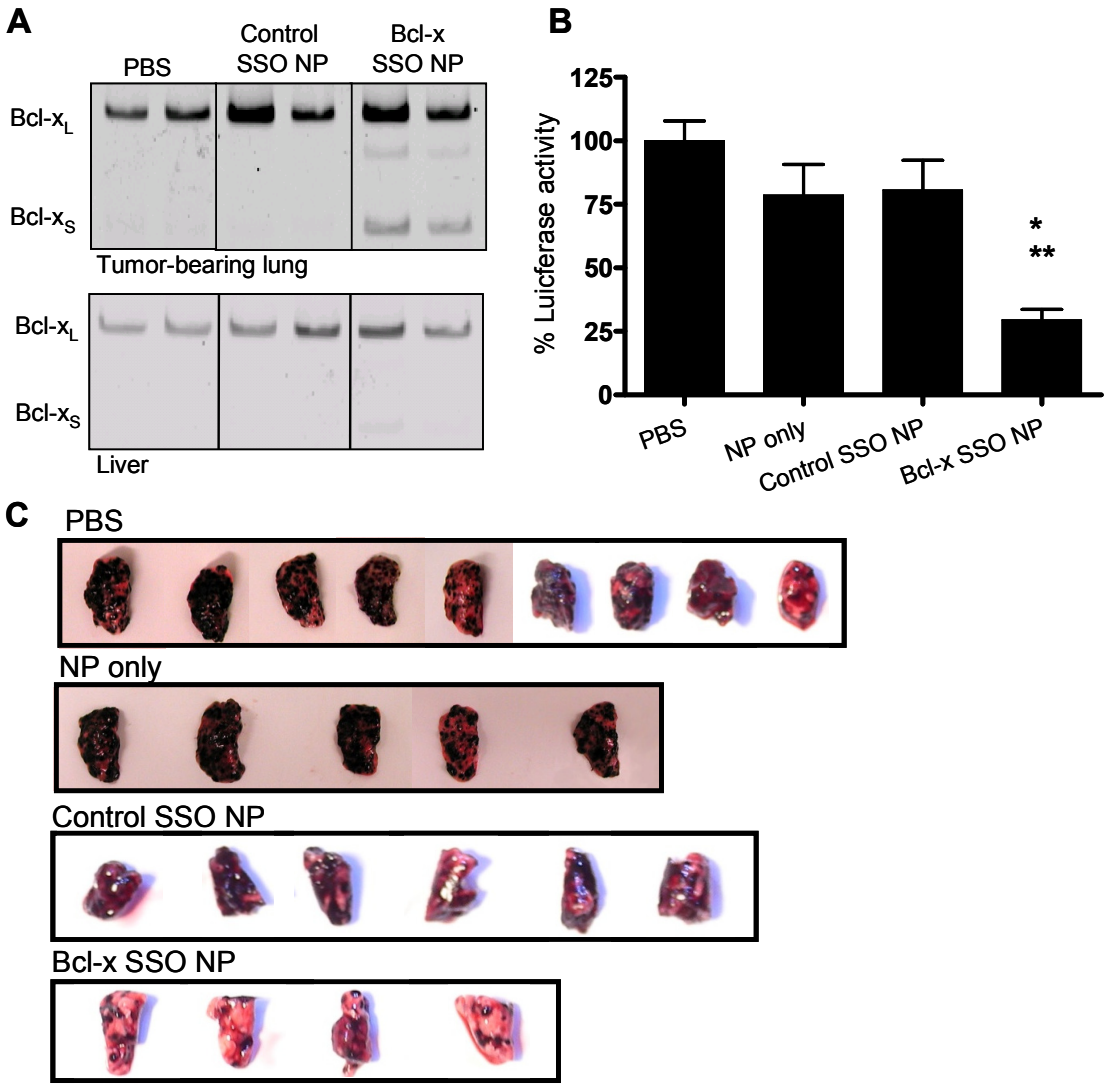

Figure 2.9 Effects of LPD-NP-delivered SSO in B16F10 tumor-bearing lungs.
(A) RT-PCR analysis of Bcl-x mRNA splicing in the tumor-bearing lungs (upper panel) and liver (lower panel) of mice treated with vehicle only (PBS), empty NP, control SSO-formulated NP and Bcl-x SSO-formulated NP. (B) Luciferase activity in the tumor-loaded lungs on day 17 after injections on days 3-6. Asterisks denote statistical significance thresholds (*$P < 0.05$, **$P < 0.001$, determined by ANOVA and Tukey's post-test). Untreated $n = 26$, NP only $n = 8$, Control SSO NP $n = 13$, Bcl-x SSO NP $n = 9$. (C) Representative images of lungs excised from tumor-bearing mice on day 17 following 4 injections of 2.4 mg/kg NP formulations on days 3-6.

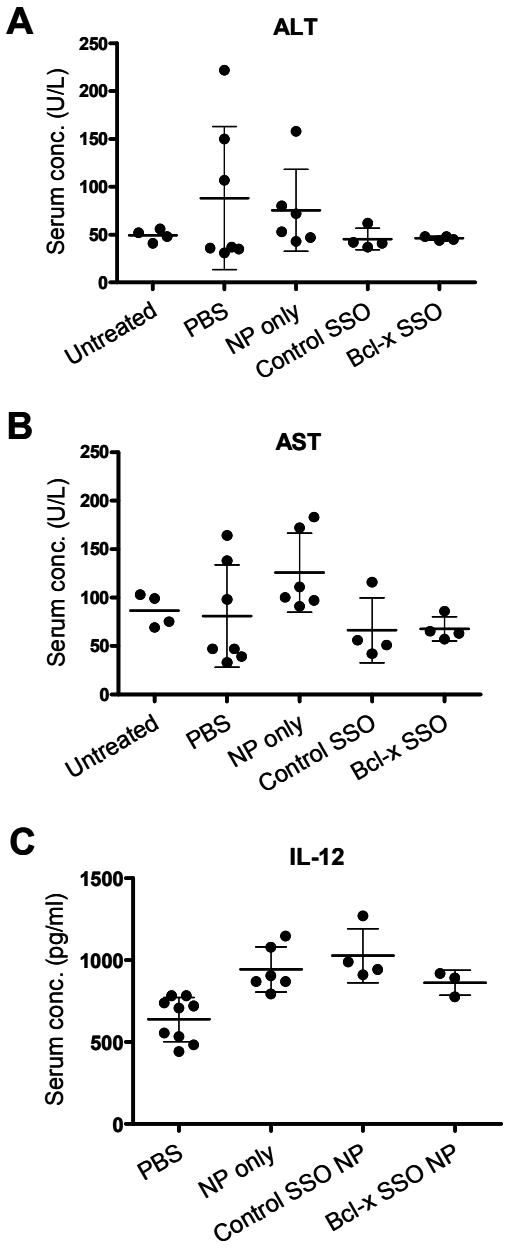

Figure 2.10 Serum enzyme and cytokine analysis.
ALT (A), AST (B) and IL-12 (C) serum levels of untreated tumor-free and tumor-bearing C57BL/6 mice 24 hours after the last of 4 consecutive daily treatments. Treatments consisted of i.v. injections of vehicle only (PBS), NP formulated with control SSO, or NP formulated with SSO targeted to Bcl-x.

Chapter 3 – Modification of Mcl-1 alternative splicing with splice-switching oligonucleotides induces apoptosis and enhances chemosensitivity

Abstract

Mcl-1 transcripts are alternatively spliced to produce proteins with opposing functions. Inclusion of all three exons produces Mcl-1_L, an anti-apoptotic protein that is highly expressed in many malignancies and confers resistance to chemotherapeutic drugs. Skipping of exon 2 leads to expression of Mcl-1_S, a potent pro-apoptotic protein expressed at low levels in most cells. We used RNAse H non-competent splice-switching oligonucleotides targeted to the 5′ and 3′ splice sites in Mcl-1 pre-mRNA, thereby blocking recognition by the spliceosome and modifying the pattern of alternative splicing. Modification of Mcl-1 splicing from Mcl-1_L to -1_S induced PARP cleavage and cell death in HeLa cells, indicative of apoptosis. Mcl-1 splice-switching also sensitized cells staurosporine. These findings validate Mcl-1 as a target for splice-switching strategies to induce apoptosis and sensitize cancer cells to chemotherapy.

Introduction

The ability of tumor cells to evade apoptosis is a hallmark of cancer (Hanahan and Weinberg, 2000), prompting the search for drugs that can restore normal apoptotic signaling in tumor cells (Fesik, 2005). Apoptosis is regulated by death receptor-mediated (extrinsic) and mitochondria-mediated (intrinsic) pathways, which converge on the activation of caspases, which in turn initiate a proteolytic cascade leading to the cell death phenotype. Apoptotic signaling through the intrinsic pathway requires permeabilization of the outer mitochondrial membrane and the consequent efflux of pro-apoptotic factors, such as cytochrome C.

Mitochondrial membrane integrity is regulated by interactions among members of the Bcl-2 family. Apoptotic stimuli prompt Bax and Bak to oligomerize at the outer

mitochondrial membrane, resulting in membrane permeability and effluc of pro-apoptotic factors such as cytochrome C. Anti-apoptotic Bcl-2 homologs, such as Bcl-2, Bcl-x_L and Mcl-1_L, bind and sequester Bax and Bak, preventing the cell from committing to apoptosis. BH3-only proteins, such as Noxa, Puma, Bad and Bim, are activated by diverse apoptotic signals, such as DNA damage and growth factor deprivation, prompting their translocation to the mitochondria, where they competitively bind the anti-apoptotic homologs, liberating Bax and Bak to oligomerize and trigger apoptosis. (Adams and Cory, 2007; Uren et al., 2007; Willis et al., 2007). The balance of BH3-only and anti-apoptotic Bcl-2 proteins thus determines whether the cell will commit to apoptosis. Upregulation of anti-apoptotic Bcl-2 homologues enables them to overcome antagonism by BH3-only proteins, causing resistance to apoptosis. Consequently, overexpression of a anti-apoptotic family member can be oncogenic and, since many chemotherapeutics induce apoptosis through activation of BH3-only proteins, the upregulation of Bcl-2 anti-apoptotic proteins by tumor cells promotes chemoresistance (Amundson et al., 2000; Huang and Strasser, 2000).

The *Mcl-1* gene encodes three exons and its pre-mRNA transcript is alternatively spliced to produce splice variants with opposing function (Figure 3.1). Inclusion of all three exons produces the anti-apoptotic Bcl-2 homolog Mcl-1_L encoding three basic helical domains (BH1-3) and a C-terminal transmembrane domain responsible for its localization at the mitochondrial. BH domains 1–3 form a hydrophobic groove on the protein surface, which is the site of interaction with Bak and BH3-only proteins, including Noxa, Puma, Bim and Bad (Chen et al., 2005; Willis et al., 2005). Mcl-1_L is overexpressed in a number of malignancies, including cervical cancer (Chung et al., 2002; Wei et al., 2001a), chronic

myeloid leukemia (Aichberger et al., 2005), and multiple myeloma (Zhang et al., 2002). High Mcl-1_L expression confers resistance to the BH3 mimetic ABT-737 (Tahir et al., 2007).

Skipping of exon 2 in Mcl-1 pre-mRNA causes a frame-shift in the translation of exon three, leading to the production of Mcl-1_S, a truncated protein encoding a BH3 domain and a novel C-terminus (Bae et al., 2000; Bingle et al., 2000). Mcl-1_S was found to potently induce apoptosis in a manner that inhibited by caspase blockade. The apoptotic activity was also inhibited fully by Mcl-1_L and partially by Bcl-x_L and Bcl-w (Bae et al., 2000). Mcl-1_S was also found to bind Mcl-1_L. Taken together, these findings sugges that Mcl-1_S act as a BH3-only protein that antagonizes Mcl-1_L (Bae et al., 2000; Bingle et al., 2000).

Over 90% of multi-exon gene transcripts undergo alternative splicing (Wang et al., 2008) and up to 50% of disease-causing mutations affect splicing (Lopez-Bigas et al., 2005). Accordingly, alternative pre-mRNA splicing has emerged as important therapeutic target (Cooper et al., 2009). Our laboratory and others have developed splice-switching oligonucleotides (SSOs), chemically modified antisense compounds that hybridize to pre-mRNA sequences involved in splicing, thereby blocking access to the transcript by splicing factors and influencing splice site usage (Dominski and Kole, 1993; Sierakowska et al., 1996). SSOs have been used to repair aberrant pre-mRNA splicing, modulate alternative splicing patterns, and induce expression of novel splice variants (Bauman et al., 2009).

Here SSOs have been employed to switch the alternative splicing pattern of Mcl-1 from predominant expression of Mcl-1_L to Mcl-1_S, thereby converting an anti-apoptotic molecule into a pro-apoptotic one. Mcl-1 splice-swtiching induced apoptosis and enhanced chemosensitivity in cells in culture.

Methods and Materials

Materials

2′-O-methyl phosphorothioate oligonucleotides targeted to the 5′ and 3′ splice sites of exon II of Mcl-1 pre-mRNA (Figure 3.1A) were synthesized by the UNC Program in Macromolecular Therapeutics Oligonucleotide Synthesis Core Facility. The sequences are available upon request. One SSO sequence for each splice site was chosen for further study and SSOs 2′-O-methoxyethyl phosphorothioate SSOs were synthesized by Integrated DNA Technologies, Inc. (IDT): 5′-GTTTCCGAAGCATGCCTGAG-3′ (5' splice site) and 5′-TCCTTAAGGCAAACTTACCC-3′ (3' splice site). An oligonucleotide targeted to aberrantly spliced human β-globin intron (5′-GCTATTACCTTAACCCAG-3′, ISIS18204) provided by ISIS Pharmaceuticals (Carlsbad, CA) (Sazani et al., 2002), was used as negative control. Plasmid DNA expressing FLAG-tagged Mcl-1_S (pcDNA3-Mcl-1_S) was generously provided by J. Bae (CHA University, South Korea).The chemotherapeutic pan-kinase inhibitor staurosporine (Sts) was purchased, already in-solution at 1 mM in DMSO, from Sigma-Aldrich (S6942; St. Louis, MO).

Cell culture and transfection

HeLa cervical cancer cells and Sk-Mel147 melanoma cells were maintained in high-glucose Dulbecco's modified Eagle's medium supplemented with 10% fetal bovine serum and a 5% penicillin/streptomycin solution (GIBCO, Grand Island, NY) at 37ºC and 5% CO_2. HeLa cells were seeded in 96- or 12-well plates at 1.0×10^3 and 1.0×10^5 cells/well, respectively, approximately 24 hours prior to transfection. Sk-Mel147 cells were seeded in 12-well plates at 1.5×10^5 cells/well. Cells were transfected with LipofectAmine 2000

(Invitrogen) in Opti-MEM (Invitrogen) per the manufacturer's recommendation. SSO and plasmid DNA transfections were performed in 1:3 serial dilutions. For Mcl-1_S plasmid transfection, half of the cells were used for isolation of total RNA and half were used for isolation of total protein.

RNA Isolation and analysis

Total RNA from cells was isolated using TRI Reagent (Molecular Research Center, Cincinnati, OH, USA) according to the manufacturer's protocol using 800 μl per well for a 24-well plate. Next, 200 ng of total RNA was subjected to RT-PCR (5′-CCTGATGCCACCTTCTAGGTCC-3′, forward primer; 5′-CTCTCGGTACCTTCGGGAGC-3′, reverse primer) with rTth polymerase (Applied Biosystems, Foster City, CA). Cycles of PCR proceeded at 95ºC for 3 min, followed by 22 cycles of 95ºC for 30 s, 56ºC for 30 s, and 72ºC for 1 min. The PCR contained Cy5-conjugated dCTP (GE Healthcare) for visualization. The PCR products were separated on a 10% nondenaturing polyacrylamide gel (Invitrogen) and bands were visualized on a Typhoon 9400 Imager (GE Healthcare). Images were quantified using ImageQuant analysis software (Version 5.2, Molecular Dynamics). The percentage of Mcl-1_S in each lane was determined by dividing the intensity of the 194 bp band (Mcl-1_S) by the total intensities of the 442 bp (Mcl-1_L) and 194 bp (Mcl-1_S) bands. The identity of the 194 bp band was confirmed by sequencing by the UNC-CH Genome Analysis Facility.

Western Blot Analysis

Cells (1.0×10^5 cells/well in a 12-well plate) were washed twice with ice-cold PBS and lysed in RIPA buffer (radioimmune precipitation assay buffer; 50 mM Tris-HCl, 150 mM NaCl, 5 mM EDTA, 1% Triton X-100, 0.1% SDS, and 1% sodium deoxycholate)

supplemented with protease inhibitor cocktail (Sigma). Total protein was quantified by BCA using the Protein Assay Reagent (Pierce). Total protein (10 μg) was separated by electrophoresis on a pre-cast 4-12% Bis-Tris gel (Invitrogen) and electrotransferred onto a polyvinylidene difluoride (PVDF) membrane. Membranes were stained with Ponceau's stain to confirm equal loading and transfer. Membranes were blocked for 30 min in Blotto, consisting of Tris-buffered saline supplemented with 0.1% Tween 20 (TBS-T) and nonfat dry milk (5% w/v). Membranes were subsequently incubated overnight at 4ºC with the following primary antibodies in Blotto: polyclonal Mcl-1 antibody (1:3000; Santa Cruz Biotechnology, S-19), polyclonal PARP antibody (1:3000; Cell Signaling 9452) and mouse anti-β-actin monoclonal antibody (1:10,000; Sigma). Membranes were then incubated for 1 hour with horseradish peroxidase-conjugated anti-mouse (1:100,000; Sigma) or goat anti-rabbit (Abcam, 1:10,000) secondary antibodies. Blots were developed with ECL Plus reagents (GE Healthcare) and exposed to film (GE Healthcare). Mcl-1_L, Mcl-1_S, β-actin, cleaved PARP and full-length PARP migrated at 40, 32, 45, 89 and 116 kDa respectively. β-actin was used to confirm equal protein loading.

Cell death and chemosensitization assays

Cell death in response to SSO, plasmid DNA or staurosporine (Sts) treatment was measured by MTS assay (Promega). Cell viability was calculated relative to mock-transfected cells. For the chemosensitization study, six hours after transfection with SSO, the cell culture medium was replaced with medium containing various doses of Sts. Cells were incubated for 48 hours and then cell viability was calculated relative to untreated cells and normalized to the lowest Sts dose for each treatment group. Cell death and dose-response

curve data were analyzed by one-way analysis of variance (ANOVA) and Dunnett's post-test using Prism statistical software (GraphPad, version 4.03).

Results

Modification of Mcl-1 pre-mRNA splicing by SSO

The pro-apoptotic protein Mcl-1_S is translated from an mRNA transcript in which exon 2 is excluded through alternative splicing. However, this isoform is expressed at low levels in most cells. We predicted that steric block of either the 5′ or 3′ splice site of exon 2 with SSOs would prompt exon exclusion, thereby increasing expression of Mcl-1_S (Figure 3 A). To test this hypothesis, we first screened 2′-*O*-methyl (2OMe) phosphorothioate (PS) SSOs designed to hybridize to sequences surrounding the 5′ and 3′ splice sites of Mcl-1 exon 2. We used 2OMe SSOs in the initial screen because they can be inexpensively synthesized and do not support RNase H. HeLa cells transfected with 25 nM SSOs targeted to either splice site (SSOs 09-16) induced a concomitant down-regulation of Mcl-1_L and an up-regulation of Mcl-1_S mRNA (Figure 3.1 B). Splice-switching efficacies did not differ dramatically among SSOs targeted to the same splice site; however, at the 25 nM SSO concentration tested, the 5′ SSOs (SSO11-16) appeared to be slightly more potent inducers of splice-switching than the 3′ SSOs (SSO05-10).

For further study we decided to use 2′-*O*-methoxyethyl (MOE) SSOs because 2OMe oligonucleotides exhibit non-specific toxicity which would complicate the interpretation of results from apoptosis studies. Accordingly, MOE PS SSOs were synthesized for further study using the sequences corresponding to SSO9 and SSO16. HeLa cells were transfected with various concentrations of SSO21 and SSO22, which hybridize to the 5′ or 3′ splice sites of exon 2, respectively. RT-PCR analysis showed a dose-dependent redirection of Mcl-1 pre-

mRNA splicing ($EC_{50} \approx 20$ nM for SSO22, $EC_{50} \approx 10$ nM for SSO21) (Figure 3.2 A). Sequence analysis confirmed joining of exons one and three in the RT-PCR product (Figure 3.2 B). As a negative control, cells were mock-transfected or transfected with an SSO targeted to intron two of aberrantly-spliced β-globin (SSO654), which had no effect on Mcl-1 pre-mRNA splicing (Figure 3.2 A). Mcl-1_S was rapidly induced by SSO22 and redirection of splicing peaked at approximately 12 hours following transfection and persisted out to 72 hours. Mcl-1 splice switching was also demonstrated in Skmel-147 cells (Figure 3.2 D). The induction of Mcl-1_S mRNA was inhibited by the transcription inhibitor actinomycin D (10μg/ml), but not the translation inhibitor cycloheximide (1 and 10μg/ml) or the pan-caspase inhibitor Z-VAD-fmk (50 μM) (Figure 3.3).

Western blot analysis of cells transfected with SSO22 showed a dose-dependent down-regulation of Mcl-1_L protein and up-regulation of Mcl-1_S protein, confirming that Mcl-1_S protein generated by SSO was translated into protein (Figure 3.4 A, B). Levels of Mcl-1_L and -1_S protein were unchanged in the negative control groups.

Apoptosis and cell death induced by Mcl-1 Splice-switching

Next, we tested the hypothesis that the observed redirection in Mcl-1 pre-mRNA splicing would lead to increased apoptosis. Cells were transfected with various concentrations of SSO22 and 24 or 48 hours later total protein lysate was isolated and subjected to SDS-PAGE. Western Blot analysis showed a dose-dependent increase in the cleavage of poly (ADP-ribose) polymerase (PARP), a target of caspase cleavage representative of apoptosis induction (Figure 3.4 A, B). There was no PARP cleavage observed in cells treated with SSO654 control. Actin was used as a loading control.

To test whether modification of Mcl-1 pre-mRNA splicing from Mcl-1_L to Mcl-1_S is sufficient to induce cell death, cells were transfected with various concentrations of SSO22 and SSO654 control. Forty-eight hours later, cell viability was measured by MTS assay. Relative to mock-transfected cells, SSO22-treated cells showed a dose-dependant reduction in cell viability absent in SSO654-treated cells (P<0.01 for 50–150 nM) (Figure 3.5 A). Plasmid expression of Mcl-1_S was also sufficient to trigger cell death, consistent with previous reports (P<0.05 for 0.17μg, P<0.05 for 0.5μg) (Bae et al., 2000; Bingle et al., 2000). The levels of Mcl-1_S expression in SSO- and plasmid-transfected cells were compared by normalizing to β-actin expression in each sample (Figure 3.5 B). The level of Mcl-1_S expression induced by 50–150 nM SSO22 transfection was similar to that which was induced by 0.06–0.16 ug Mcl-1_S plasmid transfection.

Chemosensitization induced by SSO

Next we tested the hypothesis that redirection of Mcl-1 pre-mRNA splicing could render the affected cells more sensitive to chemotherapeutic agents. Six hours after transfection with SSO22 and SSO654 control, cells were treated with various concentrations of the pan-kinase inhibitor staurosporine and incubated for 48 hours. Cells pre-treated with SSO22 exhibited a significant shift in the dose-response to staurosporine compared to mock-transfected cells (P < 0.05) (Figure 3.6).

Discussion

The anti-apoptotic protein Mcl-1_L is emerging as an important therapeutic target for the treatment of cancer. Amplification of the *Mcl-1* and high levels of Mcl-1_L have been detected in a broad range of cancer types, suggesting a general role for Mcl-1_L in the survival

of cancer cells. In this study we sought to exploit the high tumor cell expression of *Mcl-1* through the redirection of alternative splicing to generate a potent pro-apoptotic protein, Mcl-1_S, thereby reducing the tumor cell's ability to evade apoptosis. To this end, we employed SSOs comprised of RNase H non-competent 2OMe or MOE modified bases to bind and block either the 5′ or 3′ splice site of exon 2 of Mcl-1 pre-mRNA to force exon 2 skipping.

The degree of Mcl-1 splice-switching induced by a given SSO is presumably due to the relative ability of each SSO to block the interaction of the splicing machinery with sequence elements. As a result, SSOs can exhibit dramatically different efficacies despite targeting to nearby or overlapping sequences depending on the presence of splice sites or regulators sequence elements within the target sequence (Graziewicz et al., 2008; Hua et al., 2007). In our initial screen, all 2OMe SSOs targeted to the same splice site exhibited comparable splice-switching efficiencies, suggesting that they utilized the same mechanism of action, namely steric blocking of either the 5′ or 3′ splice site. Blockade of the 5' splice site resulted slightly more potent antisense activity than blockade of the 3' splice site for both 2OMe and MOE SSOs. It is not unusual for the 5′ and 3′ splice sites to exhibit different sensitivities to SSOs. For example, 5′ SSOs were more effective than 3′ SSOs at skipping of exon 2 in MyD88 pre-mRNA (Vickers et al., 2006). In a detailed analysis of exon 23 skipping in dystrophin pre-mRNA the 5′ SSOs were found to be effective while the 3′ splice site was insensitive to SSOs (Mann et al., 2002).

When investigating novel agents for potential apoptotic activity, it is critical to minimize non-specific toxicity that would compromise the interpretation of experimental results. MOE oligonucleotides have been reported to exhibit lower non-specific toxicity relative to 2OMe in cell culture (Bennett and Swayze, 2010). Hence, once Mcl-1 splice-

switching was validated by the 2OMe SSO screen, further investigation of Mcl-1 splicing-switching was carried out using MOE SSOs. As predicted by the initial screen, transfection of MOE SSO22 and SSO21 resulted in the modification of Mcl-1 pre-mRNA splicing in Hela cells. (Figure 3.1 A, B). SSO22 was chosen for subsequent experiments to avoid potential off-target confounds due to the high degree of sequence homology at the 5′ splice site of exon 2 among Bcl-2 family members (See chapter 2, Figure 2.5).

To assess if *de novo* protein synthesis was required for Mcl-1 splice-switching, we tested the effect of SSO22 in the presence of the protein synthesis inhibitor cycloheximide. Cycloheximide did not inhibit production of Mcl-1_S, suggesting that SSO-induced splice-switching did not require *de novo* protein synthesis (Figure 3.3). It is possible that the SSO led only to down-regulation of Mcl-1_L, which could trigger apoptosis and promote the caspase-dependent degradation of components of the splicing machinery, thereby causing general disruption of splicing. Indeed, spliceosomal components and RNA-binding proteins can be targets for caspases (Back et al., 2002; Waterhouse et al., 1996). However, addition of the pan-caspase inhibitor Z-VAD-fmk did not abrogate production of Mcl-1_S mRNA induced by SSO22 (Figure 3.3). To test whether mRNA transcription was required for SSO-induced splice-switching, we tested the effect of SSO22 in the presence of the transcription inhibitor actinomycin D. Actinomyin D completely inhibited the expression of Mcl-1_S induced by SSO22 (Figure 3.3). SSO22 also induced splice-switching was also observed in cell lines other than HeLa (Figure 3.2D and observations by J.A.B.), indicating that this effect was not an experimental artifact confined to HeLa cells. Taken together, these results suggest that SSO22 required transcription but not translation or capsase activation to induce expression of Mcl-1_S mRNA, which is consistent with the predicted splice-switching mechanism of action.

The modification of Mcl-1 splicing by SSO22 was rapid, achieving maximal splice-switching at approximately 12 hours post-transfection (Figure 3.2 C). The rapid induction of Mcl-1_S was consistent with the high turnover previously report for Mcl-1 mRNA (Yang et al., 1996). The observed mRNA splice-switching by SSO was accompanied by a dose-dependent decrease in Mcl-1_L protein and increases in Mcl-1_S protein and PARP cleavage (Figure 3.4 A, B). Twenty-fours post-transfection, SSO concentrations of $\geq$50 nM resulted in >75% Mcl-1_S mRNA and approximately 50% Mcl-1_S protein relative to Mcl-1_L mRNA and protein levels, respectively (Figures 3.2 A, 3.4 A). Still, our data likely underestimate the true levels of SSO-induced Mcl-1_S mRNA and protein because a significant portion of the affected cells underwent apoptosis and thus were removed from the sample from which RNA and protein could be isolated and analyzed (Figure 3.5 A). At the protein level, the total level of Mcl-1 protein (i.e. Mcl-1_L + Mcl-1_S) in SSO22-treated cells appeared to less than the total level of Mcl-1 protein detected in negative control cells. This could have been caused by more efficient apoptosis of cells expressing higher levels of Mcl-1. In this case, only low Mcl-1 expressing cells—with less Mcl-1 pre-mRNA to convert into pro-apoptotic Mcl-1_S and perhaps relying on compensatory expression of anti-apoptotic Bcl-x_L and/or Bcl-2—would remain for protein isolation, resulting in the lower total Mcl-1 protein observed by Western Blot. An alternative explanation is that the antibody used Mcl-1 detection exhibited different affinities for the two splice variants.

SSO22-induced modification of Mcl-1 splicing and PARP cleavage was accompanied by dose-dependent reduction in cell viability, indicating that SSO22 induced apoptotic cell death. We wanted to explore the extent to which the observed cell death induced by SSO22 by was due to up-regulation of Mcl-1_S. It has been shown that Mcl-1_S induces cell death

when overexpressed with plasmid DNA (Bae et al., 2000). The level of Mcl-1_S expression that can be induced by SSO is dependent on endogenous expression. By titrating the amount of DNA used for transfection, we show that Mcl-1_S can induce cell death when expressed at levels comparable to those that can be induced by SSO (Figure 3.5 A, B). However, SSO22 was evidently more effective at inducing cell death than Mcl-1_S. This suggests that cell death induced by SSO22 is a function of both Mcl-1_L down-regulation and Mcl-1_S up-regulation.

Because of the important role of Mcl-1_L in enabling tumor cells to evade apoptosis, we asked whether Mcl-1 splice-switching could render cells more sensitive to chemotherapy. Pre-treatment of cells with SSO22 caused a shift in their dose-response to staurosporine, providing evidence of chemosensitization by Mcl-1 splice-switching. This finding is important because at the highest concentration tested about half of the cells remained viable when treated with SSO22 alone. Simultaneous treatment with chemotherapeutic agents, such as staurosporine, may be necessary to maximize the apoptosis-promoting potential of Mcl-1 splice-switching.

During the course of this investigation, another group reported the modification of Mcl-1 splicing in basal carcinoma cells using PMO SSOs (Shieh et al., 2009). Interestingly, targeting both the 5′ and 3′ splice sites simultaneously failed to a shift in Mcl-1 splicing >50% at the highest PMO concentration tested. They detected a modest induction of apoptosis (25% annexin V-positive cells vs. 10% in controls) and cell death was not reported.

DNA damaging agents, such as UV irradiation, cisplatin and etoposide, were found to induce poly-ubiquitination and subsequent proteasomal degradation of Mcl-1_L via the E3 ubiquitin ligase Mule. Mule encodes a BH3 domain that is required for its poly-ubiquitation of Mcl-1_L. Like the pro-apoptotic BH3-only proteins, Mule is thought to bind via its BH3

domain to the hydrophobic pocket in Mcl-1_L formed by its BH1–3 domains. Because Mcl-1_S lacks the BH1 and BH2 domains, it cannot form this binding site and is presumably not poly-ubiquitinated by Mule in response to DNA damage. In the presence of DNA damaging agents, Mcl-1_S induced by SSO might persist while Mcl-1_L is targeted for degradation. This possibility should be further studied.

Interestingly, elimination of Mcl-1_L by RNAi or by Noxa-mediated proteasomal degradation was required but not sufficient for apoptosis in HeLa cells (Cuconati et al., 2003; Nijhawan et al., 2003). The fact that Mcl-1 splice-switching induced apoptosis in this study could be the result of Mcl-1_S up-regulation by the SSO, especially if Mcl-1_S has pro-apoptotic functions outside of Mcl-1_L antagonism. For example, Mcl-1_S could bind and antagonize other Bcl-2 family members, such as Bfl-1/A1. Based on sequence homology, Bfl-1/A1 and Mcl-1_L are more closely related to each other than to Bcl-2, Bcl-x_L or Bcl-w (Petros et al., 2004). Mcl-1_S failed to bind the latter proteins in a yeast two-hybrid assay; however, binding between Mcl-1_S and Bfl-1/A1 has not been investigated. Alternatively, apoptosis induced by Mcl-1 splice-switching could be result of differences in the particular HeLa sublcones used in the different studies.

Our results confirm that blockade of either the 5′ or 3′ splice site of exon 2 in Mcl-1 pre-mRNA with SSOs results in a modification of splicing from Mcl-1_L to -1_S. Mcl-1 splice-switching resulted in dose-dependent increases in Mcl-1_S protein expression and apoptotic cell death. We also show, for the first time, sensitization to chemotherapeutics induced by Mcl-1 splice-switching.

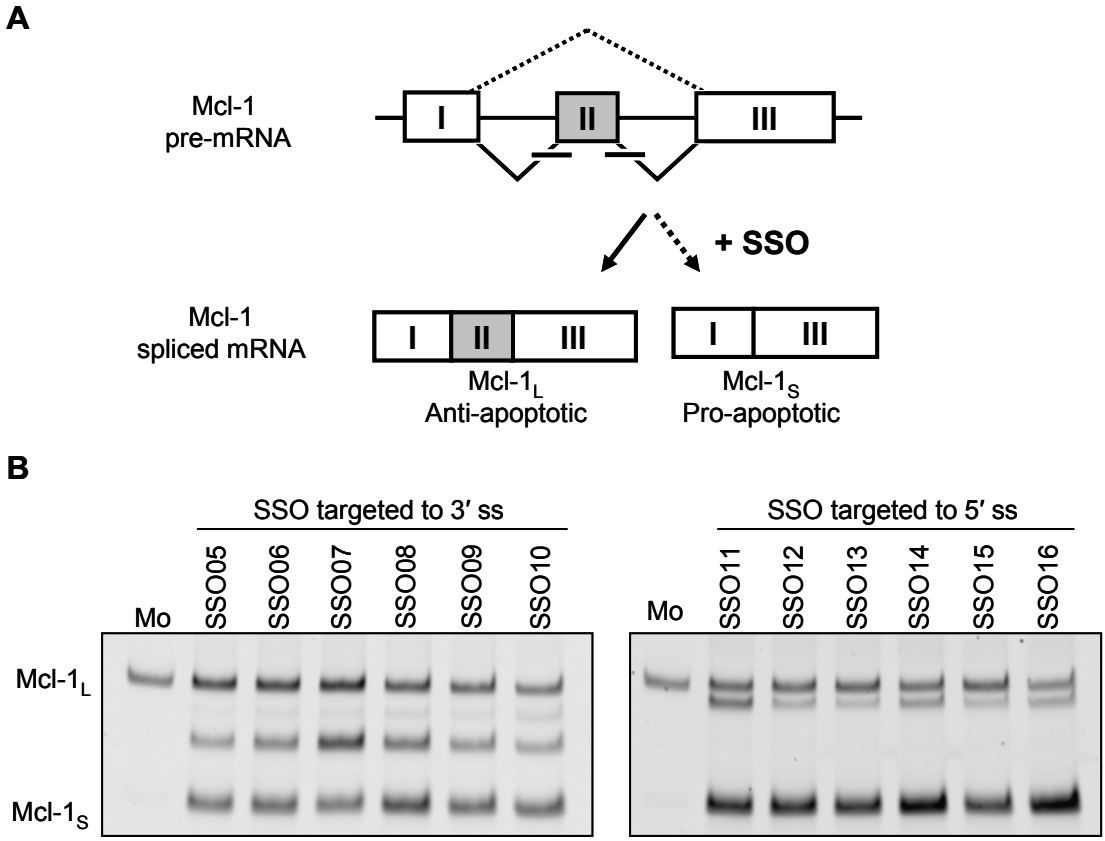

Figure 3.1. 2′-O-methyl SSOs targeted to the 3′ and 5′ splice sites of Mcl-1 exon 2 modify the pattern of alternative splicing.
(A) Inclusion of all three exons from Mcl-1 pre-mRNA results in expression of anti-apoptotic Mcl-1_L while skipping of exon 2 results in expression of pro-apoptotic Mcl-1_S. (B) RNase H non-competent 2′-O-methyl SSOs targeted to the 3′ or 5′ splice site of exon 2 induce expression of Mcl-1_S mRNA.

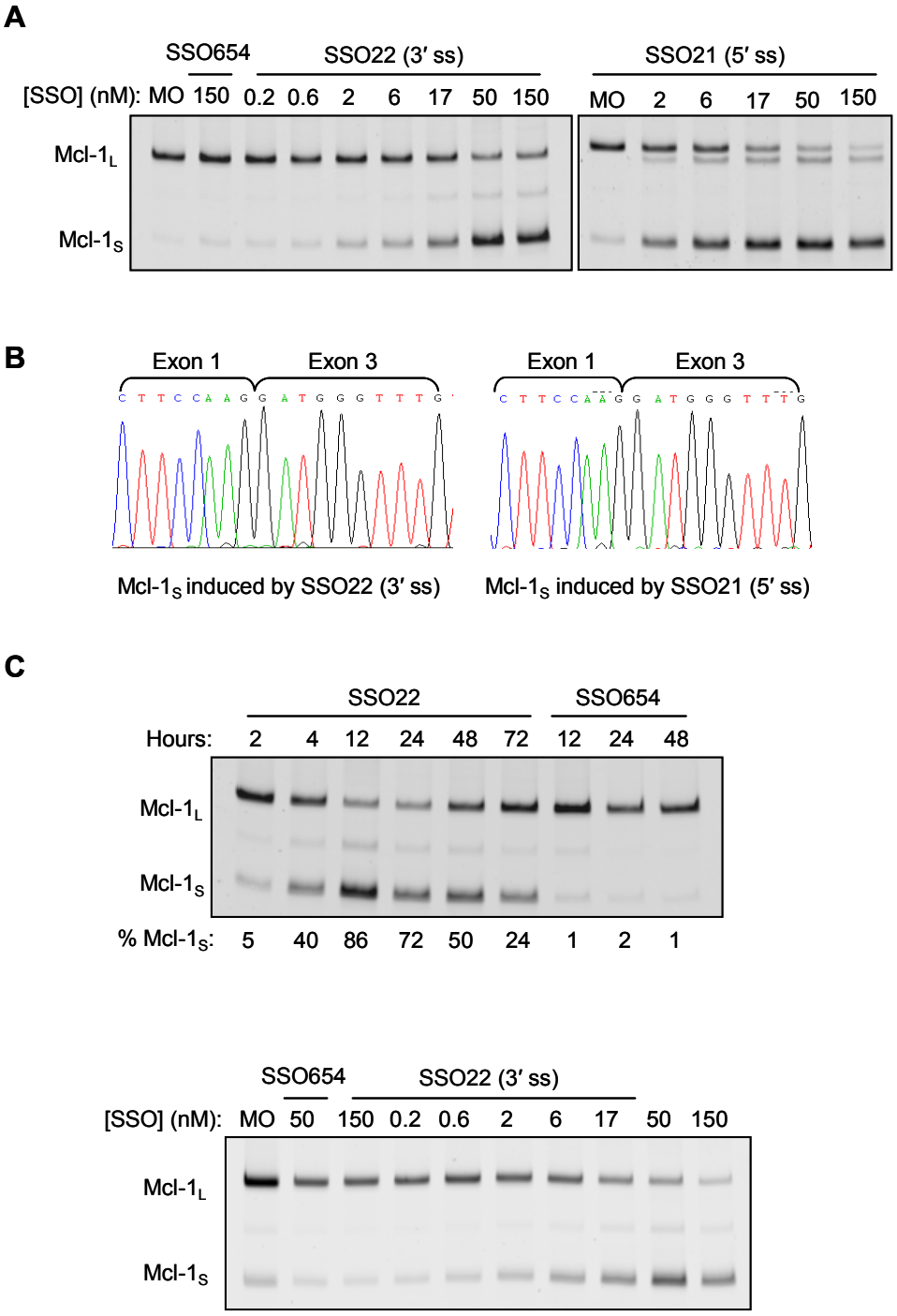
A
SSO654
SSO22 (3′ ss)
SSO21 (5′ ss)
[SSO] (nM): MO 150 0.2 0.6 2 6 17 50 150
MO 2 6 17 50 150
Mcl-1L
Mcl-1S
B
Exon 1
Exon 3
Exon 1
Exon 3
Mcl-1S induced by SSO22 (3′ ss)
Mcl-1S induced by SSO21 (5′ ss)
C
SSO22
SSO654
Hours: 2 4 12 24 48 72 12 24 48
Mcl-1L
Mcl-1S
% Mcl-1S: 5 40 86 72 50 24 1 2 1
SSO654
SSO22 (3′ ss)
[SSO] (nM): MO 50 150 0.2 0.6 2 6 17 50 150
Mcl-1L
Mcl-1S

Figure 3.2 2′-O-methoxyethyl (MOE) SSOs targeted to the 5′ or 3′ splice site of exon 2 modify the pattern of Mcl-1 alternative splicing.
(A) Modification of Mcl-1 alternative splicing using MOE SSOs targeted to the 5′ (SSO21) or 3′ splice site (SSO22) of exon 2 in Mcl-1 pre-mRNA. Splice-switching is dose-dependent and absent in cells treated with a control SSO (SSO654). (B) Sequences analysis of PCR bands corresponding to Mcl-1_S induced by SSO22 (3′ splice site) and SSO21 (5′ splice site) confirm skipping of exon 2. (C) Time-course of Mcl-1 splice-switching by SSO22. (D) SSO-induced Mcl-1 splice-switching in Skmel-147 melanoma cells indicates that SSO activity is not an artifact confined HeLa cells.

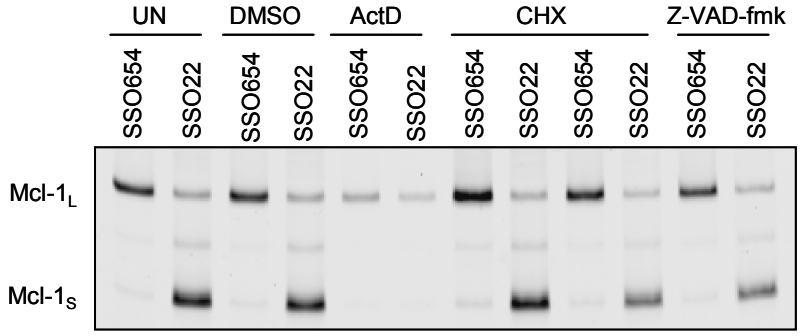

Figure 3.3 SSO induction of Mcl-1_S mRNA requires transcription but not translation or caspase activation.
HeLa cells were pre-treated with the transcriptional inhibitor actinomycin D (ActD, 10 μg/μl), the translational inhibitor cycloheximide (CHX, 1 and 1 μg/μl), and the pan-caspase inhibitor Z-VAD-fmk (50 μM), and then transfected with either negative control (SSO654) or Mcl-1 3′ SSO (SSO22). Only transcriptional inhibition blocks expression of Mcl-1_S, consistent with the SSO acting by modification of splicing, as expected.

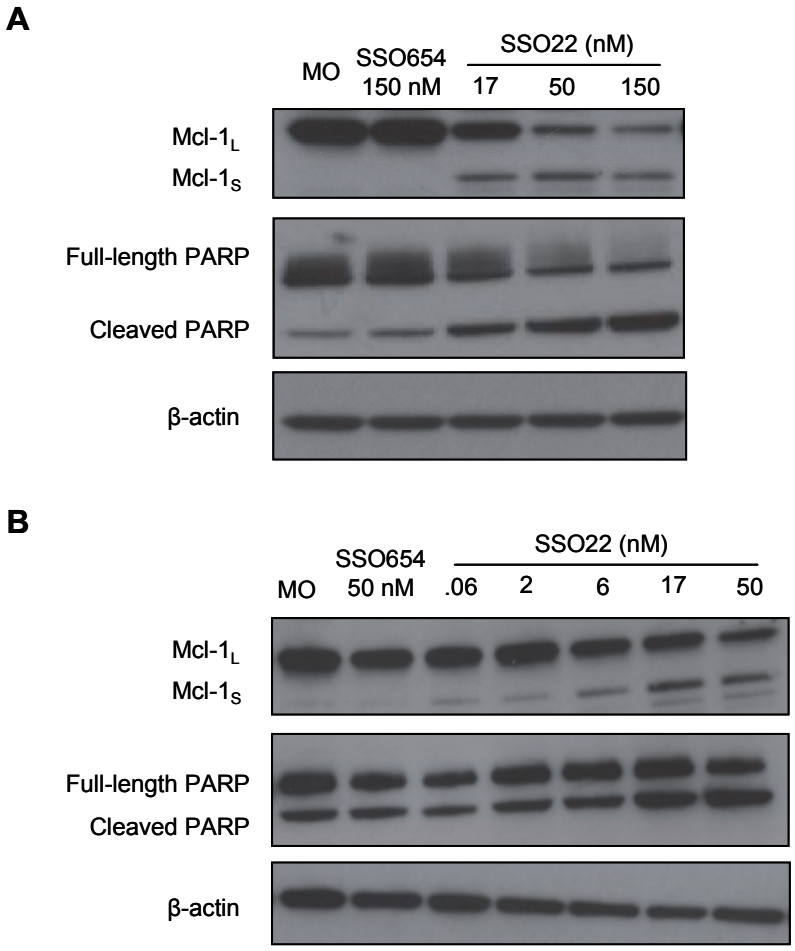

Figure 3.4 SSO induces Mcl-1_S protein expression and apoptosis in a dose-dependent manner.
Western blot analysis of cells transfected with SSO22 or SSO654 control for 24 (A) or 48 (B) hours. SSO22 induced a dose-dependent increase in Mcl-1_S protein and a concomitant decrease in Mcl-1_L expression. SSO22 also induced a dose-dependent increase in cleavage of PARP, a target of caspases. SSO654 control had no effect on the expression of Mcl-1 protein or PARP cleavage.

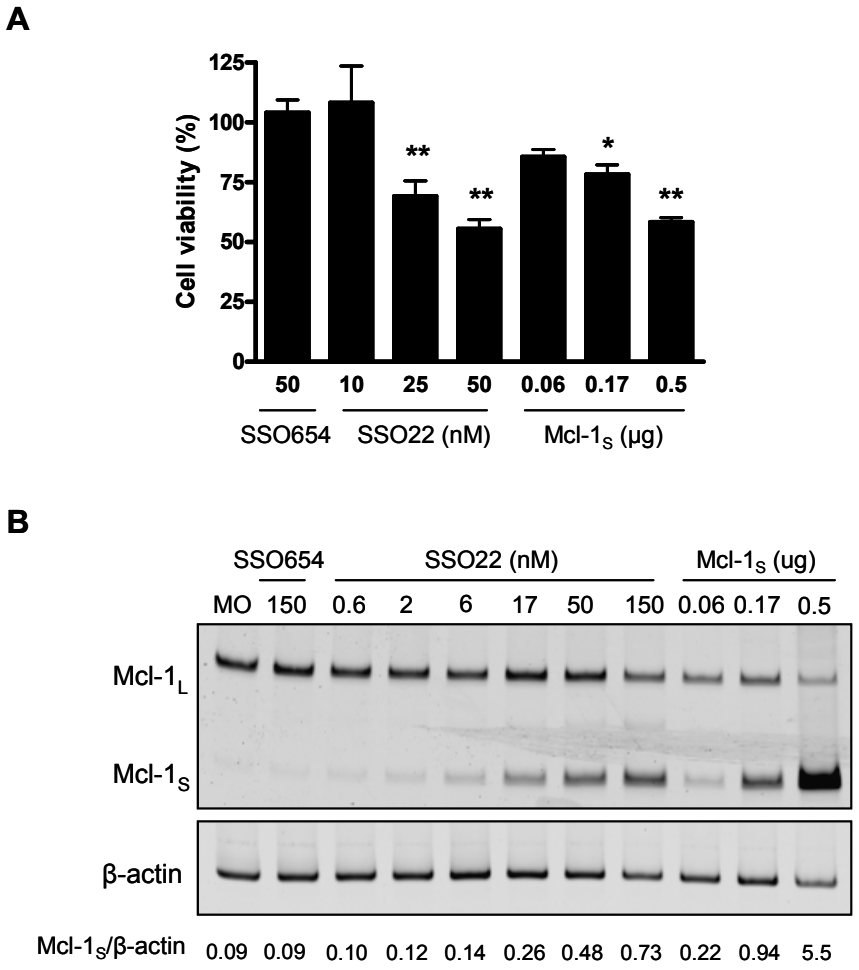

Figure 3.5 SSO-induced Mcl-1 splice-switching results in cell death.
(A) Cell transfected with SSO22 or Mcl-1_S plasmid undergo dose-dependent cell death as determine by MTS assay. * $P<0.05$, ** $P<0.01$. (B) RT-PCR analysis of mRNA from cells transfected with SSO or Mcl-1_S plasmid. Expression of Mcl-1_S mRNA was normalized to that of β-actin and the ratios of Mcl-1_S to β-actin as a measure of Mcl-1_S are listed. Expression of Mcl-1_S plasmid at levels comparable to that which can be induced by SSO22 resulted in cell death.

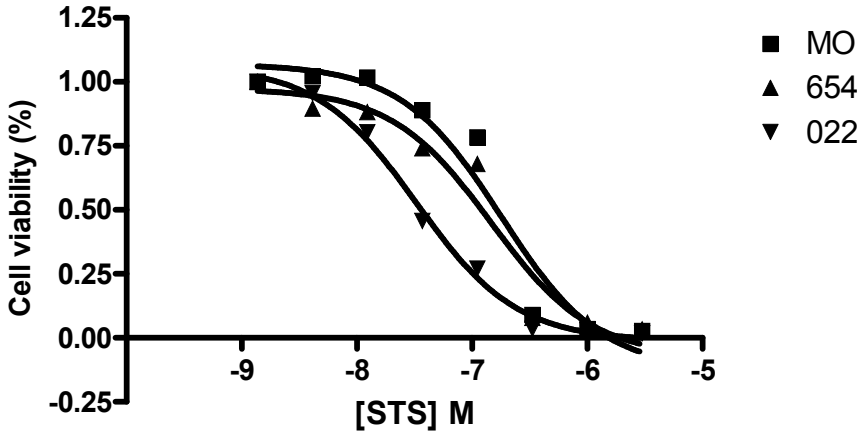

	MO	SSO654	SSO22
$LOGEC_{50}$	−6.8	−6.8	−7.5

Figure 3.6 SSO-induced Mcl-1 splice-switching sensitizes cells to staurosporine. Cell were transfected with SSO22 or SSO654 control and subsequently treated with increasing concentrations of the pan-kinase inhibitor staursporine (STS). The cells were incubated for 48 hours and then cell death was measured by MTS assay. Pre-treatment with SSO22 resulted in shift in the dose-response to staurosporine.

Chapter 4 – Summary of Results

Summary of Results

Early studies by Mercatante et al. and Taylor et al. established that RNase H non-competent splice-switching oligonucleotides (SSOs) targeted to the downstream (Bcl-x_L) 5′ splice site of exon 2 in Bcl-x pre-mRNA could modify the pattern of Bcl-x splicing *in vitro*. They further showed that Bcl-x splice-switching induced apoptotic cell death and chemosensitization in breast, prostate and lung cancer cells. I have recapitulated these results in a murine melanoma cell line. These *in vitro* results demonstrate the promise of Bcl-x splice-switching as a therapeutic strategy; however, the anti-cancer potential of Bcl-x splice-switching remained to be validated in a setting that more faithfully reproduces the microenvironment of a tumor *in vivo*. Using a lipid nanoparticle (LPD NP) to aid delivery, I showed that SSOs could induce Bcl-x splice-switching in melanoma xenografts; this result constituted the first demonstration of pre-mRNA splicing modification in tumor cells *in vivo*. Importantly, the observed Bcl-x splice-switching was associated with a reduction in tumor burden absent in the animals in negative control treatment groups.

Delivery is a chief concern for the application of oligonucleotide drugs. The first and only approved oligonucleotide drug, Vitravene, and the RNA aptamer drug Macugene, are administered by intravitreal injection, essentially circumventing many of the biological barriers typically encountered by systemically administered drugs. In order to realize the full therapeutic utility of SSOs, these barriers will have to be overcome. Lipid nanoparticles, such as the LPD NP used herein, have been effective at *in vivo* delivery of siRNA and SSO in mouse xenograft models (Bauman et al., 2010; Li et al., 2008a; Li et al., 2008b; Li et al., 2008c; Li and Huang, 2006a). These formulations are comprised of multiple components (e.g., liposomes, carrier molecules, targeting ligands) making their approval for use in

humans complicated from a regulatory and pharmaceutics perspective; immunotoxicity is also a concern. Further study and continued optimization of the LPD NP should improve upon these limitations. For example, Chono et al. showed that substituting calf thymus DNA with hyaluronic acid reduced immunostimulation caused by high doses of the NP (Chono et al., 2008). Although clinical utility of the LPD NP has not yet been established, it proved to be useful tool for the *in vivo* evaluation of Bcl-x SSOs. Future iterations of the LPD NP should be considered for the study and validation other splice-switching targets in cancer.

Several studies using animal models show that uptake, potency and cell targeting of PMO SSOs can be improved by the addition of arginine-rich cell-penetrating peptides (CPP) (Ivanova et al., 2008; Jearawiriyapaisarn et al., 2008; Jearawiriyapaisarn et al., 2010; Wu et al., 2009; Wu et al., 2008; Yin et al., 2008b; Yokota, 2008). Hence, CPP conjugates warrant further study for tumor targeting and delivery of SSOs.

In addition to Bcl-x, there are numerous alternatively-spliced transcripts implicated in cancer that constitute potential targets for splice-switching strategies (Table 4.1). Among these candidates, Mcl-1 undergoes alternative splicing to produce anti-apoptotic Mcl-1_L, which has been linked to the pathogenesis of a variety of cancers, and pro-apoptotic Mcl-1_S, which is expressed at very low levels. In this dissertation, I showed that SSOs targeted to the 5′ or 3′ splice site of exon 2 in Mcl-1 pre-mRNA modify the pattern of splicing from Mcl-1-$_L$ to -1_S. Mcl-1 splice-switching induced apoptosis and cell death, and sensitized cells to staurosporine. These findings provide evidence that Mcl-1 splice-switching is a potential anti-cancer strategy.

As with Bcl-x splice-switching, the efficacy of Mcl-1 SSOs should be evaluated for anti-cancer effects in *in vivo* systems. Multiple myeloma would make a good candidate for

future Mcl-1 splice-switching studies for several reasons. First, Mcl-1_L expression was established as a critical survival factor for multiple myeloma (Zhang et al., 2002). Second, patient samples can be readily obtained and treated with SSOs *ex vivo*; this might represent the heterogeneous disease state more accurately than immortalized cell lines. Finally, *in vivo* delivery to circulating myeloma cells might present fewer challenges than delivery to solid tumors. Numerous studies have demonstrated that knockdown of Mcl-1_L sensitizes resistant cells lines to the pan-Bcl-2 inhibitor ABT-737 (Chen et al., 2007; van Delft et al., 2006; Wesarg et al., 2007). Accordingly, the ability of Mcl-1 SSOs to synergize with ABT-737 and other cancer therapeutics warrants future study.

The finding that Bcl-x splice-switching resulted in anti-cancer activity *in vivo* adds to the mounting evidence supporting the therapeutic utility of ASOs in general and SSOs in particular. The approval of Vitravene in 1998, indicated for the treatment of cytomegalovirus retinitis in immunocompromised patients, demonstrates the capacity of antisense drugs to meet regulatory requirements for safety and efficacy. Promising RNase H-active ASOs in late-stage clinical trials include Mipomersan, which targets Apolipoprotein-B100 for treatment of hypercholesterolemia, and OGX-011, which targets clusterin for treatment of cancer. In addition, SSOs that restore dystrophin expression in DMD patients are progressing in the clinic (Table 4.2) (Kinali et al., 2009; Sazani et al., 2010; van Deutekom et al., 2007).

As illustrated in Table 4.2, there are now numerous oligonucleotide therapeutics currently under clinical investigation for treatment of cancer. All of these drug candidates utilize the RNase H or siRNA mechanism of action, and therefore down-regulate gene expression. Despite a rich and growing pool of cancer targets suitable for splice-switching strategies (Table 4.1) there are presently no ongoing clinical trials using SSOs for the

treatment of cancer. This observation, coupled with the recent progress of SSOs for non-cancer indications, indicate that SSOs aimed at cancer therapy occupy a largely unexploited niche at the intersection of splice-switching and anti-cancer drugs. This is likely the result of poor delivery of previously tested oligonucleotides to tumors, a problem which I have begun to address with the research presented in this dissertation. As delivery vehicles continue to improve, splice-switching as a strategy for cancer therapy should move closer to becoming a reality. Importantly, Bcl-x and Mcl-1 have recently been validated as key genes in numerous cancers (Beroukhim et al., 2010), providing additional impetus for continuation of the work initiated here.

Role in cancer	Gene	Splice variants	Cellular effect
Apoptosis	Bcl-x	Bcl-x_L	Anti-apoptotic, up-regulated in cancers, promotes chemoresistance
		Bcl-x_S	Pro-apoptotic, antagonizes Bcl-x_L and Bcl-2
	Mcl-1	Mcl-1_L	Anti-apoptotic, up-regulated in cancers, promotes chemoresistance
		Mcl-1_S	Pro-apoptotic, antagonizes Mcl-1_L
	Caspase-2	Caspase-2L	Pro-apoptotic
		Caspase-2S	Anti-apoptotic, protects against chemotherapeutics
	Caspase-9	Caspase-9	Pro-apoptotic
		Caspase-9B	Anti-apoptotic, inhibits apoptosome formation
	Survivin	Survivin	Anti-apoptotic, up-regulated in cancers
		Survivin-2B	Pro-apoptotic, antagonizes survivin
Cell proliferation	Fas	Fas	Mediates apoptotic signaling
		FasExo8Del	Inhibits Fas-mediated apoptosis, up-regulated in certain cancers
	HER2	HER2	Promotes proliferation and survival of cancer cells
		Herstatin	Pro-apoptotic, soluble dominant-negative inhibitor or HER2
		Δ15HER2	Pro-apoptotic, soluble dominant-negative inhibitor or HER2
	Rac1	Rac1	Regulates cell proliferation and cytoskeletal reorganization
		Rac1b	Increased rate of GDP/GTP exchange leads to constitutive activation, transforms cells in culture, expressed exclusively in tumors tissue
Angiogenesis	VEGF	VEGFA	Promotes angiogenesis through activations of VEGF receptors 1 and 2, up-regulated in many cancers
		VEGF165b	Inhibits angiogenesis through competitive inhibition of VEGF receptor 2
Transcription factors	p53	p53	Tumor suppressor, transcription factor
		p47	Antagonizes p53 tumor suppressor
	KLF6	KLF6	Tumor suppressor, transcription factor
		KLF6-SV1	Antagonizes KLF6, up-regulated in certain cancers

Table 4.1 Alternatively-spliced gene transcripts important in cancer.
Listed are examples of genes involved in the proliferation, survival and chemoresistance of cancer cells that express splice variants with different functions [Comprehensively reviewed in (David and Manley, 2010; Mercatante and Kole, 2002; Schwerk and Schulze-Osthoff, 2005)]. This non-comprehensive list suggests a richness of potential targets for splice-switching strategies for cancer therapy.

Drug	Indication	Target	Mechanism	Chemsitry	Route	Status
Fomiversen	Cytomegalovirus	IE2 gene	RNase H	PS ODN	Intravitreal	Approved
Genasense	Cancer	Bcl-2	RNase H	PS DNA	Systemic	Phase 3
Mipomersen	Cardiovascular	Apolipoprotein B	RNase H	MOE gapmer	Systemic	Phase 3
Trabederen	Cancer	Transforming growth factor-β	RNase H	PS DNA	Intratumoral	Phase 3
LOR-2040	Cancer	Ribonucleotide reductase	RNase H	PS DNA	Systemic	Phase 3
Archexin	Cancer	AKT-1	RNase H	PS DNA	Systemic	Phase 3
Custirsen	Cancer	Clusterin	RNase H	MOE gapmer	Systemic	Phase 3
TPI ASM8	Asthma	CCR3 and IL-5 (two oligomers)	RNase H	PS DNA	Inhaled	Phase 2
Alicaforsen	Colitis	Intracellular adhesion molecule-1	RNase H	PS DNA	Enema	Phase 2
AEG35156	Cancer	X-IAP	RNase H	2OMe gapmer	Systemic	Phase 2
TV.ATL1102	Multiple sclerosis	CD49D	RNase H	2OMe gapmer	Systemic	Phase 2
LY2181308	Cancer	Survivin	RNase H	MOE gapmer	Systemic	Phase 2
ISIS111317	Diabetes, type 2	Protein tyrosine phosphatase-B	RNase H	MOE gapmer	Systemic	Phase 2
Monarsen	Myasthenia gravis	Acetylcholine esterase	RNase H	MOE gapmer	Oral	Phase 2
PRO-051	DMD	Dystrophin	Splice-switching	2OMe	Systemic	Phase 2
AVI-4658	DMD	Dystrophin	Splice-switching	PMO	Systemic	Phase 2
ALNSRV-01	Respiratory syncytial virus	Nucleocapsid N gene	siRNA	dsRNA (unmodified)	Inhaled	Phase 2
PF-4523655	Age-related macular degeneracy	RTP801	siRNA	dsRNA (unmodified)	Intravitreal	Phase 2
AIR 645	Asthma	eIF-4E	RNase H	MOE gapmer	Inhaled	Phase 1
ISIS-CRP	Diabetes	Sodium-dependent glucose transporter 2	RNase H	MOE gapmer	Intravitreal	Phase 1
iCO-007	Macular degeneration	C-raf kinase	RNase H	MOE gapmer	Systemic	Phase 1
LY2275796	Cancer	eIF-4E	RNase H	MOE gapmer	Systemic	Phase 1
OGX-427	Cancer	Heat shock protein 27	RNase H	MOE gapmer	Systemic	Phase 1
SPC2996	Cancer	Bcl-2	RNase H	LNA gapmer	Systemic	Phase 1/2
EZN2968	Cancer	Hypoxia inducing factor 1-α	RNase H	LNA gapmer	Systemic	Phase 1
EZN3042	Cancer	Survivin	RNase H	LNA gapmer	Systemic	Phase 1
PRO044	DMD	Dystrophin	Splice-switching	2OMe	Systemic	Phase 1
QPI-1102	Acute kidney injury	p53	siRNA	dsRNA	Systemic	Phase 1
ALN-VSP	Cancer	Vascular endothelial growth factor	siRNA	Modified dsRNA in liposome formulation	Systemic	Phase 1
CALAA-01	Cancer	Ribonucleotide reductase	siRNA	dsRNA in nanoparticulate formulation	Systemic	Phase 1

Table 4.2 Oligonucleotide drugs currently in clinical trials or marketed.
Listed are examples of oligonucleotide drugs in clinical trials. There are currently three SSO drugs in clinical trials, all for treatment of Duchenne Muscular Dystrophy. All of the drug candidates indicated for cancer utilize the RNase H or siRNA mechanism of action, and thus are all down-regulate target gene expression. Many of the late-phase candidates utilize PS DNA chemistry, which is vulnerable to enzymatic cleavage and is rapidly cleared. For this reason, early-phase candidates utilizing PMO, MOE and LNA chemistries are more likely to gain approval and commercial success. Source: www.ClinicalTrials.gov.

LITERATURE CITED

Aartsma-Rus, A., Janson, A. A., Kaman, W. E., Bremmer-Bout, M., den Dunnen, J. T., Baas, F., van Ommen, G. J., and van Deutekom, J. C. (2003). Therapeutic antisense-induced exon skipping in cultured muscle cells from six different DMD patients. Hum Mol Genet *12*, 907-914.

Aartsma-Rus, A., Kaman, W. E., Bremmer-Bout, M., Janson, A. A., den Dunnen, J. T., van Ommen, G. J., and van Deutekom, J. C. (2004). Comparative analysis of antisense oligonucleotide analogs for targeted DMD exon 46 skipping in muscle cells. Gene Ther *11*, 1391-1398.

Abes, S., Williams, D., Prevot, P., Thierry, A., Gait, M. J., and Lebleu, B. (2006). Endosome trapping limits the efficiency of splicing correction by PNA-oligolysine conjugates. J Control Release *110*, 595-604.

Adams, J. M., and Cory, S. (2007). The Bcl-2 apoptotic switch in cancer development and therapy. Oncogene *26*, 1324-1337.

Aichberger, K. J., Mayerhofer, M., Krauth, M. T., Skvara, H., Florian, S., Sonneck, K., Akgul, C., Derdak, S., Pickl, W. F., Wacheck, V.*, et al.* (2005). Identification of mcl-1 as a BCR/ABL-dependent target in chronic myeloid leukemia (CML): evidence for cooperative antileukemic effects of imatinib and mcl-1 antisense oligonucleotides. Blood *105*, 3303-3311.

Akhtar, S., and Benter, I. F. (2007). Nonviral delivery of synthetic siRNAs in vivo. J Clin Invest *117*, 3623-3632.

Alam, M. R., Dixit, V., Kang, H., Li, Z. B., Chen, X., Trejo, J., Fisher, M., and Juliano, R. L. (2008). Intracellular delivery of an anionic antisense oligonucleotide via receptor-mediated endocytosis. Nucleic Acids Res *36*, 2764-2776.

Alter, J., Lou, F., Rabinowitz, A., Yin, H., Rosenfeld, J., Wilton, S. D., Partridge, T. A., and Lu, Q. L. (2006). Systemic delivery of morpholino oligonucleotide restores dystrophin expression bodywide and improves dystrophic pathology. Nat Med *12*, 175-177.

Amundson, S. A., Myers, T. G., Scudiero, D., Kitada, S., Reed, J. C., and Fornace, A. J., Jr. (2000). An informatics approach identifying markers of chemosensitivity in human cancer cell lines. Cancer Res *60*, 6101-6110.

Back, S. H., Shin, S., and Jang, S. K. (2002). Polypyrimidine tract-binding proteins are cleaved by caspase-3 during apoptosis. J Biol Chem *277*, 27200-27209.

Backus, H. H., Van Groeningen, C. J., Vos, W., Dukers, D. F., Bloemena, E., Wouters, D., Pinedo, H. M., and Peters, G. J. (2002). Differential expression of cell cycle and apoptosis related proteins in colorectal mucosa, primary colon tumours, and liver metastases. J Clin Pathol *55*, 206-211.

Bae, J., Leo, C. P., Hsu, S. Y., and Hsueh, A. J. (2000). MCL-1S, a splicing variant of the antiapoptotic BCL-2 family member MCL-1, encodes a proapoptotic protein possessing only the BH3 domain. J Biol Chem *275*, 25255-25261.

Baker, B. F., Lot, S. S., Condon, T. P., Cheng-Flournoy, S., Lesnik, E. A., Sasmor, H. M., and Bennett, C. F. (1997). 2'-O-(2-Methoxy)ethyl-modified anti-intercellular adhesion molecule 1 (ICAM-1) oligonucleotides selectively increase the ICAM-1 mRNA level and inhibit formation of the ICAM-1 translation initiation complex in human umbilical vein endothelial cells. J Biol Chem *272*, 11994-12000.

Ban, J., Eckhart, L., Weninger, W., Mildner, M., and Tschachler, E. (1998). Identification of a human cDNA encoding a novel Bcl-x isoform. Biochem Biophys Res Commun *248*, 147-152.

Banerjee, R., Tyagi, P., Li, S., and Huang, L. (2004). Anisamide-targeted stealth liposomes: a potent carrier for targeting doxorubicin to human prostate cancer cells. Int J Cancer *112*, 693-700.

Baughan, T., Shababi, M., Coady, T. H., Dickson, A. M., Tullis, G. E., and Lorson, C. L. (2006). Stimulating full-length SMN2 expression by delivering bifunctional RNAs via a viral vector. Mol Ther *14*, 54-62.

Bauman, J., Jearawiriyapaisarn, N., and Kole, R. (2009). Therapeutic potential of splice-switching oligonucleotides. Oligonucleotides *19*, 1-13.

Bauman, J. A., Li, S. D., Yang, A., Huang, L., and Kole, R. (2010). Anti-tumor activity of splice-switching oligonucleotides. Nucleic Acids Res.

Bem, W. T., Thomas, G. E., Mamone, J. Y., Homan, S. M., Levy, B. K., Johnson, F. E., and Coscia, C. J. (1991). Overexpression of sigma receptors in nonneural human tumors. Cancer Res *51*, 6558-6562.

Bennett, C. F. (2008). Pharmacological Properties of 2'-O-Methoxyethyl-Modified Oligonucleotides. In Antisense Drug Technology: Principles, Strategies, and Applications, S. T. Crooke, ed. (CRC Press: Boca Raton, FL), pp. 273-304.

Bennett, C. F., and Swayze, E. E. (2010). RNA targeting therapeutics: molecular mechanisms of antisense oligonucleotides as a therapeutic platform. Annu Rev Pharmacol Toxicol *50*, 259-293.

Beroukhim, R., Mermel, C. H., Porter, D., Wei, G., Raychaudhuri, S., Donovan, J., Barretina, J., Boehm, J. S., Dobson, J., Urashima, M.*, et al.* (2010). The landscape of somatic copy-number alteration across human cancers. Nature *463*, 899-905.

Bingle, C. D., Craig, R. W., Swales, B. M., Singleton, V., Zhou, P., and Whyte, M. K. (2000). Exon skipping in Mcl-1 results in a bcl-2 homology domain 3 only gene product that promotes cell death. J Biol Chem *275*, 22136-22146.

Black, D. L. (2003). Mechanisms of alternative pre-messenger RNA splicing. Annu Rev Biochem *72*, 291-336.

Boise, L. H., Gonzalez-Garcia, M., Postema, C. E., Ding, L., Lindsten, T., Turka, L. A., Mao, X., Nunez, G., and Thompson, C. B. (1993). bcl-x, a bcl-2-related gene that functions as a dominant regulator of apoptotic cell death. Cell *74*, 597-608.

Boisvert-Adamo, K., Longmate, W., Abel, E. V., and Aplin, A. E. (2009). Mcl-1 is required for melanoma cell resistance to anoikis. Mol Cancer Res *7*, 549-556.

Boulares, A. H., Yakovlev, A. G., Ivanova, V., Stoica, B. A., Wang, G., Iyer, S., and Smulson, M. (1999). Role of poly(ADP-ribose) polymerase (PARP) cleavage in apoptosis. Caspase 3-resistant PARP mutant increases rates of apoptosis in transfected cells. J Biol Chem *274*, 22932-22940.

Brannon-Peppas, L., and Blanchette, J. O. (2004). Nanoparticle and targeted systems for cancer therapy. Adv Drug Deliv Rev *56*, 1649-1659.

Brown, D. A., Kang, S. H., Gryaznov, S. M., DeDionisio, L., Heidenreich, O., Sullivan, S., Xu, X., and Nerenberg, M. I. (1994). Effect of phosphorothioate modification of oligodeoxynucleotides on specific protein binding. J Biol Chem *269*, 26801-26805.

Caceres, J. F., Misteli, T., Screaton, G. R., Spector, D. L., and Krainer, A. R. (1997). Role of the modular domains of SR proteins in subnuclear localization and alternative splicing specificity. J Cell Biol *138*, 225-238.

Cartegni, L., and Krainer, A. R. (2002). Disruption of an SF2/ASF-dependent exonic splicing enhancer in SMN2 causes spinal muscular atrophy in the absence of SMN1. Nat Genet *30*, 377-384.

Cartegni, L., and Krainer, A. R. (2003). Correction of disease-associated exon skipping by synthetic exon-specific activators. Nat Struct Biol *10*, 120-125.

Castilla, C., Congregado, B., Chinchon, D., Torrubia, F. J., Japon, M. A., and Saez, C. (2006). Bcl-xL is overexpressed in hormone-resistant prostate cancer and promotes survival of LNCaP cells via interaction with proapoptotic Bak. Endocrinology *147*, 4960-4967.

Chalfant, C. E., Rathman, K., Pinkerman, R. L., Wood, R. E., Obeid, L. M., Ogretmen, B., and Hannun, Y. A. (2002). De novo ceramide regulates the alternative splicing of caspase 9 and Bcl-x in A549 lung adenocarcinoma cells. Dependence on protein phosphatase-1. J Biol Chem *277*, 12587-12595.

Chang, B. S., Kelekar, A., Harris, M. H., Harlan, J. E., Fesik, S. W., and Thompson, C. B. (1999). The BH3 domain of Bcl-x(S) is required for inhibition of the antiapoptotic function of Bcl-x(L). Mol Cell Biol *19*, 6673-6681.

Chen, L., Willis, S. N., Wei, A., Smith, B. J., Fletcher, J. I., Hinds, M. G., Colman, P. M., Day, C. L., Adams, J. M., and Huang, D. C. (2005). Differential targeting of prosurvival Bcl-2 proteins by their BH3-only ligands allows complementary apoptotic function. Mol Cell *17*, 393-403.

Chen, S., Dai, Y., Harada, H., Dent, P., and Grant, S. (2007). Mcl-1 down-regulation potentiates ABT-737 lethality by cooperatively inducing Bak activation and Bax translocation. Cancer Res *67*, 782-791.

Cheng, E. H., Kirsch, D. G., Clem, R. J., Ravi, R., Kastan, M. B., Bedi, A., Ueno, K., and Hardwick, J. M. (1997). Conversion of Bcl-2 to a Bax-like death effector by caspases. Science *278*, 1966-1968.

Cheng, E. H., Wei, M. C., Weiler, S., Flavell, R. A., Mak, T. W., Lindsten, T., and Korsmeyer, S. J. (2001). BCL-2, BCL-X(L) sequester BH3 domain-only molecules preventing BAX- and BAK-mediated mitochondrial apoptosis. Mol Cell *8*, 705-711.

Choi, J. S., MacKay, J. A., and Szoka, F. C., Jr. (2003). Low-pH-sensitive PEG-stabilized plasmid-lipid nanoparticles: preparation and characterization. Bioconjug Chem *14*, 420-429.

Chonghaile, T. N., and Letai, A. (2008). Mimicking the BH3 domain to kill cancer cells. Oncogene *27 Suppl 1*, S149-157.

Chono, S., Li, S. D., Conwell, C. C., and Huang, L. (2008). An efficient and low immunostimulatory nanoparticle formulation for systemic siRNA delivery to the tumor. J Control Release *131*, 64-69.

Chung, T. K., Cheung, T. H., Lo, W. K., Yim, S. F., Yu, M. Y., Krajewski, S., Reed, J. C., and Wong, Y. F. (2002). Expression of apoptotic regulators and their significance in cervical cancer. Cancer Lett *180*, 63-68.

Cooper, T. A., Wan, L., and Dreyfuss, G. (2009). RNA and disease. Cell *136*, 777-793.

Cory, S., and Adams, J. M. (2002). The Bcl2 family: regulators of the cellular life-or-death switch. Nat Rev Cancer *2*, 647-656.

Craig, R. W. (2002). MCL1 provides a window on the role of the BCL2 family in cell proliferation, differentiation and tumorigenesis. Leukemia *16*, 444-454.

Cuconati, A., Mukherjee, C., Perez, D., and White, E. (2003). DNA damage response and MCL-1 destruction initiate apoptosis in adenovirus-infected cells. Genes Dev *17*, 2922-2932.

David, C. J., and Manley, J. L. (2010). Alternative pre-mRNA splicing regulation in cancer: pathways and programs unhinged. Genes Dev *24*, 2343-2364.

Deas, T. S., Binduga-Gajewska, I., Tilgner, M., Ren, P., Stein, D. A., Moulton, H. M., Iversen, P. L., Kauffman, E. B., Kramer, L. D., and Shi, P. Y. (2005). Inhibition of flavivirus infections by antisense oligomers specifically suppressing viral translation and RNA replication. J Virol *79*, 4599-4609.

Dijkers, P. F., Medema, R. H., Lammers, J. W., Koenderman, L., and Coffer, P. J. (2000). Expression of the pro-apoptotic Bcl-2 family member Bim is regulated by the forkhead transcription factor FKHR-L1. Curr Biol *10*, 1201-1204.

Ding, Q., He, X., Xia, W., Hsu, J. M., Chen, C. T., Li, L. Y., Lee, D. F., Yang, J. Y., Xie, X., Liu, J. C., and Hung, M. C. (2007). Myeloid cell leukemia-1 inversely correlates with glycogen synthase kinase-3beta activity and associates with poor prognosis in human breast cancer. Cancer Res *67*, 4564-4571.

Dominski, Z., and Kole, R. (1992). Cooperation of pre-mRNA sequence elements in splice site selection. Mol Cell Biol *12*, 2108-2114.

Dominski, Z., and Kole, R. (1993). Restoration of correct splicing in thalassemic pre-mRNA by antisense oligonucleotides. Proc Natl Acad Sci U S A *90*, 8673-8677.

Du, L., Pollard, J. M., and Gatti, R. A. (2007). Correction of prototypic ATM splicing mutations and aberrant ATM function with antisense morpholino oligonucleotides. Proc Natl Acad Sci U S A *104*, 6007-6012.

Dunckley, M. G., Manoharan, M., Villiet, P., Eperon, I. C., and Dickson, G. (1998). Modification of splicing in the dystrophin gene in cultured Mdx muscle cells by antisense oligoribonucleotides. Hum Mol Genet *7*, 1083-1090.

Eckstein, F. (2000). Phosphorothioate oligodeoxynucleotides: what is their origin and what is unique about them? Antisense Nucleic Acid Drug Dev *10*, 117-121.

Edelstein, M. L., Abedi, M. R., Wixon, J., and Edelstein, R. M. (2004). Gene therapy clinical trials worldwide 1989-2004-an overview. J Gene Med *6*, 597-602.

Edwards, S. W., Derouet, M., Howse, M., and Moots, R. J. (2004). Regulation of neutrophil apoptosis by Mcl-1. Biochem Soc Trans *32*, 489-492.

Fesik, S. W. (2005). Promoting apoptosis as a strategy for cancer drug discovery. Nat Rev Cancer *5*, 876-885.

Fletcher, S., Honeyman, K., Fall, A. M., Harding, P. L., Johnsen, R. D., Steinhaus, J. P., Moulton, H. M., Iversen, P. L., and Wilton, S. D. (2007). Morpholino oligomer-mediated exon skipping averts the onset of dystrophic pathology in the mdx mouse. Mol Ther *15*, 1587-1592.

Garneau, D., Revil, T., Fisette, J. F., and Chabot, B. (2005). Heterogeneous nuclear ribonucleoprotein F/H proteins modulate the alternative splicing of the apoptotic mediator Bcl-x. J Biol Chem *280*, 22641-22650.

Gaur, R. K., Valcarcel, J., and Green, M. R. (1995). Sequential recognition of the pre-mRNA branch point by U2AF65 and a novel spliceosome-associated 28-kDa protein. Rna *1*, 407-417.

Geary, R., Yu, R., Siwkowski, A., and Levin, A. (2008). Pharmacokinetic/Pharmacodynamic Properties of Phosphorothioate 2'-O-(Methoxyethyl)-Modified Antisense Oligonucleotides in Animals and Man. In Antisense Drug Technology, S. Crooke, ed. (Baton Rouge, FL, CRC Press), pp. 305-326.

Geary, R. S., Wancewicz, E., Matson, J., Pearce, M., Siwkowski, A., Swayze, E., and Bennett, F. (2009). Effect of dose and plasma concentration on liver uptake and pharmacologic activity of a 2'-methoxyethyl modified chimeric antisense oligonucleotide targeting PTEN. Biochem Pharmacol *78*, 284-291.

Gilad, S., Chessa, L., Khosravi, R., Russell, P., Galanty, Y., Piane, M., Gatti, R. A., Jorgensen, T. J., Shiloh, Y., and Bar-Shira, A. (1998). Genotype-phenotype relationships in ataxia-telangiectasia and variants. Am J Hum Genet *62*, 551-561.

Giorgini, S., Trisciuoglio, D., Gabellini, C., Desideri, M., Castellini, L., Colarossi, C., Zangemeister-Wittke, U., Zupi, G., and Del Bufalo, D. (2007). Modulation of bcl-xL in tumor cells regulates angiogenesis through CXCL8 expression. Mol Cancer Res *5*, 761-771.

Goldstrohm, A. C., Greenleaf, A. L., and Garcia-Blanco, M. A. (2001). Co-transcriptional splicing of pre-messenger RNAs: considerations for the mechanism of alternative splicing. Gene *277*, 31-47.

Gonzalez-Garcia, M., Garcia, I., Ding, L., O'Shea, S., Boise, L. H., Thompson, C. B., and Nunez, G. (1995). bcl-x is expressed in embryonic and postnatal neural tissues and functions to prevent neuronal cell death. Proc Natl Acad Sci U S A *92*, 4304-4308.

Gonzalez-Garcia, M., Perez-Ballestero, R., Ding, L., Duan, L., Boise, L. H., Thompson, C. B., and Nunez, G. (1994). bcl-XL is the major bcl-x mRNA form expressed during murine development and its product localizes to mitochondria. Development *120*, 3033-3042.

Graziewicz, M. A., Tarrant, T. K., Buckley, B., Roberts, J., Fulton, L., Hansen, H., Orum, H., Kole, R., and Sazani, P. (2008). An endogenous TNF-alpha antagonist induced by splice-switching oligonucleotides reduces inflammation in hepatitis and arthritis mouse models. Mol Ther *16*, 1316-1322.

Han, S. P., Tang, Y. H., and Smith, R. (2010). Functional diversity of the hnRNPs: past, present and perspectives. Biochem J *430*, 379-392.

Hanahan, D., and Weinberg, R. A. (2000). The hallmarks of cancer. Cell *100*, 57-70.

Harvie, P., Wong, F. M., and Bally, M. B. (2000). Use of poly(ethylene glycol)-lipid conjugates to regulate the surface attributes and transfection activity of lipid-DNA particles. J Pharm Sci *89*, 652-663.

Hoffman, E. P., Morgan, J. E., Watkins, S. C., and Partridge, T. A. (1990). Somatic reversion/suppression of the mouse mdx phenotype in vivo. J Neurol Sci *99*, 9-25.

Hossini, A. M., Eberle, J., Fecker, L. F., Orfanos, C. E., and Geilen, C. C. (2003). Conditional expression of exogenous Bcl-X(S) triggers apoptosis in human melanoma cells in vitro and delays growth of melanoma xenografts. FEBS Lett *553*, 250-256.

Hsieh, A. C., and Moasser, M. M. (2007). Targeting HER proteins in cancer therapy and the role of the non-target HER3. Br J Cancer *97*, 453-457.

Hsu, S. Y., Kaipia, A., McGee, E., Lomeli, M., and Hsueh, A. J. (1997). Bok is a pro-apoptotic Bcl-2 protein with restricted expression in reproductive tissues and heterodimerizes with selective anti-apoptotic Bcl-2 family members. Proc Natl Acad Sci U S A *94*, 12401-12406.

Hua, Y., Vickers, T. A., Baker, B. F., Bennett, C. F., and Krainer, A. R. (2007). Enhancement of SMN2 exon 7 inclusion by antisense oligonucleotides targeting the exon. PLoS Biol *5*, e73.

Hua, Y., Vickers, T. A., Okunola, H. L., Bennett, C. F., and Krainer, A. R. (2008). Antisense masking of an hnRNP A1/A2 intronic splicing silencer corrects SMN2 splicing in transgenic mice. Am J Hum Genet *82*, 834-848.

Huang, D. C., and Strasser, A. (2000). BH3-Only proteins-essential initiators of apoptotic cell death. Cell *103*, 839-842.

Hui, J., Hung, L. H., Heiner, M., Schreiner, S., Neumuller, N., Reither, G., Haas, S. A., and Bindereif, A. (2005). Intronic CA-repeat and CA-rich elements: a new class of regulators of mammalian alternative splicing. Embo J *24*, 1988-1998.

Ivanova, G. D., Arzumanov, A., Abes, R., Yin, H., Wood, M. J., Lebleu, B., and Gait, M. J. (2008). Improved cell-penetrating peptide-PNA conjugates for splicing redirection in HeLa cells and exon skipping in mdx mouse muscle. Nucleic Acids Res *36*, 6418-6428.

Jacobson, M. D., Weil, M., and Raff, M. C. (1997). Programmed cell death in animal development. Cell *88*, 347-354.

Jain, R. K. (1999). Transport of molecules, particles, and cells in solid tumors. Annu Rev Biomed Eng *1*, 241-263.

Janssens, S., Burns, K., Tschopp, J., and Beyaert, R. (2002). Regulation of interleukin-1- and lipopolysaccharide-induced NF-kappaB activation by alternative splicing of MyD88. Curr Biol *12*, 467-471.

Jearawiriyapaisarn, N., Moulton, H. M., Buckley, B., Roberts, J., Sazani, P., Fucharoen, S., Iversen, P. L., and Kole, R. (2008). Sustained dystrophin expression induced by peptide-conjugated morpholino oligomers in the muscles of mdx mice. Mol Ther *16*, 1624-1629.

Jearawiriyapaisarn, N., Moulton, H. M., Sazani, P., Kole, R., and Willis, M. S. (2010). Long-term improvement in mdx cardiomyopathy after therapy with peptide-conjugated morpholino oligomers. Cardiovasc Res *85*, 444-453.

Jeffs, L. B., Palmer, L. R., Ambegia, E. G., Giesbrecht, C., Ewanick, S., and MacLachlan, I. (2005). A scalable, extrusion-free method for efficient liposomal encapsulation of plasmid DNA. Pharm Res *22*, 362-372.

John, C. S., Bowen, W. D., Varma, V. M., McAfee, J. G., and Moody, T. W. (1995). Sigma receptors are expressed in human non-small cell lung carcinoma. Life Sci *56*, 2385-2392.

Juliano, R., Bauman, J., Kang, H., and Ming, X. (2009a). Biological barriers to therapy with antisense and siRNA oligonucleotides. Mol Pharm *6*, 686-695.

Juliano, R. L., Bauman, J., Kang, H., and Ming, X. (2009b). Biological Barriers to Therapy with Antisense and siRNA Oligonucleotides. Mol Pharm.

Kang, H., Alam, M. R., Dixit, V., Fisher, M., and Juliano, R. L. (2008). Cellular delivery and biological activity of antisense oligonucleotides conjugated to a targeted protein carrier. Bioconjug Chem *19*, 2182-2188.

Kang, S. H., Cho, M. J., and Kole, R. (1998). Up-regulation of luciferase gene expression with antisense oligonucleotides: implications and applications in functional assay development. Biochemistry *37*, 6235-6239.

Karl, E., Zhang, Z., Dong, Z., Neiva, K. G., Soengas, M. S., Koch, A. E., Polverini, P. J., Nunez, G., and Nor, J. E. (2007). Unidirectional crosstalk between Bcl-xL and Bcl-2 enhances the angiogenic phenotype of endothelial cells. Cell Death Differ *14*, 1657-1666.

Kashima, T., and Manley, J. L. (2003). A negative element in SMN2 exon 7 inhibits splicing in spinal muscular atrophy. Nat Genet *34*, 460-463.

Kerbel, R. S. (2003). Human tumor xenografts as predictive preclinical models for anticancer drug activity in humans: better than commonly perceived-but they can be improved. Cancer Biol Ther *2*, S134-139.

Kerr, J. F., Wyllie, A. H., and Currie, A. R. (1972). Apoptosis: a basic biological phenomenon with wide-ranging implications in tissue kinetics. Br J Cancer *26*, 239-257.

Kinali, M., Arechavala-Gomeza, V., Feng, L., Cirak, S., Hunt, D., Adkin, C., Guglieri, M., Ashton, E., Abbs, S., Nihoyannopoulos, P.*, et al.* (2009). Local restoration of dystrophin expression with the morpholino oligomer AVI-4658 in Duchenne muscular dystrophy: a single-blind, placebo-controlled, dose-escalation, proof-of-concept study. Lancet Neurol *8*, 918-928.

Klein, C. J., Coovert, D. D., Bulman, D. E., Ray, P. N., Mendell, J. R., and Burghes, A. H. (1992). Somatic reversion/suppression in Duchenne muscular dystrophy (DMD): evidence supporting a frame-restoring mechanism in rare dystrophin-positive fibers. Am J Hum Genet *50*, 950-959.

Kole, R. (2010). Oligonucleotide Therapeutics Society Annual Meeting.

Kole, R., Vacek, M., and Williams, T. (2004). Modification of alternative splicing by antisense therapeutics. Oligonucleotides *14*, 65-74.

Konopleva, M., Contractor, R., Tsao, T., Samudio, I., Ruvolo, P. P., Kitada, S., Deng, X., Zhai, D., Shi, Y. X., Sneed, T.*, et al.* (2006). Mechanisms of apoptosis sensitivity and resistance to the BH3 mimetic ABT-737 in acute myeloid leukemia. Cancer Cell *10*, 375-388.

Krajewski, S., Krajewska, M., Shabaik, A., Wang, H. G., Irie, S., Fong, L., and Reed, J. C. (1994). Immunohistochemical analysis of in vivo patterns of Bcl-X expression. Cancer Res *54*, 5501-5507.

Lacerra, G., Sierakowska, H., Carestia, C., Fucharoen, S., Summerton, J., Weller, D., and Kole, R. (2000). Restoration of hemoglobin A synthesis in erythroid cells from peripheral blood of thalassemic patients. Proc Natl Acad Sci U S A *97*, 9591-9596.

Lander, E. S., Linton, L. M., Birren, B., Nusbaum, C., Zody, M. C., Baldwin, J., Devon, K., Dewar, K., Doyle, M., FitzHugh, W.*, et al.* (2001). Initial sequencing and analysis of the human genome. Nature *409*, 860-921.

Legartova, S., Krejci, J., Harnicarova, A., Hajek, R., Kozubek, S., and Bartova, E. (2009). Nuclear topography of the 1q21 genomic region and Mcl-1 protein levels associated with pathophysiology of multiple myeloma. Neoplasma *56*, 404-413.

Leiter, U., Schmid, R. M., Kaskel, P., Peter, R. U., and Krahn, G. (2000). Antiapoptotic bcl-2 and bcl-xL in advanced malignant melanoma. Arch Dermatol Res *292*, 225-232.

Levin, A., Yu, R., and Geary, R. (2008). Basic Principles of the Pharmacokinetics of Antisense Oligonucleotide Drugs. In Antisense Drug Technology, S. Crooke, ed. (New York, CRC Press), pp. 183-215.

Levin, A. A. (1999). A review of the issues in the pharmacokinetics and toxicology of phosphorothioate antisense oligonucleotides. Biochim Biophys Acta *1489*, 69-84.

Lewis, J., Yang, B., Kim, R., Sierakowska, H., Kole, R., Smithies, O., and Maeda, N. (1998). A common human beta globin splicing mutation modeled in mice. Blood *91*, 2152-2156.

Li, H., Zhu, H., Xu, C. J., and Yuan, J. (1998). Cleavage of BID by caspase 8 mediates the mitochondrial damage in the Fas pathway of apoptosis. Cell *94*, 491-501.

Li, S. D., Chen, Y. C., Hackett, M. J., and Huang, L. (2008a). Tumor-targeted delivery of siRNA by self-assembled nanoparticles. Mol Ther *16*, 163-169.

Li, S. D., Chono, S., and Huang, L. (2008b). Efficient gene silencing in metastatic tumor by siRNA formulated in surface-modified nanoparticles. J Control Release *126*, 77-84.

Li, S. D., Chono, S., and Huang, L. (2008c). Efficient oncogene silencing and metastasis inhibition via systemic delivery of siRNA. Mol Ther *16*, 942-946.

Li, S. D., and Huang, L. (2006a). Surface-modified LPD nanoparticles for tumor targeting. Ann N Y Acad Sci *1082*, 1-8.

Li, S. D., and Huang, L. (2006b). Targeted delivery of antisense oligodeoxynucleotide and small interference RNA into lung cancer cells. Mol Pharm *3*, 579-588.

Li, S. D., and Huang, L. (2008). Pharmacokinetics and biodistribution of nanoparticles. Mol Pharm *5*, 496-504.

Li, S. D., and Huang, L. (2009). Nanoparticles evading the reticuloendothelial system: role of the supported bilayer. Biochim Biophys Acta *1788*, 2259-2266.

Li, W., Huang, Z., MacKay, J. A., Grube, S., and Szoka, F. C., Jr. (2005). Low-pH-sensitive poly(ethylene glycol) (PEG)-stabilized plasmid nanolipoparticles: effects of PEG chain length, lipid composition and assembly conditions on gene delivery. J Gene Med *7*, 67-79.

Lim, L. P., and Burge, C. B. (2001). A computational analysis of sequence features involved in recognition of short introns. Proc Natl Acad Sci U S A *98*, 11193-11198.

Lim, S. R., and Hertel, K. J. (2001). Modulation of survival motor neuron pre-mRNA splicing by inhibition of alternative 3' splice site pairing. J Biol Chem *276*, 45476-45483.

Lima, W., Wu, H., and Crooke, S. (2008). The RNase H Mechanism. In Antisense Drug Technology, S. Crooke, ed. (Baton Rouge, CRC Press), pp. 47-74.

Lindenboim, L., Borner, C., and Stein, R. (2001). Bcl-x(S) can form homodimers and heterodimers and its apoptotic activity requires localization of Bcl-x(S) to the mitochondria and its BH3 and loop domains. Cell Death Differ *8*, 933-942.

Lindsten, T., Ross, A. J., King, A., Zong, W. X., Rathmell, J. C., Shiels, H. A., Ulrich, E., Waymire, K. G., Mahar, P., Frauwirth, K.*, et al.* (2000). The combined functions of proapoptotic Bcl-2 family members bak and bax are essential for normal development of multiple tissues. Mol Cell *6*, 1389-1399.

Lopez-Bigas, N., Audit, B., Ouzounis, C., Parra, G., and Guigo, R. (2005). Are splicing mutations the most frequent cause of hereditary disease? FEBS Lett *579*, 1900-1903.

Lu, Q. L., Mann, C. J., Lou, F., Bou-Gharios, G., Morris, G. E., Xue, S. A., Fletcher, S., Partridge, T. A., and Wilton, S. D. (2003). Functional amounts of dystrophin produced by skipping the mutated exon in the mdx dystrophic mouse. Nat Med *9*, 1009-1014.

Lu, Q. L., Morris, G. E., Wilton, S. D., Ly, T., Artem'yeva, O. V., Strong, P., and Partridge, T. A. (2000). Massive idiosyncratic exon skipping corrects the nonsense mutation in dystrophic mouse muscle and produces functional revertant fibers by clonal expansion. J Cell Biol *148*, 985-996.

Lu, Q. L., Rabinowitz, A., Chen, Y. C., Yokota, T., Yin, H., Alter, J., Jadoon, A., Bou-Gharios, G., and Partridge, T. (2005). Systemic delivery of antisense oligoribonucleotide restores dystrophin expression in body-wide skeletal muscles. Proc Natl Acad Sci U S A *102*, 198-203.

Lv, H., Zhang, S., Wang, B., Cui, S., and Yan, J. (2006). Toxicity of cationic lipids and cationic polymers in gene delivery. J Control Release *114*, 100-109.

Mailman, M. D., Heinz, J. W., Papp, A. C., Snyder, P. J., Sedra, M. S., Wirth, B., Burghes, A. H., and Prior, T. W. (2002). Molecular analysis of spinal muscular atrophy and modification of the phenotype by SMN2. Genet Med *4*, 20-26.

Mann, C. J., Honeyman, K., Cheng, A. J., Ly, T., Lloyd, F., Fletcher, S., Morgan, J. E., Partridge, T. A., and Wilton, S. D. (2001). Antisense-induced exon skipping and synthesis of dystrophin in the mdx mouse. Proc Natl Acad Sci U S A *98*, 42-47.

Mann, C. J., Honeyman, K., McClorey, G., Fletcher, S., and Wilton, S. D. (2002). Improved antisense oligonucleotide induced exon skipping in the mdx mouse model of muscular dystrophy. J Gene Med *4*, 644-654.

Marlin, F., Simon, P., Saison-Behmoaras, T., and Giovannangeli, C. (2010). Delivery of oligonucleotides and analogues: the oligonucleotide conjugate-based approach. Chembiochem *11*, 1493-1500.

Martinez-Contreras, R., Cloutier, P., Shkreta, L., Fisette, J. F., Revil, T., and Chabot, B. (2007). hnRNP proteins and splicing control. Adv Exp Med Biol *623*, 123-147.

Massiello, A., Roesser, J. R., and Chalfant, C. E. (2006). SAP155 Binds to ceramide-responsive RNA cis-element 1 and regulates the alternative 5' splice site selection of Bcl-x pre-mRNA. Faseb J *20*, 1680-1682.

Matlin, A. J., Clark, F., and Smith, C. W. (2005). Understanding alternative splicing: towards a cellular code. Nat Rev Mol Cell Biol *6*, 386-398.

McClorey, G., Moulton, H. M., Iversen, P. L., Fletcher, S., and Wilton, S. D. (2006). Antisense oligonucleotide-induced exon skipping restores dystrophin expression in vitro in a canine model of DMD. Gene Ther *13*, 1373-1381.

McCullough, A. J., and Berget, S. M. (2000). An intronic splicing enhancer binds U1 snRNPs to enhance splicing and select 5' splice sites. Mol Cell Biol *20*, 9225-9235.

Mercatante, D. R., Bortner, C. D., Cidlowski, J. A., and Kole, R. (2001). Modification of alternative splicing of Bcl-x pre-mRNA in prostate and breast cancer cells. analysis of apoptosis and cell death. J Biol Chem *276*, 16411-16417.

Mercatante, D. R., and Kole, R. (2002). Control of alternative splicing by antisense oligonucleotides as a potential chemotherapy: effects on gene expression. Biochim Biophys Acta *1587*, 126-132.

Mercatante, D. R., Mohler, J. L., and Kole, R. (2002). Cellular response to an antisense-mediated shift of Bcl-x pre-mRNA splicing and antineoplastic agents. J Biol Chem *277*, 49374-49382.

Merdzhanova, G., Edmond, V., De Seranno, S., Van den Broeck, A., Corcos, L., Brambilla, C., Brambilla, E., Gazzeri, S., and Eymin, B. (2008). E2F1 controls alternative splicing pattern of genes involved in apoptosis through upregulation of the splicing factor SC35. Cell Death Differ *15*, 1815-1823.

Minn, A. J., Boise, L. H., and Thompson, C. B. (1996). Bcl-x(S) anatagonizes the protective effects of Bcl-x(L). J Biol Chem *271*, 6306-6312.

Miyajima, H., Miyaso, H., Okumura, M., Kurisu, J., and Imaizumi, K. (2002). Identification of a cis-acting element for the regulation of SMN exon 7 splicing. J Biol Chem *277*, 23271-23277.

Monaco, A. P., Bertelson, C. J., Liechti-Gallati, S., Moser, H., and Kunkel, L. M. (1988). An explanation for the phenotypic differences between patients bearing partial deletions of the DMD locus. Genomics *2*, 90-95.

Monia, B. P., Lesnik, E. A., Gonzalez, C., Lima, W. F., McGee, D., Guinosso, C. J., Kawasaki, A. M., Cook, P. D., and Freier, S. M. (1993). Evaluation of 2'-modified oligonucleotides containing 2'-deoxy gaps as antisense inhibitors of gene expression. J Biol Chem *268*, 14514-14522.

Morcos, P. A. (2007). Achieving targeted and quantifiable alteration of mRNA splicing with Morpholino oligos. Biochem Biophys Res Commun *358*, 521-527.

Mosser, D. M., and Edwards, J. P. (2008). Exploring the full spectrum of macrophage activation. Nat Rev Immunol *8*, 958-969.

Moulton, H. M., Fletcher, S., Neuman, B. W., McClorey, G., Stein, D. A., Abes, S., Wilton, S. D., Buchmeier, M. J., Lebleu, B., and Iversen, P. L. (2007). Cell-penetrating peptide-morpholino conjugates alter pre-mRNA splicing of DMD (Duchenne muscular dystrophy) and inhibit murine coronavirus replication in vivo. Biochem Soc Trans *35*, 826-828.

Nakano, K., and Vousden, K. H. (2001). PUMA, a novel proapoptotic gene, is induced by p53. Mol Cell *7*, 683-694.

Nasim, F. U., Hutchison, S., Cordeau, M., and Chabot, B. (2002). High-affinity hnRNP A1 binding sites and duplex-forming inverted repeats have similar effects on 5' splice site selection in support of a common looping out and repression mechanism. Rna *8*, 1078-1089.

Nechushtan, A., Smith, C. L., Hsu, Y. T., and Youle, R. J. (1999). Conformation of the Bax C-terminus regulates subcellular location and cell death. Embo J *18*, 2330-2341.

Nemunaitis, J., Holmlund, J. T., Kraynak, M., Richards, D., Bruce, J., Ognoskie, N., Kwoh, T. J., Geary, R., Dorr, A., Von Hoff, D., and Eckhardt, S. G. (1999). Phase I evaluation of ISIS 3521, an antisense oligodeoxynucleotide to protein kinase C-alpha, in patients with advanced cancer. J Clin Oncol *17*, 3586-3595.

Neri, M., Torelli, S., Brown, S., Ugo, I., Sabatelli, P., Merlini, L., Spitali, P., Rimessi, P., Gualandi, F., Sewry, C.*, et al.* (2007). Dystrophin levels as low as 30% are sufficient to avoid muscular dystrophy in the human. Neuromuscul Disord *17*, 913-918.

Nguyen, M., Marcellus, R. C., Roulston, A., Watson, M., Serfass, L., Murthy Madiraju, S. R., Goulet, D., Viallet, J., Belec, L., Billot, X.*, et al.* (2007). Small molecule obatoclax (GX15-070) antagonizes MCL-1 and overcomes MCL-1-mediated resistance to apoptosis. Proc Natl Acad Sci U S A *104*, 19512-19517.

Nicholson, L. V., Davison, K., Johnson, M. A., Slater, C. R., Young, C., Bhattacharya, S., Gardner-Medwin, D., and Harris, J. B. (1989). Dystrophin in skeletal muscle. II. Immunoreactivity in patients with Xp21 muscular dystrophy. J Neurol Sci *94*, 137-146.

Nijhawan, D., Fang, M., Traer, E., Zhong, Q., Gao, W., Du, F., and Wang, X. (2003). Elimination of Mcl-1 is required for the initiation of apoptosis following ultraviolet irradiation. Genes Dev *17*, 1475-1486.

Nikiforov, M. A., Riblett, M., Tang, W. H., Gratchouck, V., Zhuang, D., Fernandez, Y., Verhaegen, M., Varambally, S., Chinnaiyan, A. M., Jakubowiak, A. J., and Soengas, M. S. (2007). Tumor cell-selective regulation of NOXA by c-MYC in response to proteasome inhibition. Proc Natl Acad Sci U S A *104*, 19488-19493.

Oda, E., Ohki, R., Murasawa, H., Nemoto, J., Shibue, T., Yamashita, T., Tokino, T., Taniguchi, T., and Tanaka, N. (2000). Noxa, a BH3-only member of the Bcl-2 family and candidate mediator of p53-induced apoptosis. Science *288*, 1053-1058.

Okada, H., and Mak, T. W. (2004). Pathways of apoptotic and non-apoptotic death in tumour cells. Nat Rev Cancer *4*, 592-603.

Olayioye, M. A., Neve, R. M., Lane, H. A., and Hynes, N. E. (2000). The ErbB signaling network: receptor heterodimerization in development and cancer. Embo J *19*, 3159-3167.

Olopade, O. I., Adeyanju, M. O., Safa, A. R., Hagos, F., Mick, R., Thompson, C. B., and Recant, W. M. (1997). Overexpression of BCL-x protein in primary breast cancer is associated with high tumor grade and nodal metastases. Cancer J Sci Am *3*, 230-237.

Olsen, N. J., and Stein, C. M. (2004). New drugs for rheumatoid arthritis. N Engl J Med *350*, 2167-2179.

Oltersdorf, T., Elmore, S. W., Shoemaker, A. R., Armstrong, R. C., Augeri, D. J., Belli, B. A., Bruncko, M., Deckwerth, T. L., Dinges, J., Hajduk, P. J.*, et al.* (2005). An inhibitor of Bcl-2 family proteins induces regression of solid tumours. Nature *435*, 677-681.

Opferman, J. T., Iwasaki, H., Ong, C. C., Suh, H., Mizuno, S., Akashi, K., and Korsmeyer, S. J. (2005). Obligate role of anti-apoptotic MCL-1 in the survival of hematopoietic stem cells. Science *307*, 1101-1104.

Paronetto, M. P., Achsel, T., Massiello, A., Chalfant, C. E., and Sette, C. (2007). The RNA-binding protein Sam68 modulates the alternative splicing of Bcl-x. J Cell Biol *176*, 929-939.

Petros, A. M., Olejniczak, E. T., and Fesik, S. W. (2004). Structural biology of the Bcl-2 family of proteins. Biochim Biophys Acta *1644*, 83-94.

Pham, T. Q., Berghofer, P., Liu, X., Greguric, I., Dikic, B., Ballantyne, P., Mattner, F., Nguyen, V., Loc'h, C., and Katsifis, A. (2007). Preparation and biologic evaluation of a novel

radioiodinated benzylpiperazine, 123I-MEL037, for malignant melanoma. J Nucl Med *48*, 1348-1356.

Pincus, T., O'Dell, J. R., and Kremer, J. M. (1999). Combination therapy with multiple disease-modifying antirheumatic drugs in rheumatoid arthritis: a preventive strategy. Ann Intern Med *131*, 768-774.

Pollard, A. J., Krainer, A. R., Robson, S. C., and Europe-Finner, G. N. (2002). Alternative splicing of the adenylyl cyclase stimulatory G-protein G alpha(s) is regulated by SF2/ASF and heterogeneous nuclear ribonucleoprotein A1 (hnRNPA1) and involves the use of an unusual TG 3'-splice Site. J Biol Chem *277*, 15241-15251.

Pollard, A. J., Sparey, C., Robson, S. C., Krainer, A. R., and Europe-Finner, G. N. (2000). Spatio-temporal expression of the trans-acting splicing factors SF2/ASF and heterogeneous ribonuclear proteins A1/A1B in the myometrium of the pregnant human uterus: a molecular mechanism for regulating regional protein isoform expression in vivo. J Clin Endocrinol Metab *85*, 1928-1936.

Pramono, Z. A., Takeshima, Y., Alimsardjono, H., Ishii, A., Takeda, S., and Matsuo, M. (1996). Induction of exon skipping of the dystrophin transcript in lymphoblastoid cells by transfecting an antisense oligodeoxynucleotide complementary to an exon recognition sequence. Biochem Biophys Res Commun *226*, 445-449.

Puthalakath, H., O'Reilly, L. A., Gunn, P., Lee, L., Kelly, P. N., Huntington, N. D., Hughes, P. D., Michalak, E. M., McKimm-Breschkin, J., Motoyama, N.*, et al.* (2007). ER stress triggers apoptosis by activating BH3-only protein Bim. Cell *129*, 1337-1349.

Reeve, J. G., Xiong, J., Morgan, J., and Bleehen, N. M. (1996). Expression of apoptosis-regulatory genes in lung tumour cell lines: relationship to p53 expression and relevance to acquired drug resistance. Br J Cancer *73*, 1193-1200.

Rimessi, P., Sabatelli, P., Fabris, M., Braghetta, P., Bassi, E., Spitali, P., Vattemi, G., Tomelleri, G., Mari, L., Perrone, D.*, et al.* (2009). Cationic PMMA nanoparticles bind and deliver antisense oligoribonucleotides allowing restoration of dystrophin expression in the mdx mouse. Mol Ther *17*, 820-827.

Rippe, B., Rosengren, B. I., Carlsson, O., and Venturoli, D. (2002). Transendothelial transport: the vesicle controversy. J Vasc Res *39*, 375-390.

Roberts, J., Palma, E., Sazani, P., Orum, H., Cho, M., and Kole, R. (2006). Efficient and persistent splice switching by systemically delivered LNA oligonucleotides in mice. Mol Ther *14*, 471-475.

Roscigno, R. F., and Garcia-Blanco, M. A. (1995). SR proteins escort the U4/U6.U5 tri-snRNP to the spliceosome. Rna *1*, 692-706.

Sato, T., Hanada, M., Bodrug, S., Irie, S., Iwama, N., Boise, L. H., Thompson, C. B., Golemis, E., Fong, L., Wang, H. G., and et al. (1994). Interactions among members of the Bcl-2 protein family analyzed with a yeast two-hybrid system. Proc Natl Acad Sci U S A *91*, 9238-9242.

Sazani, P., Astriab-Fischer, A., and Kole, R. (2003). Effects of base modifications on antisense properties of 2'-O-methoxyethyl and PNA oligonucleotides. Antisense Nucleic Acid Drug Dev *13*, 119-128.

Sazani, P., Gemignani, F., Kang, S. H., Maier, M. A., Manoharan, M., Persmark, M., Bortner, D., and Kole, R. (2002). Systemically delivered antisense oligomers upregulate gene expression in mouse tissues. Nat Biotechnol *20*, 1228-1233.

Sazani P, G. M., Kole R (2007). Splice switching oligonucleotides as potential therapeutics. In Antisense Drug Technology (CRC Press Taylor & Francis Group), pp. 89-114.

Sazani, P., Kang, S. H., Maier, M. A., Wei, C., Dillman, J., Summerton, J., Manoharan, M., and Kole, R. (2001). Nuclear antisense effects of neutral, anionic and cationic oligonucleotide analogs. Nucleic Acids Res *29*, 3965-3974.

Sazani, P., Weller, D. L., and Shrewsbury, S. B. (2010). Safety pharmacology and genotoxicity evaluation of AVI-4658. Int J Toxicol *29*, 143-156.

Schwerk, C., and Schulze-Osthoff, K. (2005). Regulation of apoptosis by alternative pre-mRNA splicing. Mol Cell *19*, 1-13.

Schwickart, M., Huang, X., Lill, J. R., Liu, J., Ferrando, R., French, D. M., Maecker, H., O'Rourke, K., Bazan, F., Eastham-Anderson, J*., et al.* (2010). Deubiquitinase USP9X stabilizes MCL1 and promotes tumour cell survival. Nature *463*, 103-107.

Sharma, S., Falick, A. M., and Black, D. L. (2005). Polypyrimidine tract binding protein blocks the 5' splice site-dependent assembly of U2AF and the prespliceosomal E complex. Mol Cell *19*, 485-496.

Sharpless, N. E., and Depinho, R. A. (2006). The mighty mouse: genetically engineered mouse models in cancer drug development. Nat Rev Drug Discov *5*, 741-754.

Shepard, P. J., and Hertel, K. J. (2009). The SR protein family. Genome Biol *10*, 242.

Shieh, J. J., Liu, K. T., Huang, S. W., Chen, Y. J., and Hsieh, T. Y. (2009). Modification of alternative splicing of Mcl-1 pre-mRNA using antisense morpholino oligonucleotides induces apoptosis in basal cell carcinoma cells. J Invest Dermatol *129*, 2497-2506.

Shiraiwa, N., Inohara, N., Okada, S., Yuzaki, M., Shoji, S., and Ohta, S. (1996). An additional form of rat Bcl-x, Bcl-xbeta, generated by an unspliced RNA, promotes apoptosis in promyeloid cells. J Biol Chem *271*, 13258-13265.

Sierakowska, H., Sambade, M. J., Agrawal, S., and Kole, R. (1996). Repair of thalassemic human beta-globin mRNA in mammalian cells by antisense oligonucleotides. Proc Natl Acad Sci U S A *93*, 12840-12844.

Sigova, A., and Zamore, P. (2008). Small RNA Silencing Pathways. In Antisense Drug Technology, S. Crooke, ed. (Baton Rouge, CRC Press), pp. 75-88.

Singh, N. K., Singh, N. N., Androphy, E. J., and Singh, R. N. (2006). Splicing of a critical exon of human Survival Motor Neuron is regulated by a unique silencer element located in the last intron. Mol Cell Biol *26*, 1333-1346.

Singh, N. N., Androphy, E. J., and Singh, R. N. (2004). An extended inhibitory context causes skipping of exon 7 of SMN2 in spinal muscular atrophy. Biochem Biophys Res Commun *315*, 381-388.

Skordis, L. A., Dunckley, M. G., Yue, B., Eperon, I. C., and Muntoni, F. (2003). Bifunctional antisense oligonucleotides provide a trans-acting splicing enhancer that stimulates SMN2 gene expression in patient fibroblasts. Proc Natl Acad Sci U S A *100*, 4114-4119.

Soleymanlou, N., Jurisicova, A., Wu, Y., Chijiiwa, M., Ray, J. E., Detmar, J., Todros, T., Zamudio, S., Post, M., and Caniggia, I. (2007). Hypoxic switch in mitochondrial myeloid cell leukemia factor-1/Mtd apoptotic rheostat contributes to human trophoblast cell death in preeclampsia. Am J Pathol *171*, 496-506.

Sorek, R., and Ast, G. (2003). Intronic sequences flanking alternatively spliced exons are conserved between human and mouse. Genome Res *13*, 1631-1637.

Sorek, R., Shemesh, R., Cohen, Y., Basechess, O., Ast, G., and Shamir, R. (2004). A non-EST-based method for exon-skipping prediction. Genome Res *14*, 1617-1623.

Staknis, D., and Reed, R. (1994). SR proteins promote the first specific recognition of Pre-mRNA and are present together with the U1 small nuclear ribonucleoprotein particle in a general splicing enhancer complex. Mol Cell Biol *14*, 7670-7682.

Staley, J. P., and Guthrie, C. (1998). Mechanical devices of the spliceosome: motors, clocks, springs, and things. Cell *92*, 315-326.

Storey, S. (2008). Targeting apoptosis: selected anticancer strategies. Nature Reviews Drug Discovery *7*, 971-972.

Surono, A., Van Khanh, T., Takeshima, Y., Wada, H., Yagi, M., Takagi, M., Koizumi, M., and Matsuo, M. (2004). Chimeric RNA/ethylene-bridged nucleic acids promote dystrophin expression in myocytes of duchenne muscular dystrophy by inducing skipping of the nonsense mutation-encoding exon. Hum Gene Ther *15*, 749-757.

Suwanmanee, T., Sierakowska, H., Fucharoen, S., and Kole, R. (2002a). Repair of a splicing defect in erythroid cells from patients with beta-thalassemia/HbE disorder. Mol Ther *6*, 718-726.

Suwanmanee, T., Sierakowska, H., Lacerra, G., Svasti, S., Kirby, S., Walsh, C. E., Fucharoen, S., and Kole, R. (2002b). Restoration of human beta-globin gene expression in murine and human IVS2-654 thalassemic erythroid cells by free uptake of antisense oligonucleotides. Mol Pharmacol *62*, 545-553.

Svasti, S., Suwanmanee, T., Fucharoen, S., Moulton, H. M., Nelson, M. H., Maeda, N., Smithies, O., and Kole, R. (2009). RNA repair restores hemoglobin expression in IVS2-654 thalassemic mice. Proc Natl Acad Sci U S A *106*, 1205-1210.

Tahir, S. K., Yang, X., Anderson, M. G., Morgan-Lappe, S. E., Sarthy, A. V., Chen, J., Warner, R. B., Ng, S. C., Fesik, S. W., Elmore, S. W.*, et al.* (2007). Influence of Bcl-2 family members on the cellular response of small-cell lung cancer cell lines to ABT-737. Cancer Res *67*, 1176-1183.

Takahashi, A., Alnemri, E. S., Lazebnik, Y. A., Fernandes-Alnemri, T., Litwack, G., Moir, R. D., Goldman, R. D., Poirier, G. G., Kaufmann, S. H., and Earnshaw, W. C. (1996). Cleavage of lamin A by Mch2 alpha but not CPP32: multiple interleukin 1 beta-converting enzyme-related proteases with distinct substrate recognition properties are active in apoptosis. Proc Natl Acad Sci U S A *93*, 8395-8400.

Takehara, T., Liu, X., Fujimoto, J., Friedman, S. L., and Takahashi, H. (2001). Expression and role of Bcl-xL in human hepatocellular carcinomas. Hepatology *34*, 55-61.

Takeshima, Y., Nishio, H., Sakamoto, H., Nakamura, H., and Matsuo, M. (1995). Modulation of in vitro splicing of the upstream intron by modifying an intra-exon sequence which is deleted from the dystrophin gene in dystrophin Kobe. J Clin Invest *95*, 515-520.

Tang, L., Tron, V. A., Reed, J. C., Mah, K. J., Krajewska, M., Li, G., Zhou, X., Ho, V. C., and Trotter, M. J. (1998). Expression of apoptosis regulators in cutaneous malignant melanoma. Clin Cancer Res *4*, 1865-1871.

Taylor, J. K., Zhang, Q. Q., Wyatt, J. R., and Dean, N. M. (1999). Induction of endogenous Bcl-xS through the control of Bcl-x pre-mRNA splicing by antisense oligonucleotides. Nat Biotechnol *17*, 1097-1100.

Tennyson, C. N., Shi, Q., and Worton, R. G. (1996). Stability of the human dystrophin transcript in muscle. Nucleic Acids Res *24*, 3059-3064.

Teraoka, S. N., Telatar, M., Becker-Catania, S., Liang, T., Onengut, S., Tolun, A., Chessa, L., Sanal, O., Bernatowska, E., Gatti, R. A., and Concannon, P. (1999). Splicing defects in the ataxia-telangiectasia gene, ATM: underlying mutations and consequences. Am J Hum Genet *64*, 1617-1631.

Thanaraj, T. A., Clark, F., and Muilu, J. (2003). Conservation of human alternative splice events in mouse. Nucleic Acids Res *31*, 2544-2552.

Thornberry, N. A., and Lazebnik, Y. (1998). Caspases: enemies within. Science *281*, 1312-1316.

Thornberry, N. A., Rano, T. A., Peterson, E. P., Rasper, D. M., Timkey, T., Garcia-Calvo, M., Houtzager, V. M., Nordstrom, P. A., Roy, S., Vaillancourt, J. P.*, et al.* (1997). A combinatorial approach defines specificities of members of the caspase family and granzyme B. Functional relationships established for key mediators of apoptosis. J Biol Chem *272*, 17907-17911.

Trudel, S., Li, Z. H., Rauw, J., Tiedemann, R. E., Wen, X. Y., and Stewart, A. K. (2007). Preclinical studies of the pan-Bcl inhibitor obatoclax (GX015-070) in multiple myeloma. Blood *109*, 5430-5438.

Tu, Y., Renner, S., Xu, F., Fleishman, A., Taylor, J., Weisz, J., Vescio, R., Rettig, M., Berenson, J., Krajewski, S.*, et al.* (1998). BCL-X expression in multiple myeloma: possible indicator of chemoresistance. Cancer Res *58*, 256-262.

Underhill, D. M., and Ozinsky, A. (2002). Phagocytosis of microbes: complexity in action. Annu Rev Immunol *20*, 825-852.

Uren, R. T., Dewson, G., Chen, L., Coyne, S. C., Huang, D. C., Adams, J. M., and Kluck, R. M. (2007). Mitochondrial permeabilization relies on BH3 ligands engaging multiple prosurvival Bcl-2 relatives, not Bak. J Cell Biol *177*, 277-287.

Valcarcel, J., Gaur, R. K., Singh, R., and Green, M. R. (1996). Interaction of U2AF65 RS region with pre-mRNA branch point and promotion of base pairing with U2 snRNA [corrected]. Science *273*, 1706-1709.

van Delft, M. F., Wei, A. H., Mason, K. D., Vandenberg, C. J., Chen, L., Czabotar, P. E., Willis, S. N., Scott, C. L., Day, C. L., Cory, S.*, et al.* (2006). The BH3 mimetic ABT-737 targets selective Bcl-2 proteins and efficiently induces apoptosis via Bak/Bax if Mcl-1 is neutralized. Cancer Cell *10*, 389-399.

van Deutekom, J. C., Bremmer-Bout, M., Janson, A. A., Ginjaar, I. B., Baas, F., den Dunnen, J. T., and van Ommen, G. J. (2001). Antisense-induced exon skipping restores dystrophin expression in DMD patient derived muscle cells. Hum Mol Genet *10*, 1547-1554.

van Deutekom, J. C., Janson, A. A., Ginjaar, I. B., Frankhuizen, W. S., Aartsma-Rus, A., Bremmer-Bout, M., den Dunnen, J. T., Koop, K., van der Kooi, A. J., Goemans, N. M.*, et al.* (2007). Local dystrophin restoration with antisense oligonucleotide PRO051. N Engl J Med *357*, 2677-2686.

Vickers, T. A., Zhang, H., Graham, M. J., Lemonidis, K. M., Zhao, C., and Dean, N. M. (2006). Modification of MyD88 mRNA splicing and inhibition of IL-1beta signaling in cell culture and in mice with a 2'-O-methoxyethyl-modified oligonucleotide. J Immunol *176*, 3652-3661.

Vilner, B. J., John, C. S., and Bowen, W. D. (1995). Sigma-1 and sigma-2 receptors are expressed in a wide variety of human and rodent tumor cell lines. Cancer Res *55*, 408-413.

Vitiello, L., Bassi, N., Campagnolo, P., Zaccariotto, E., Occhi, G., Malerba, A., Pigozzo, S., Reggiani, C., Ausoni, S., Zaglia, T.*, et al.* (2008). In vivo delivery of naked antisense oligos in aged mdx mice: Analysis of dystrophin restoration in skeletal and cardiac muscle. Neuromuscul Disord.

Wacheck, V., Selzer, E., Gunsberg, P., Lucas, T., Meyer, H., Thallinger, C., Monia, B. P., and Jansen, B. (2003). Bcl-x(L) antisense oligonucleotides radiosensitise colon cancer cells. Br J Cancer *89*, 1352-1357.

Wagner, E. J., Baraniak, A. P., Sessions, O. M., Mauger, D., Moskowitz, E., and Garcia-Blanco, M. A. (2005). Characterization of the intronic splicing silencers flanking FGFR2 exon IIIb. J Biol Chem *280*, 14017-14027.

Wahl, M. C., Will, C. L., and Luhrmann, R. (2009). The spliceosome: design principles of a dynamic RNP machine. Cell *136*, 701-718.

Wahlestedt, C., Salmi, P., Good, L., Kela, J., Johnsson, T., Hokfelt, T., Broberger, C., Porreca, F., Lai, J., Ren, K.*, et al.* (2000). Potent and nontoxic antisense oligonucleotides containing locked nucleic acids. Proc Natl Acad Sci U S A *97*, 5633-5638.

Wan, J., Sazani, P., and Kole, R. (2008). Modification of HER2 pre-mRNA alternative splicing and its effects on breast cancer cells. International Journal of Cancer.

Wan, J., Sazani, P., and Kole, R. (2009). Modification of HER2 pre-mRNA alternative splicing and its effects on breast cancer cells. Int J Cancer *124*, 772-777.

Wan, L., Battle, D. J., Yong, J., Gubitz, A. K., Kolb, S. J., Wang, J., and Dreyfuss, G. (2005). The survival of motor neurons protein determines the capacity for snRNP assembly: biochemical deficiency in spinal muscular atrophy. Mol Cell Biol *25*, 5543-5551.

Wang, E. T., Sandberg, R., Luo, S., Khrebtukova, I., Zhang, L., Mayr, C., Kingsmore, S. F., Schroth, G. P., and Burge, C. B. (2008). Alternative isoform regulation in human tissue transcriptomes. Nature *456*, 470-476.

Wang, X. (2001). The expanding role of mitochondria in apoptosis. Genes Dev *15*, 2922-2933.

Wang, Z., and Burge, C. B. (2008). Splicing regulation: from a parts list of regulatory elements to an integrated splicing code. Rna *14*, 802-813.

Wang, Z., Rolish, M. E., Yeo, G., Tung, V., Mawson, M., and Burge, C. B. (2004). Systematic identification and analysis of exonic splicing silencers. Cell *119*, 831-845.

Wang, Z., Xiao, X., Van Nostrand, E., and Burge, C. B. (2006). General and specific functions of exonic splicing silencers in splicing control. Mol Cell *23*, 61-70.

Warr, M. R., and Shore, G. C. (2008). Unique biology of Mcl-1: therapeutic opportunities in cancer. Curr Mol Med *8*, 138-147.

Watanabe, J., Kushihata, F., Honda, K., Mominoki, K., Matsuda, S., and Kobayashi, N. (2002). Bcl-xL overexpression in human hepatocellular carcinoma. Int J Oncol *21*, 515-519.

Waterhouse, N., Kumar, S., Song, Q., Strike, P., Sparrow, L., Dreyfuss, G., Alnemri, E. S., Litwack, G., Lavin, M., and Watters, D. (1996). Heteronuclear ribonucleoproteins C1 and C2, components of the spliceosome, are specific targets of interleukin 1beta-converting enzyme-like proteases in apoptosis. J Biol Chem *271*, 29335-29341.

Wei, L. H., Kuo, M. L., Chen, C. A., Chou, C. H., Cheng, W. F., Chang, M. C., Su, J. L., and Hsieh, C. Y. (2001a). The anti-apoptotic role of interleukin-6 in human cervical cancer is mediated by up-regulation of Mcl-1 through a PI 3-K/Akt pathway. Oncogene *20*, 5799-5809.

Wei, M. C., Zong, W. X., Cheng, E. H., Lindsten, T., Panoutsakopoulou, V., Ross, A. J., Roth, K. A., MacGregor, G. R., Thompson, C. B., and Korsmeyer, S. J. (2001b). Proapoptotic BAX and BAK: a requisite gateway to mitochondrial dysfunction and death. Science *292*, 727-730.

Wesarg, E., Hoffarth, S., Wiewrodt, R., Kroll, M., Biesterfeld, S., Huber, C., and Schuler, M. (2007). Targeting BCL-2 family proteins to overcome drug resistance in non-small cell lung cancer. Int J Cancer *121*, 2387-2394.

Wheeler, J. J., Palmer, L., Ossanlou, M., MacLachlan, I., Graham, R. W., Zhang, Y. P., Hope, M. J., Scherrer, P., and Cullis, P. R. (1999). Stabilized plasmid-lipid particles: construction and characterization. Gene Ther *6*, 271-281.

Willis, S. N., and Adams, J. M. (2005). Life in the balance: how BH3-only proteins induce apoptosis. Curr Opin Cell Biol *17*, 617-625.

Willis, S. N., Chen, L., Dewson, G., Wei, A., Naik, E., Fletcher, J. I., Adams, J. M., and Huang, D. C. (2005). Proapoptotic Bak is sequestered by Mcl-1 and Bcl-xL, but not Bcl-2, until displaced by BH3-only proteins. Genes Dev *19*, 1294-1305.

Willis, S. N., Fletcher, J. I., Kaufmann, T., van Delft, M. F., Chen, L., Czabotar, P. E., Ierino, H., Lee, E. F., Fairlie, W. D., Bouillet, P.*, et al.* (2007). Apoptosis initiated when BH3 ligands engage multiple Bcl-2 homologs, not Bax or Bak. Science *315*, 856-859.

Wilton, S. D., Lloyd, F., Carville, K., Fletcher, S., Honeyman, K., Agrawal, S., and Kole, R. (1999). Specific removal of the nonsense mutation from the mdx dystrophin mRNA using antisense oligonucleotides. Neuromuscul Disord *9*, 330-338.

Wilusz, J. E., Devanney, S. C., and Caputi, M. (2005). Chimeric peptide nucleic acid compounds modulate splicing of the bcl-x gene in vitro and in vivo. Nucleic Acids Res *33*, 6547-6554.

Wu, B., Li, Y., Morcos, P. A., Doran, T. J., Lu, P., and Lu, Q. L. (2009). Octa-guanidine morpholino restores dystrophin expression in cardiac and skeletal muscles and ameliorates pathology in dystrophic mdx mice. Mol Ther *17*, 864-871.

Wu, B., Moulton, H. M., Iversen, P. L., Jiang, J., Li, J., Li, J., Spurney, C. F., Sali, A., Guerron, A. D., Nagaraju, K.*, et al.* (2008). Effective rescue of dystrophin improves cardiac function in dystrophin-deficient mice by a modified morpholino oligomer. Proc Natl Acad Sci U S A *105*, 14814-14819.

Wu, S., Romfo, C. M., Nilsen, T. W., and Green, M. R. (1999). Functional recognition of the 3' splice site AG by the splicing factor U2AF35. Nature *402*, 832-835.

Yang, T., Buchan, H. L., Townsend, K. J., and Craig, R. W. (1996). MCL-1, a member of the BLC-2 family, is induced rapidly in response to signals for cell differentiation or death, but not to signals for cell proliferation. J Cell Physiol *166*, 523-536.

Yarden, Y., and Sliwkowski, M. X. (2001). Untangling the ErbB signalling network. Nat Rev Mol Cell Biol *2*, 127-137.

Yeo, G. W., Van Nostrand, E. L., and Liang, T. Y. (2007). Discovery and analysis of evolutionarily conserved intronic splicing regulatory elements. PLoS Genet *3*, e85.

Yin, H., Lu, Q., and Wood, M. (2008a). Effective exon skipping and restoration of dystrophin expression by peptide nucleic acid antisense oligonucleotides in mdx mice. Mol Ther *16*, 38-45.

Yin, H., Moulton, H. M., Seow, Y., Boyd, C., Boutilier, J., Iverson, P., and Wood, M. J. (2008b). Cell-penetrating peptide-conjugated antisense oligonucleotides restore systemic muscle and cardiac dystrophin expression and function. Hum Mol Genet *17*, 3909-3918.

Yokota, T., Lu, Q., Partridge, T., Kobayashi, M., Nakamura, A., takeda, S., and Hoffman, E. P. (2008). Body-wide restoration of dystrophin expression and amelioration of pathology in dystrophic dogs using a morpholino cocktail. Mol Ther *16 Supplement 1*, S143.

Yokota, T., Lu, G, Partridge, TA, Kobayashi, M, Nakamura, A, Takeda, S, Hoffman, EP (2008). Body-wide restoration of Dystrophin expression and amelioration of pathology in dystrophic dogs using a morpholino cocktail. Molecular Therapy *16*.

Youle, R. J., and Strasser, A. (2008). The BCL-2 protein family: opposing activities that mediate cell death. Nat Rev Mol Cell Biol *9*, 47-59.

Yu, D., Kandimalla, E. R., Roskey, A., Zhao, Q., Chen, L., Chen, J., and Agrawal, S. (2000). Stereo-enriched phosphorothioate oligodeoxynucleotides: synthesis, biophysical and biological properties. Bioorg Med Chem *8*, 275-284.

Zha, J., Harada, H., Yang, E., Jockel, J., and Korsmeyer, S. J. (1996). Serine phosphorylation of death agonist BAD in response to survival factor results in binding to 14-3-3 not BCL-X(L). Cell *87*, 619-628.

Zhai, D., Jin, C., Huang, Z., Satterthwait, A. C., and Reed, J. C. (2008). Differential regulation of Bax and Bak by anti-apoptotic Bcl-2 family proteins Bcl-B and Mcl-1. J Biol Chem *283*, 9580-9586.

Zhang, B., Gojo, I., and Fenton, R. G. (2002). Myeloid cell factor-1 is a critical survival factor for multiple myeloma. Blood *99*, 1885-1893.

Zhang, N., Peairs, J. J., Yang, P., Tyrrell, J., Roberts, J., Kole, R., and Jaffe, G. J. (2007). The importance of Bcl-xL in the survival of human RPE cells. Invest Ophthalmol Vis Sci *48*, 3846-3853.

Zhang, Y. P., Sekirov, L., Saravolac, E. G., Wheeler, J. J., Tardi, P., Clow, K., Leng, E., Sun, R., Cullis, P. R., and Scherrer, P. (1999). Stabilized plasmid-lipid particles for regional gene therapy: formulation and transfection properties. Gene Ther *6*, 1438-1447.

Zhong, Q., Gao, W., Du, F., and Wang, X. (2005). Mule/ARF-BP1, a BH3-only E3 ubiquitin ligase, catalyzes the polyubiquitination of Mcl-1 and regulates apoptosis. Cell *121*, 1085-1095.

Zhou, A., Ou, A. C., Cho, A., Benz, E. J., Jr., and Huang, S. C. (2008). Novel splicing factor RBM25 modulates Bcl-x pre-mRNA 5' splice site selection. Mol Cell Biol *28*, 5924-5936.

Zhu, J., Mayeda, A., and Krainer, A. R. (2001). Exon identity established through differential antagonism between exonic splicing silencer-bound hnRNP A1 and enhancer-bound SR proteins. Mol Cell *8*, 1351-1361.

Zhuang, L., Lee, C. S., Scolyer, R. A., McCarthy, S. W., Zhang, X. D., Thompson, J. F., and Hersey, P. (2007). Mcl-1, Bcl-XL and Stat3 expression are associated with progression of melanoma whereas Bcl-2, AP-2 and MITF levels decrease during progression of melanoma. Mod Pathol *20*, 416-426.

Zimmermann, K. C., Bonzon, C., and Green, D. R. (2001). The machinery of programmed cell death. Pharmacol Ther *92*, 57-70.